# Semiconductor heterostructures – quantum wells

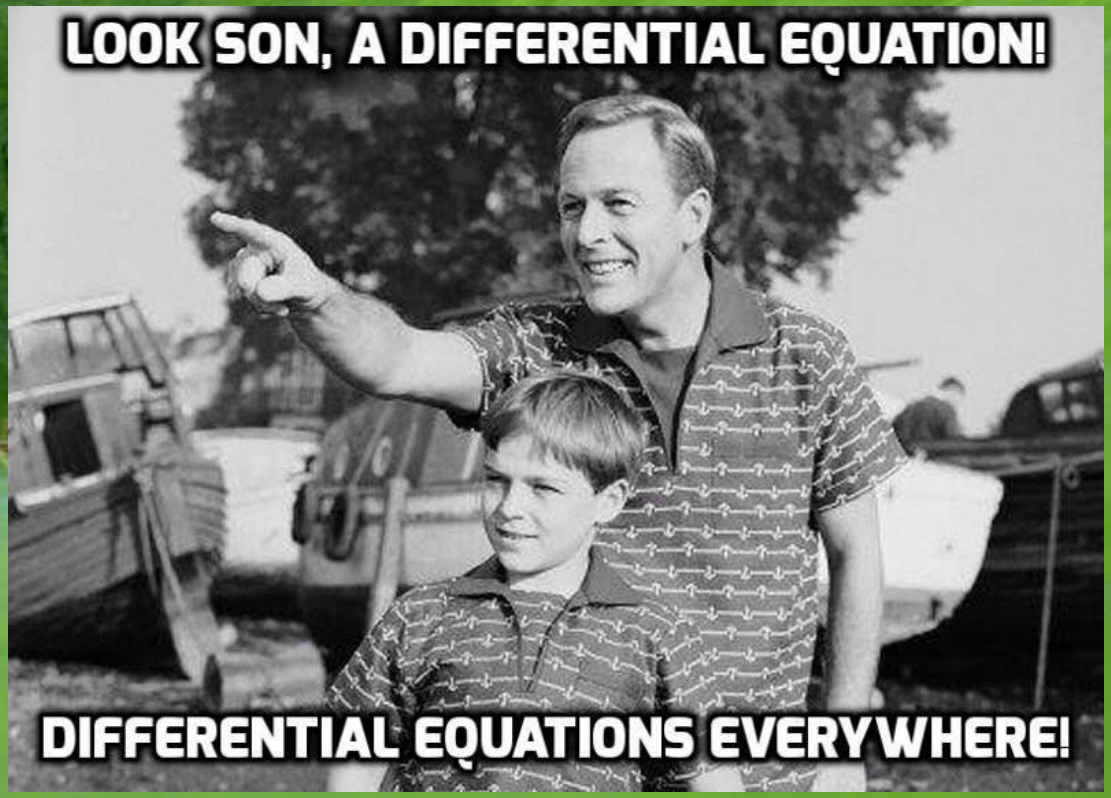


Faculty of Physics UW

Jacek.Szczytko@fuw.edu.pl

inżynieria nanostruktur

# Low dimensional structures

$$\psi_{k_x,k_y,n}(x,y,z) = \exp(ik_x x)\exp(ik_y y)\,u_n(z) = \psi_{\boldsymbol{k},n}(\boldsymbol{r},z) = \exp(i\boldsymbol{k}\cdot\boldsymbol{r})\,u_n(z)$$

$$E_n(k_x,k_y) = \varepsilon_n + \frac{\hbar^2 k_x^2}{2m} + \frac{\hbar^2 k_y^2}{2m} \qquad E_n(\boldsymbol{k}) = \varepsilon_n + \frac{\hbar^2 \boldsymbol{k}^2}{2m}$$

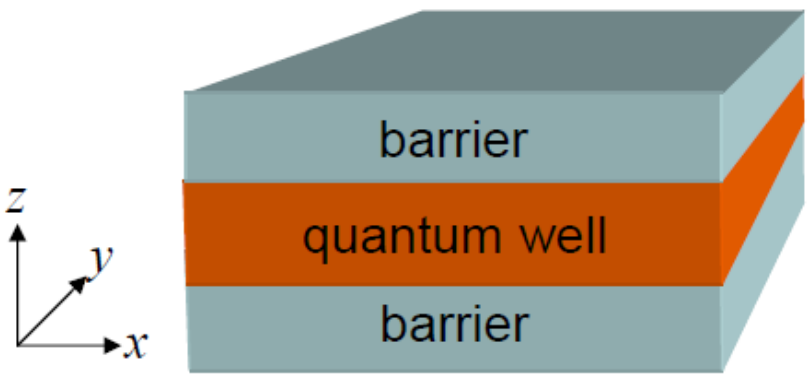


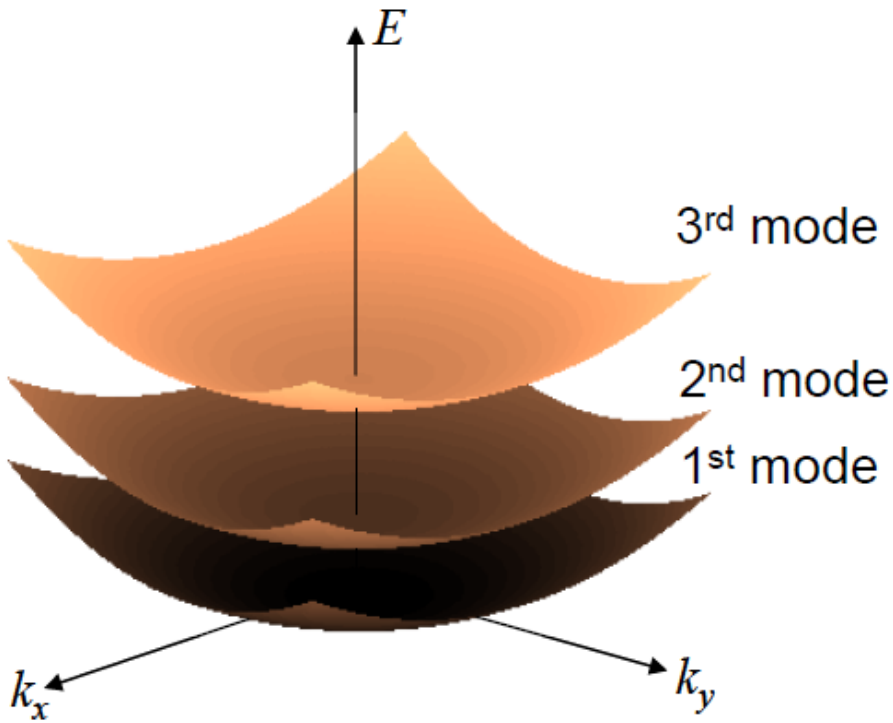


Marc Baldo MIT OpenCourseWare Publication May 2011

# Low dimensional structures

Full Hamiltonian in our universe has three spatial dimensions $(x, y, z, t) = (\vec{R}, t)$

$$\left[-\frac{\hbar^2}{2m}\nabla^2 + V(\vec{R})\right]\psi(\vec{R}) = E\psi(\vec{R})$$

For $V(\vec{R}) = V(z)$ we obtain:

$$\left[-\frac{\hbar^2}{2m}\left(\frac{\partial^2}{\partial x^2} + \frac{\partial^2}{\partial y^2} + \frac{\partial^2}{\partial z^2}\right) + V(z)\right]\psi(x, y, z) = E\psi(x, y, z)$$

Along directions $x$ and $y$ we have uniform motion (*ruch swobodny*):

$$\psi(x, y, z) = \exp(ik_x x)\exp(ik_y y)\, u(z)$$

We can show (on the blackboard!), that final eigenenergies of the potential $V(z)$ are:

$$\left[-\frac{\hbar^2}{2m}\frac{d^2}{dz^2} + V(z)\right]u(z) = \varepsilon u(z)$$

$$\varepsilon = E - \frac{\hbar^2 k_x^2}{2m} - \frac{\hbar^2 k_y^2}{2m}$$

131

# Low dimensional structures

$$\psi_{k_x,k_y,n}(x,y,z) = \exp(ik_x x)\exp(ik_y y)\,u_n(z) = \psi_{\boldsymbol{k},n}(\boldsymbol{r},z) = \exp(i\boldsymbol{k}\cdot\boldsymbol{r})\,u_n(z)$$

$$E_n(k_x,k_y) = \varepsilon_n + \frac{\hbar^2 k_x^2}{2m} + \frac{\hbar^2 k_y^2}{2m} \qquad E_n(\boldsymbol{k}) = \varepsilon_n + \frac{\hbar^2 \boldsymbol{k}^2}{2m}$$

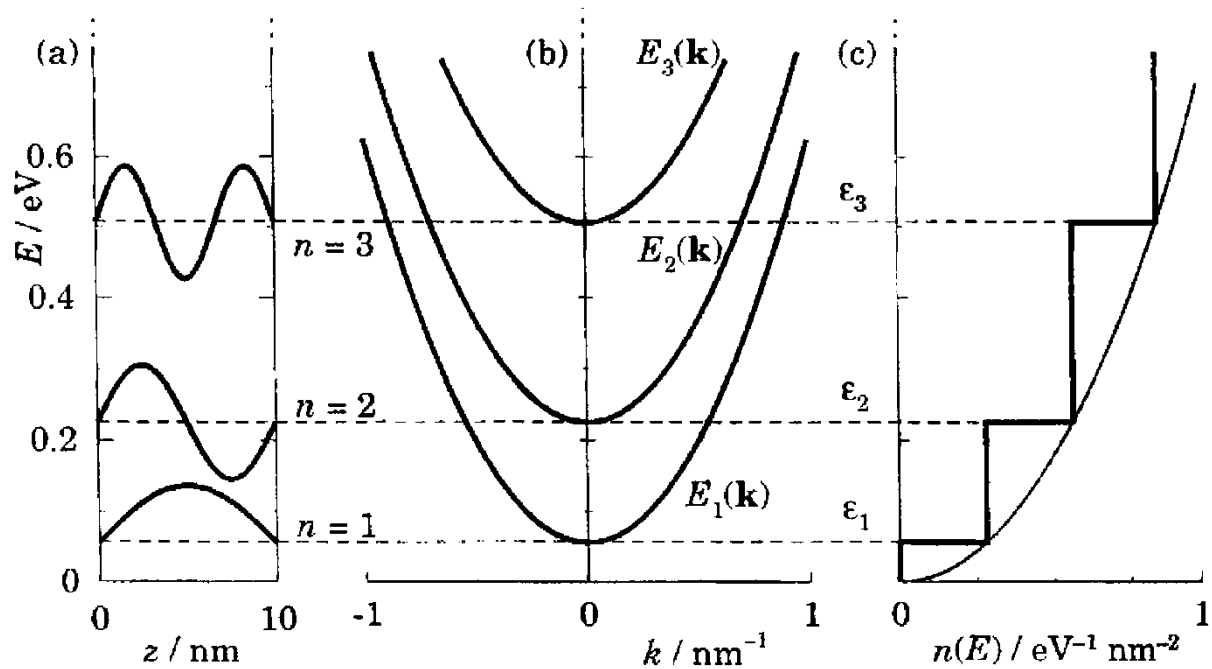


**FIGURE 4.7.** (a) Potential well with energy levels, (b) total energy including the transverse kinetic energy for each subband, and (c) steplike density of states of a quasi-two-dimensional system. The example is an infinitely deep square well in GaAs of width 10 nm. The thin curve in (c) is the parabolic density of states for unconfined three-dimensional electrons.

# Low dimensional structures

$$\psi_{k_x,k_y,n}(x,y,z) = \exp(ik_x x)\exp\left(ik_y y\right)u_n(z) = \psi_{\boldsymbol{k},n}(\boldsymbol{r},z) = \exp(i\boldsymbol{k}\cdot\boldsymbol{r})\,u_n(z)$$

$$E_n\left(k_x,k_y\right) = \varepsilon_n + \frac{\hbar^2 k_x^2}{2m} + \frac{\hbar^2 k_y^2}{2m} \qquad E_n(\boldsymbol{k}) = \varepsilon_n + \frac{\hbar^2 \boldsymbol{k}^2}{2m}$$

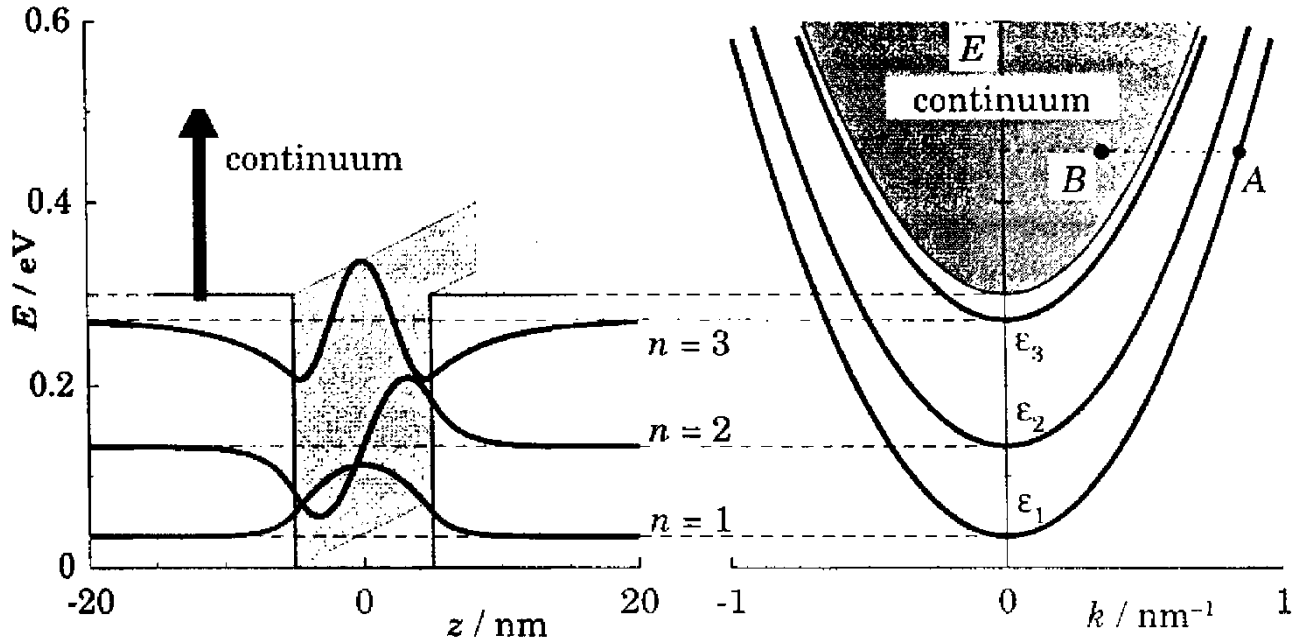


**FIGURE 4.9.** Quasi-two-dimensional system in a potential well of finite depth. Electrons with the same total energy can be bound in the well ($A$) or free ($B$).

# Low dimensional structures

Effective mass in the barrier $m_B$ and in the well $m_W$

$$\left[-\frac{\hbar^2}{2m_0\, m_{W,B}}\nabla^2 + V(\vec{R})\right]\psi(\vec{R}) = E\psi(\vec{R})$$

For separated wave functions: $\psi(\vec{R}) = \psi_{\boldsymbol{k},n}(\boldsymbol{r}, z) = \exp(i\boldsymbol{k}\cdot\boldsymbol{r})\, u_n(z)$

$$\left[-\frac{\hbar^2}{2m_0\, m_W}\nabla^2 + E_W\right]\psi(\vec{R}) = E\psi(\vec{R})$$

$$\left[-\frac{\hbar^2}{2m_0\, m_B}\nabla^2 + E_B\right]\psi(\vec{R}) = E\psi(\vec{R})$$

We got (on the blackboard!):

$$\left[-\frac{\hbar^2}{2m_0\, m_W}\frac{d^2}{dz^2} + \frac{\hbar^2\boldsymbol{k}^2}{2m_0\, m_W} + E_W\right]u_n(z) = \varepsilon u_n(z)$$

$$\left[-\frac{\hbar^2}{2m_0\, m_B}\frac{d^2}{dz^2} + \frac{\hbar^2\boldsymbol{k}^2}{2m_0\, m_B} + E_B\right]u_n(z) = \varepsilon u_n(z)$$

# Low dimensional structures

The particle moves in the well which potential depends on $\boldsymbol{k}$, in fact $k = |\boldsymbol{k}|$

$$\left[-\frac{\hbar^2}{2m_0\, m_W}\frac{d^2}{dz^2} + \frac{\hbar^2 \boldsymbol{k}^2}{2m_0\, m_W} + E_W\right] u_n(z) = \varepsilon u_n(z)$$

$$\left[-\frac{\hbar^2}{2m_0\, m_B}\frac{d^2}{dz^2} + \frac{\hbar^2 \boldsymbol{k}^2}{2m_0\, m_B} + E_B\right] u_n(z) = \varepsilon u_n(z)$$

$$V_0(k) = (E_B - E_W) + \frac{\hbar^2 k^2}{2m_0}\left(\frac{1}{m_B} - \frac{1}{m_W}\right)$$

The particle gains partially the effective mass of the barrier:

E.g. in GaAs-AlGaAs heterostructure $m_B > m_W$ thus the well gets „shallow"

$$E_n(k) = \varepsilon_n(k) + \frac{\hbar^2 k^2}{2m_0 m_W} \approx \varepsilon_n(k=0) + \frac{\hbar^2 k^2}{2m_0 m_{eff}}$$

energy of the bound state depends on $k$

$$m_{eff} \approx m_W P_W + m_B P_B$$

the probability of finding a particle

# Low dimensional structures

The particle moves in the well which potential depends on $\boldsymbol{k}$, in fact $k = |\boldsymbol{k}|$

$$\left[-\frac{\hbar^2}{2m_0\, m_W}\frac{d^2}{dz^2} + \frac{\hbar^2 \boldsymbol{k}^2}{2m_0\, m_W} + E_W\right] u_n(z) = \varepsilon u_n(z)$$

$$\left[-\frac{\hbar^2}{2m_0\, m_B}\frac{d^2}{dz^2} + \frac{\hbar^2 \boldsymbol{k}^2}{2m_0\, m_B} + E_B\right] u_n(z) = \varepsilon u_n(z)$$

$$V_0(k) = (E_B - E_W) + \frac{\hbar^2 k^2}{2m_0}\left(\frac{1}{m_B} - \frac{1}{m_W}\right)$$

E.g. in GaAs-AlGaAs heterostructure $m_B > m_W$ thus the well gets „shallow"

**TABLE 4.2** Dependence on transverse wave vector $\mathbf{k}_\perp$ of the energies of the states bound in a well 5 nm wide and 1 eV deep, with effective mass $m_W = 0.067$ inside the well and $m_B = 0.15$ outside.

| $k$ (nm$^{-1}$) | $\frac{\hbar^2 k^2}{2m_0 m_W}$ (eV) | $\frac{\hbar^2 k^2}{2m_0 m_B}$ (eV) | $V_0(k)$ (eV) | $\varepsilon_1$ (eV) | $\varepsilon_2$ (eV) | $\varepsilon_3$ (eV) | $m_{eff}$ |
|---|---|---|---|---|---|---|---|
| 0.0 | 0.000 | 0.000 | 1.000 | 0.108 | 0.446 | 0.969 | 0.067 |
| 0.5 | 0.142 | 0.064 | 0.921 | 0.106 | 0.435 | 0.919 | 0.069 |
| 1.0 | 0.570 | 0.254 | 0.685 | 0.096 | 0.397 | — | 0.076 |

# Optical transitions

$$\varepsilon_{e,n_e} = E_c^{GaAs} + \frac{\hbar^2\pi^2 n_e^2}{2m_0 m_e a^2}$$

$$\varepsilon_{h,n_h} = E_v^{GaAs} - \frac{\hbar^2\pi^2 n_h^2}{2m_0 m_h a^2}$$

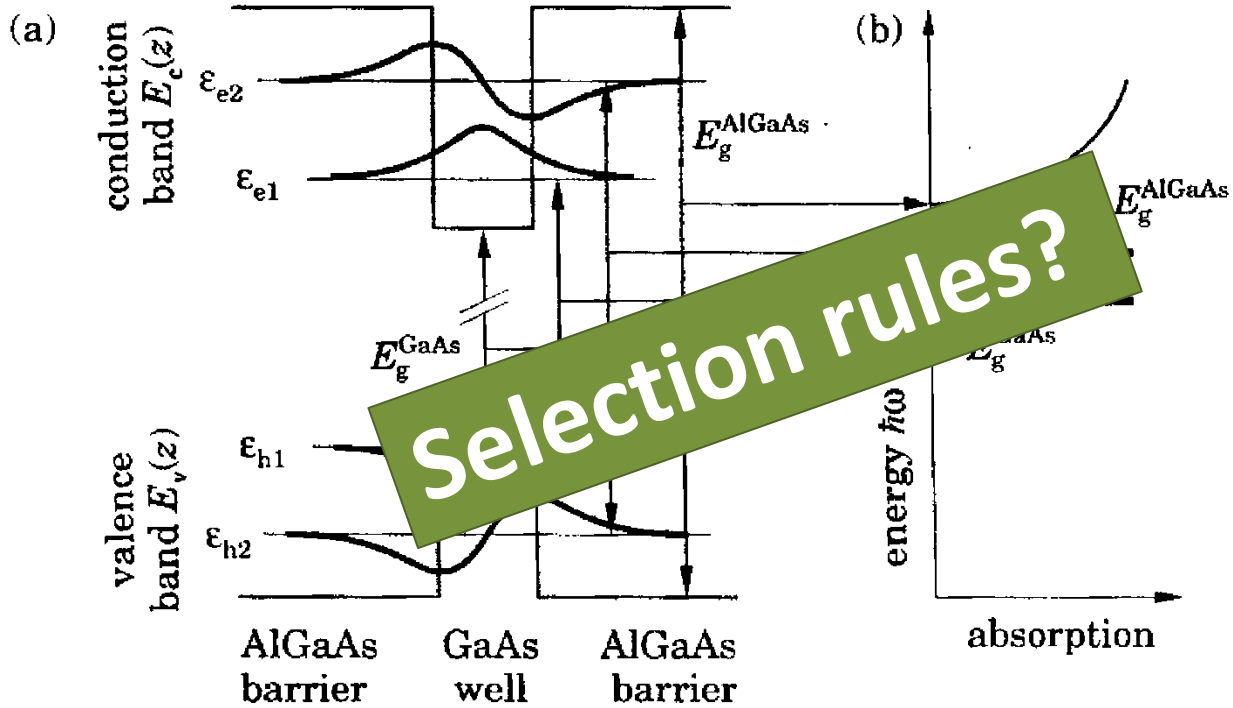


$$\hbar\omega_n = \varepsilon_{e,n_e} - \varepsilon_{h,n_h} = E_g^{GaAs} + \frac{\hbar^2\pi^2 n^2}{2m_0 a^2}\left(\frac{1}{m_e} + \frac{1}{m_h}\right) = E_g^{GaAs} + \frac{\hbar^2\pi^2 n^2}{2m_0 m_{eh} a^2}$$

Optical effective mass $\frac{1}{m_{eh}} = \frac{1}{m_e} + \frac{1}{m_h}$

# Quantum wire

$$\psi_{k_x,m,n}(x,y,z) = u_{m,n}(x,y)\exp(ik_z z) = \text{albo np.} = u_{n,l}(r,\theta)\exp(ik_z z)$$

$$E_n(k_x,k_y) = \varepsilon_{m,n} + \frac{\hbar^2 k_z^2}{2m}$$

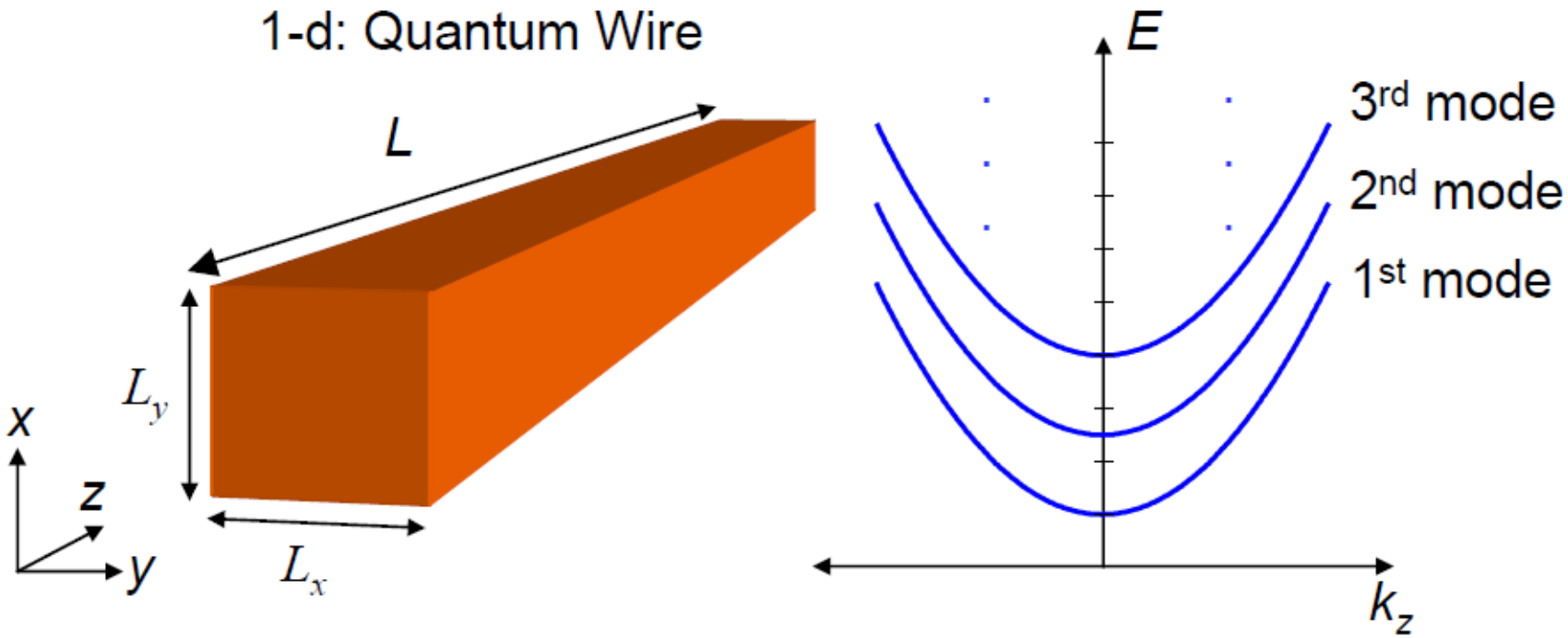


Marc Baldo MIT OpenCourseWare Publication May 2011

# Quantum wire

$$\psi_{k_x,m,n}(x,y,z) = u_{m,n}(x,y)\exp(ik_z z) = \text{albo np.} = u_{n,l}(r,\theta)\exp(ik_z z)$$

$$E_n(k_x,k_y) = \varepsilon_{m,n} + \frac{\hbar^2 k_z^2}{2m}$$

Square quantum well 2D $L_x L_y$, infinite potential:

$$\psi_{k_x,m,n}(x,y,z) = u_{m,n}(x,y)\exp(ik_z z) = \exp(ik_m x)\exp(ik_n y)\exp(ik_z z)$$

With boundary conditions $L_x k_m = n_x \pi$ and $L_y k_n = n_y \pi$ (dicrete spectrum)

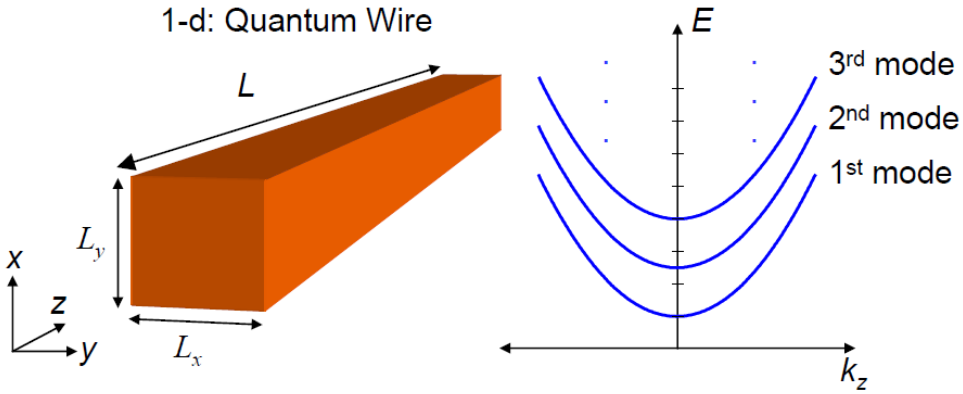


Marc Baldo MIT OpenCourseWare Publication May 2011

# Quantum wire

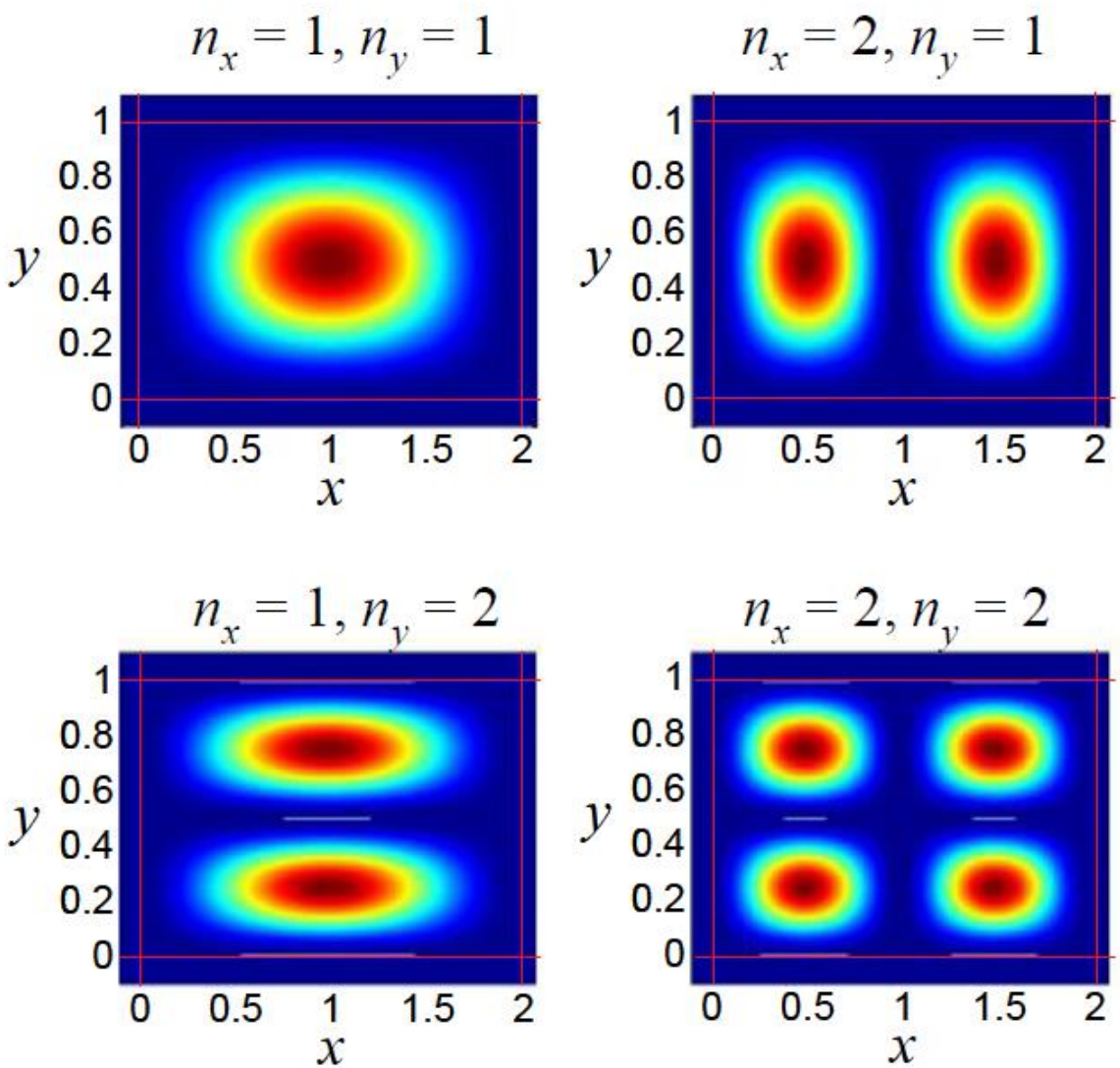


**Fig. 2.13.** The first four modes of the quantum wire. Since in this example, $L_x > L_y$ the $n_x = 2$, $n_y = 1$ mode has lower energy than the $n_x = 1$, $n_y = 2$ mode.

# Quantum wire

Rectangular wire $(a \times b)$ – solutions like:

$$\varepsilon_{n_x,n_y} = \frac{\hbar^2\pi^2}{2m}\left(\frac{n_x^2}{L_x^2} + \frac{n_y^2}{L_y^2}\right)$$

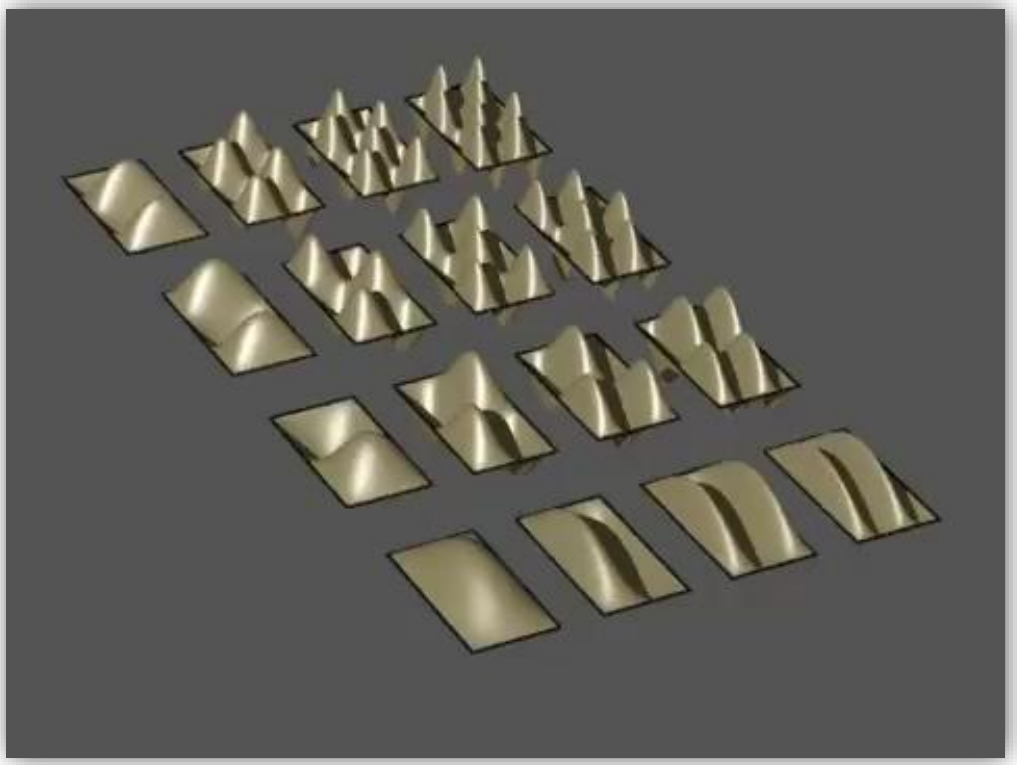

http://wn.com/2d_and_3d_standing_wave

# Quantum wells 2D and 3D

Rectangular wire $(a \times b)$ – solutions like:

$$\varepsilon_{n_x,n_y} = \frac{\hbar^2\pi^2}{2m}\left(\frac{n_x^2}{a^2} + \frac{n_y^2}{b^2}\right)$$

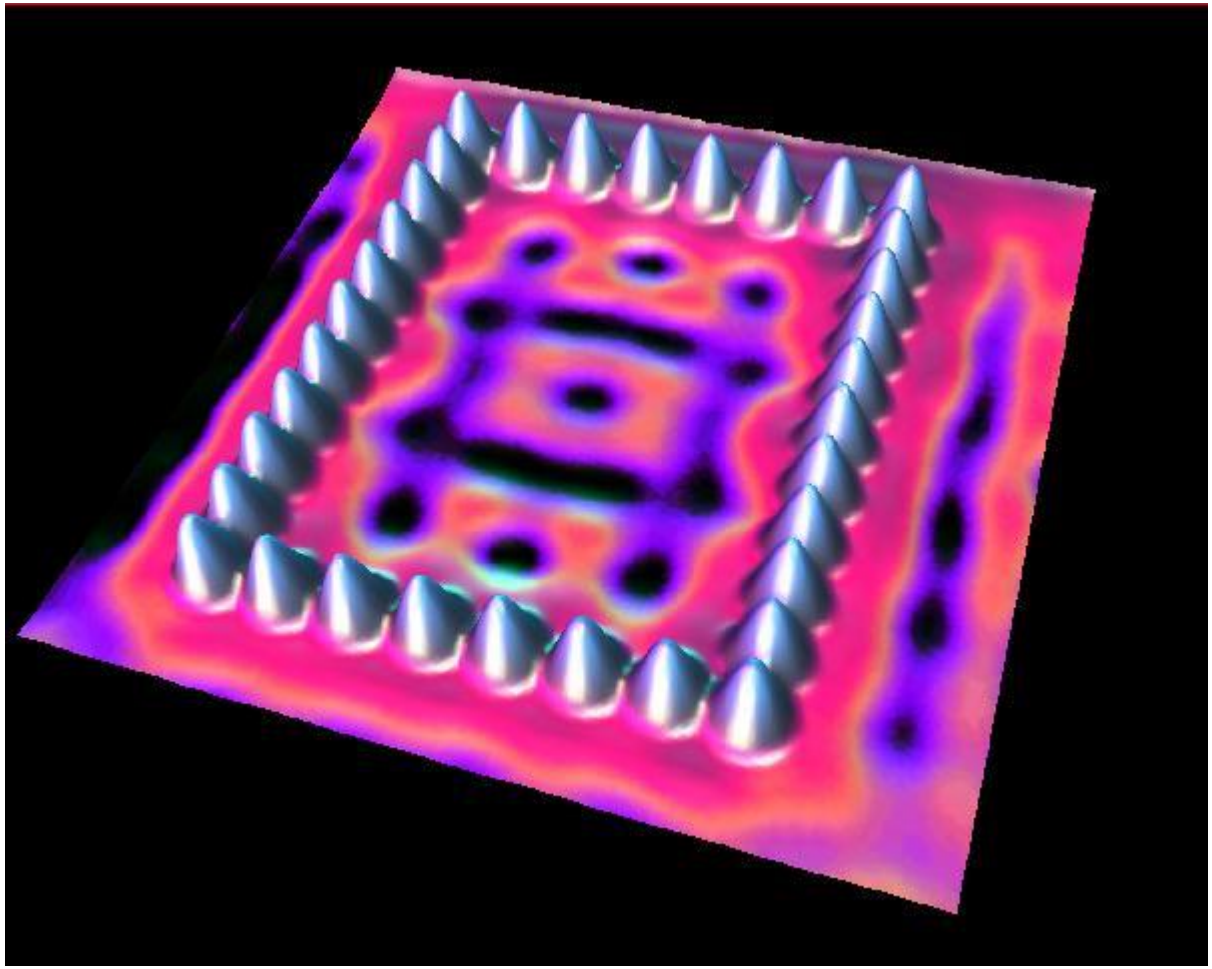

http://www.almaden.ibm.com/vis/stm/images/stm14.jpg

# Quantum wells 2D and 3D

Cylindrical well (with infinite walls)

$$-\frac{\hbar^2}{2m}\left(\frac{\partial^2}{\partial r^2}+\frac{1}{r}\frac{\partial}{\partial r}+\frac{1}{r^2}\frac{\partial^2}{\partial\theta^2}+V_0\right)\psi(r,\theta)=E\psi(r,\theta)$$

$$\psi(r,\theta)=u(r)\exp(il\theta)$$

the depth of the potential depends on $l^2$

$$\left[-\frac{\hbar^2}{2m}\left(\frac{\partial^2}{\partial r^2}+\frac{1}{r}\frac{\partial}{\partial r}\right)+\frac{\hbar^2 l^2}{2mr^2}+V_0\right]u(r)=Eu(r)$$

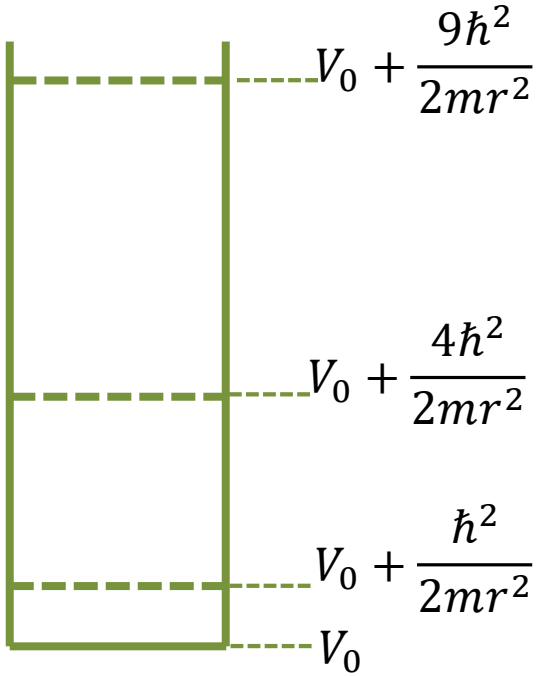


What gives solutions in the form Bessel functions

$$r^2\frac{d^2u}{dr^2}+r\frac{du}{dr}+[(kr)^2-l^2]u=0$$

$$J_l(kr)\sim\sqrt{\frac{2}{\pi kr}}\cos\left(kr-\frac{1}{2}l\pi-\frac{1}{4}\pi\right)$$

$$k=\sqrt{2m(E-V_0)}/\hbar$$

$$\phi_{nl}(r)\propto J_l\left(\frac{j_{l,n}r}{a}\right)\exp(il\theta)$$

$$\varepsilon_{nl}=\frac{\hbar^2 j_{l,n}^2}{2ma}$$

Zeros of the Besseel function are $j_{l,n}$

# Quantum wells 2D and 3D

Cylindrical well

low temperature scanning tunneling microscope (STM)

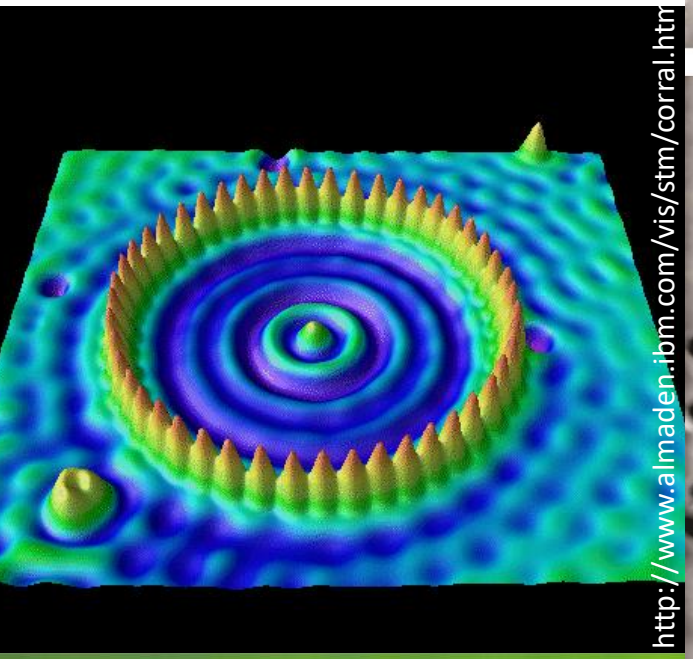

http://www.almaden.ibm.com/vis/stm/corral.html#stm16

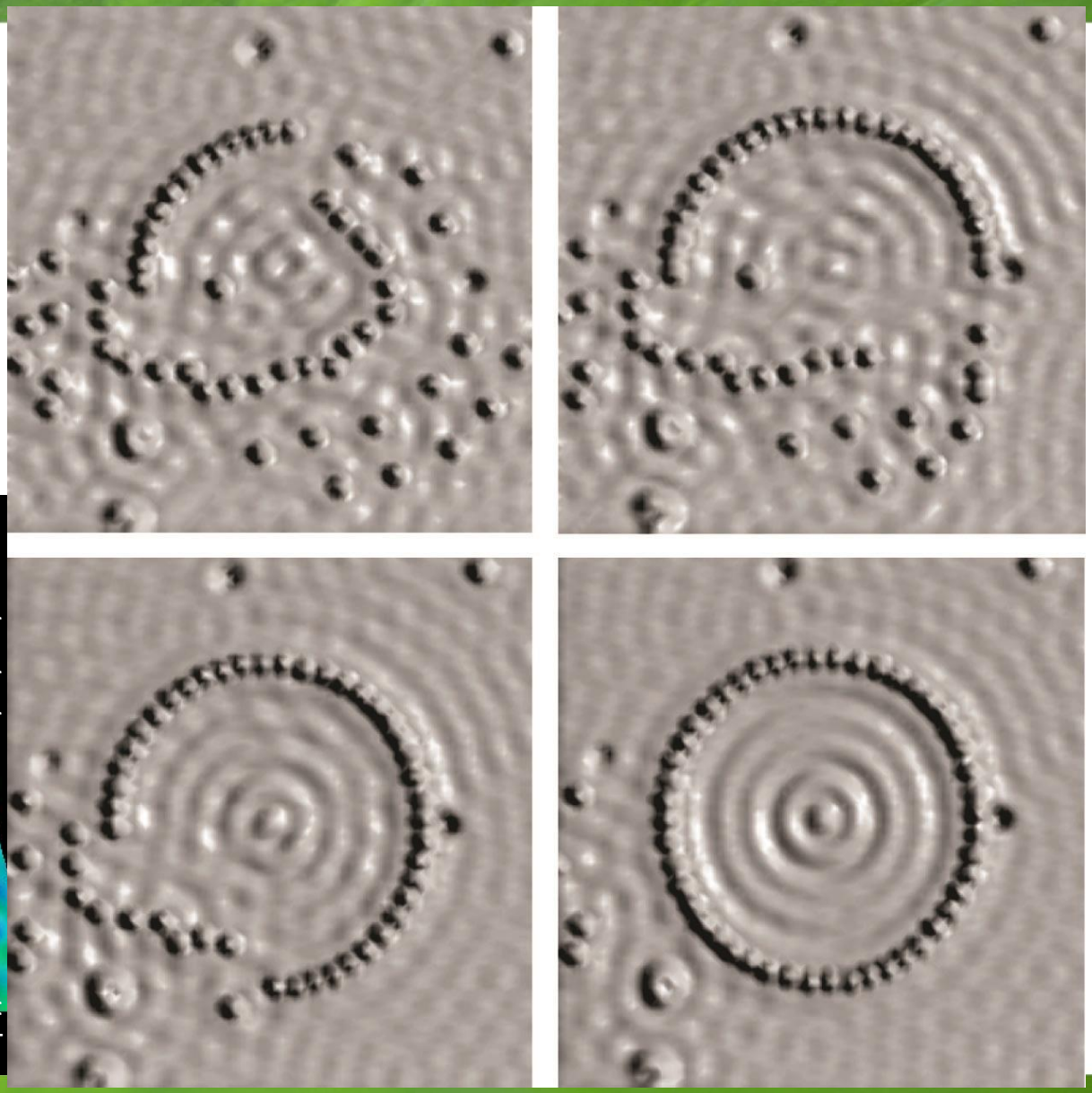

# Quantum wells 2D and 3D

Cylindrical well

low temperature scanning tunneling microscope (STM)

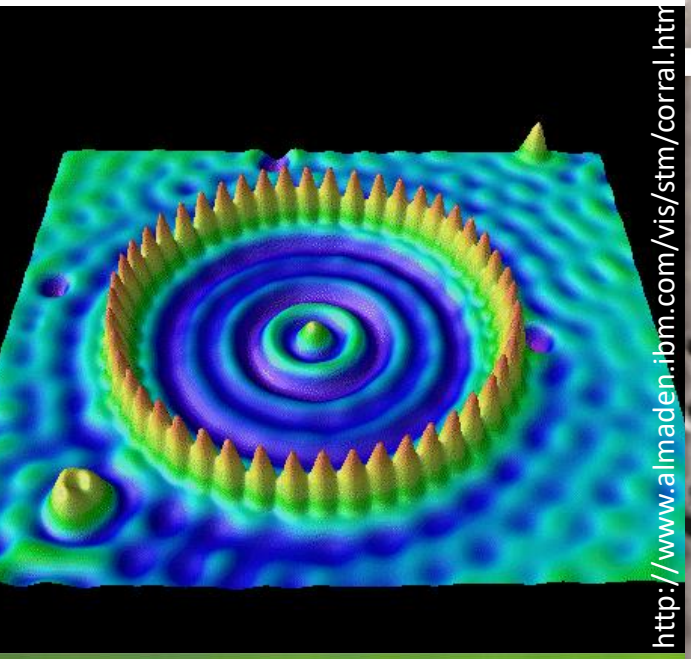

http://www.almaden.ibm.com/vis/stm/corral.html#stm16

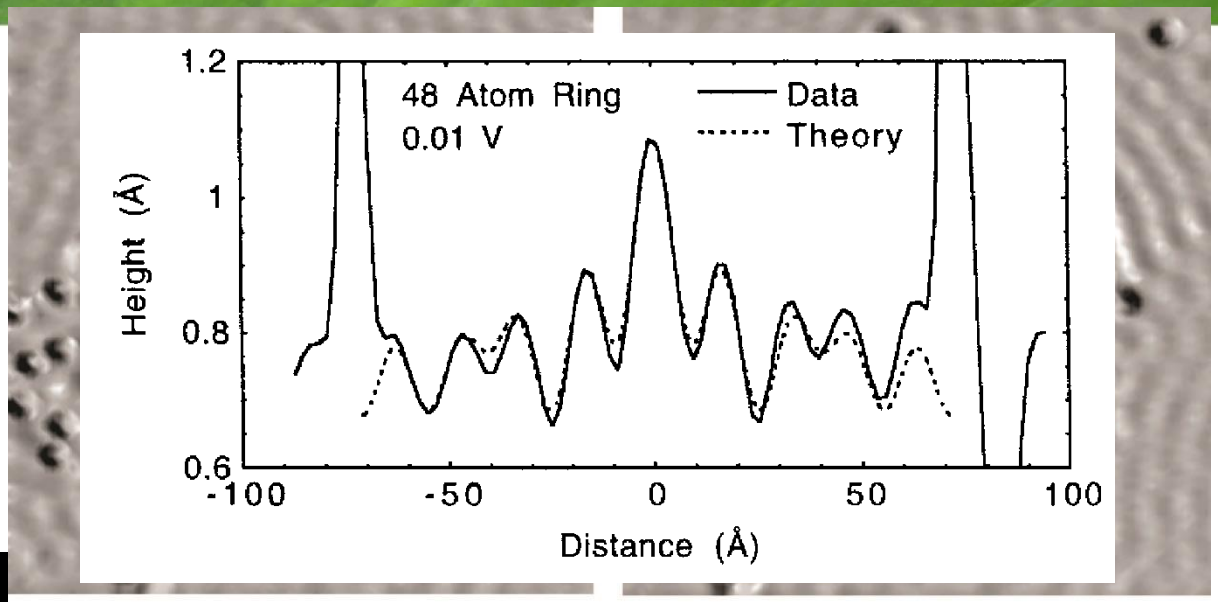


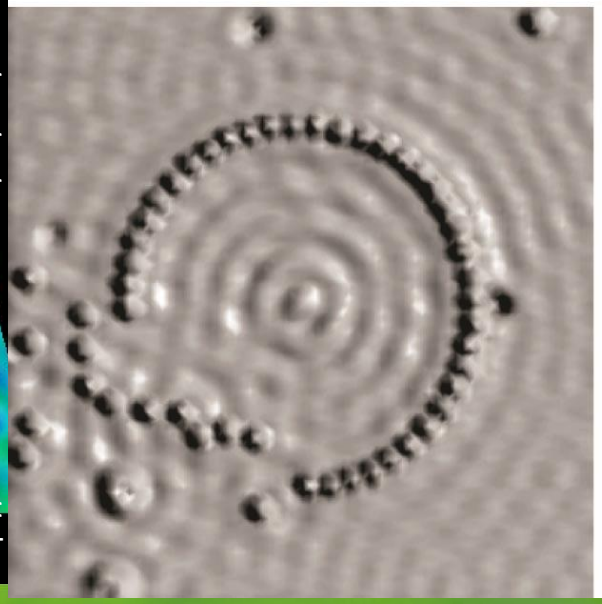

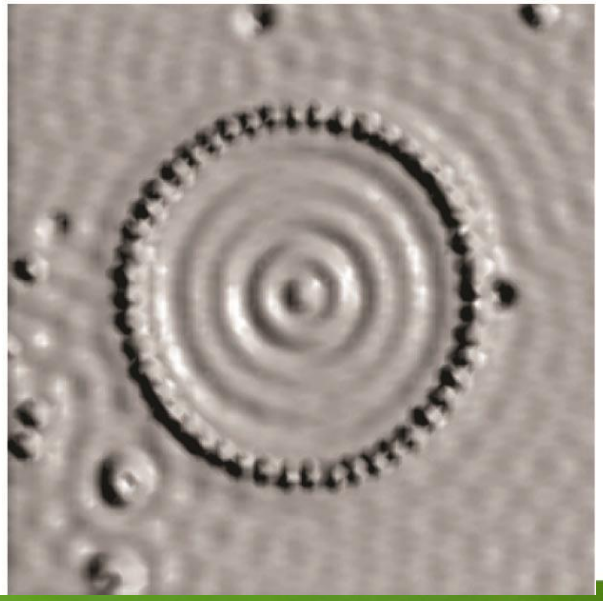

# Quantum wells 2D and 3D

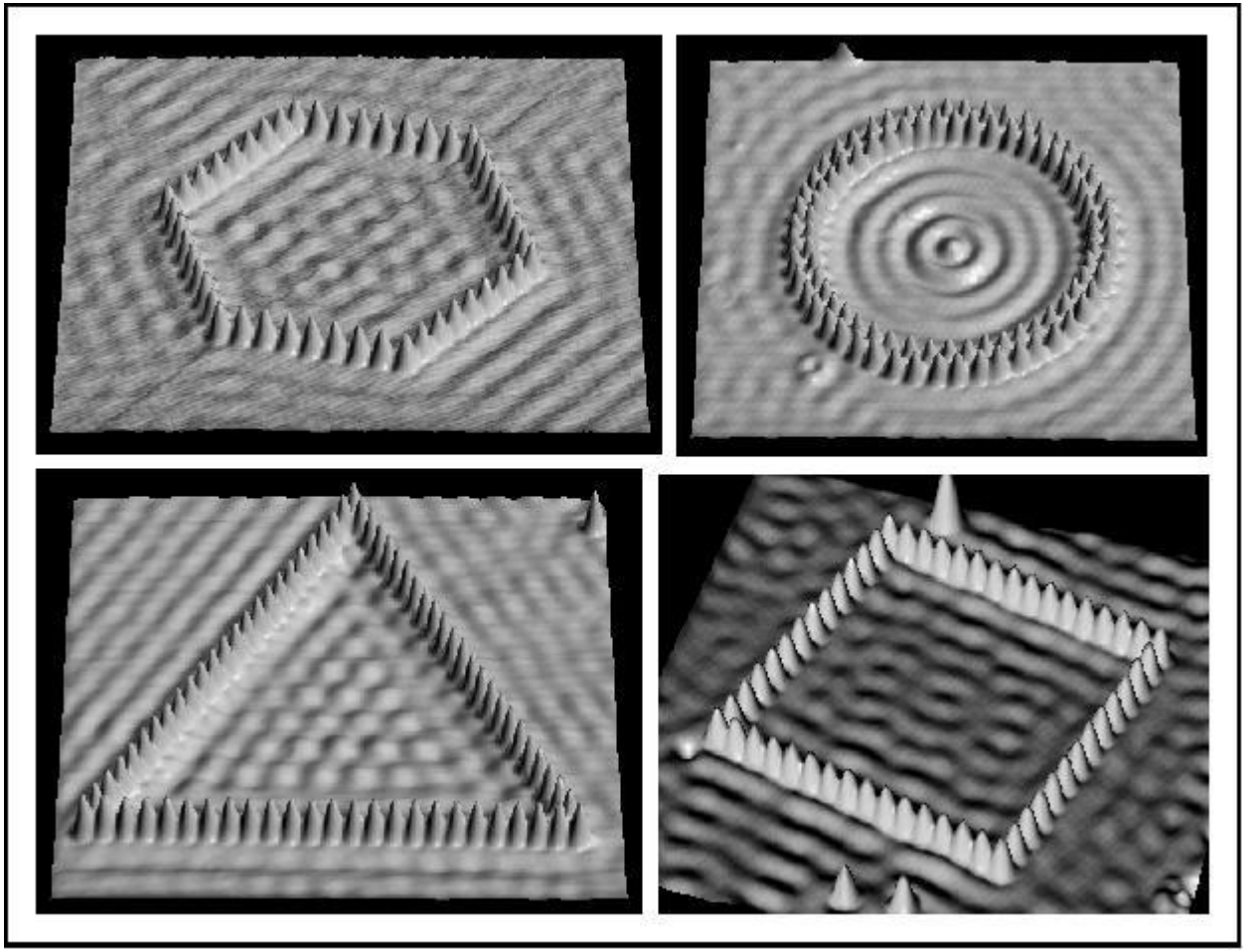

http://www.almaden.ibm.com/vis/stm/images/stm17.jpg

TUTAJ 2017.03.20

# Quantum wires

**Figure 8** The trend of the reduction of semiconductor laser threshold

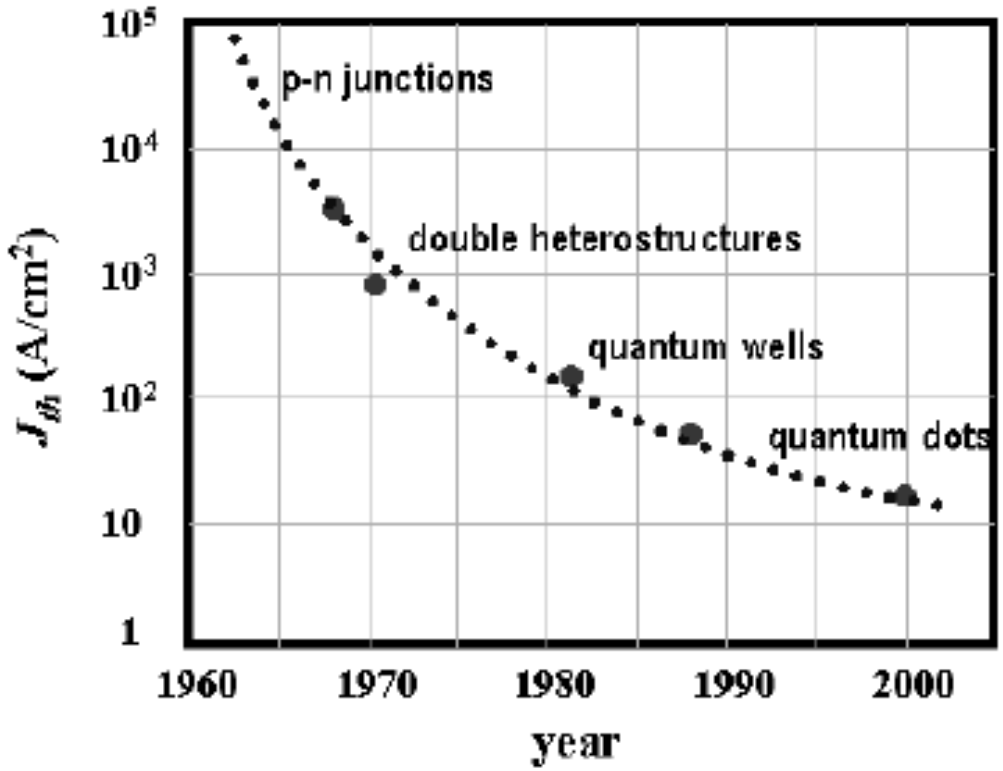

# Quantum wires

PHYSICAL REVIEW B VOLUME 52, NUMBER 15 15 OCTOBER 1995-I

**Dimensionality effects on strain and quantum confinement in lattice-mismatched $InAs_xP_{1-x}$/InP quantum wires**

M. Notomi*
*NTT Opto-electronics Laboratories, 3-1 Morinosato-Wakamiya, Atsugi, Kanagawa 243-01, Japan*

J. Hammersberg and H. Weman
*Department of Physics and Measurement Technology, Linköping University, S-581 83 Linköping, Sweden*

S. Nojima, H. Sugiura, M. Okamoto, and T. Tamamura
*NTT Opto-electronics Laboratories, 3-1 Morinosato-Wakamiya, Atugi, Kan*

M. Potemski
*Grenoble High Magnetic Field Laboratory, Max-Planck Institute für Fe*
*and Centre National de la Recherche Scientifique, 38042 Grenob*
(Received 29 March 1995)

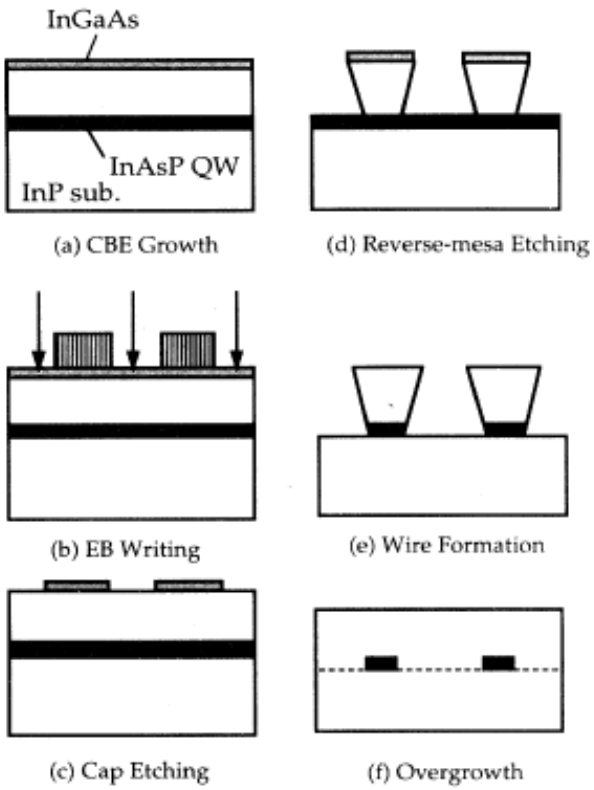


FIG. 1. Fabrication process of strained InAsP/InP quantum wires.

# Quantum wires

42 Int. J. of Nanotechnology, Vol. 1, Nos. 1/2, 2004

**Nanolasers: Lasing from nanoscale quantum wires**

Samuel S. Mao

**Figure 9** Quantum wire fabrication based on nanoscale etching and re-growth

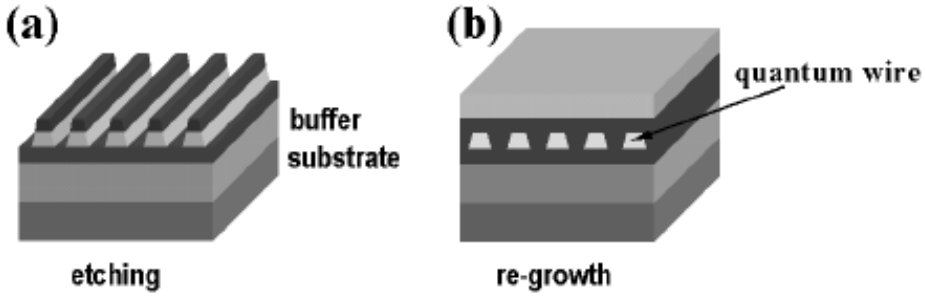


**Figure 10** Formation of one-dimensional nanoscale quantum wires by strain-induced lateral ordering

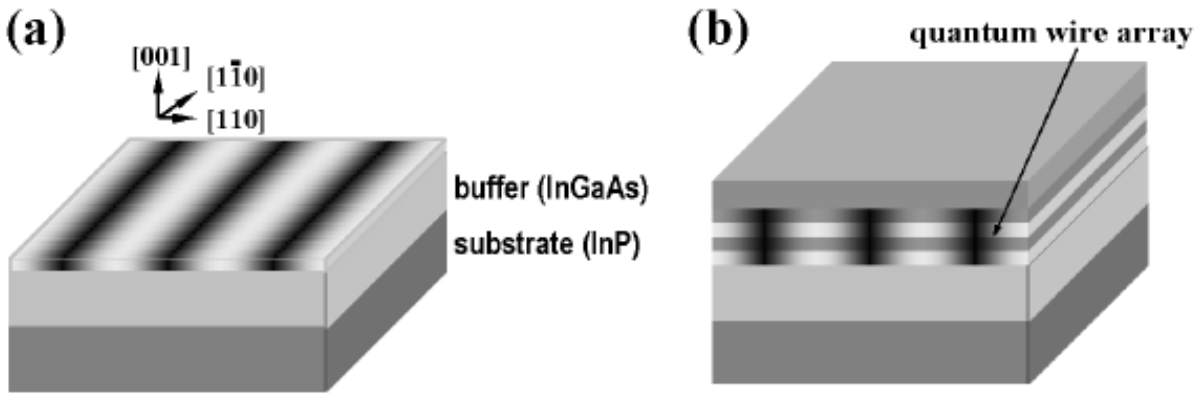

# Quantum wires

42 Int. J. of Nanotechnology, Vol. 1, Nos. 1/2, 2004

**Nanolasers: Lasing from nanoscale quantum wires**

Samuel S. Mao

**Figure 11** Growth of quantum wires on a vicinal surface with multiatomic steps

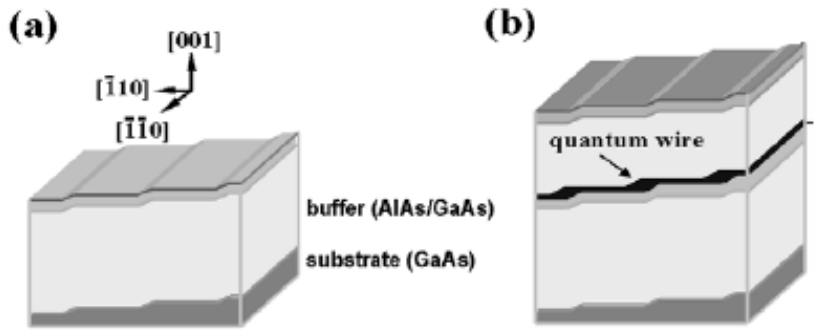


**Figure 12** Selective growth of quantum wires on a pre-patterned V-groove substrate

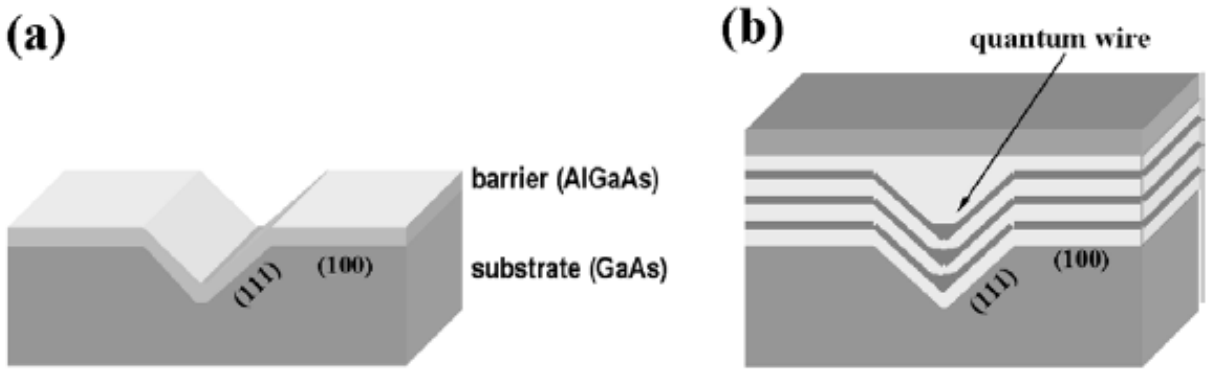

# Quantum wires

42 Int. J. of Nanotechnology, Vol. 1, Nos. 1/2, 2004

**Nanolasers: Lasing from nanoscale quantum wires**

Samuel S. Mao

**Figure 13** Selective growth of quantum wires on a pre-patterned Λ-ridge substrate

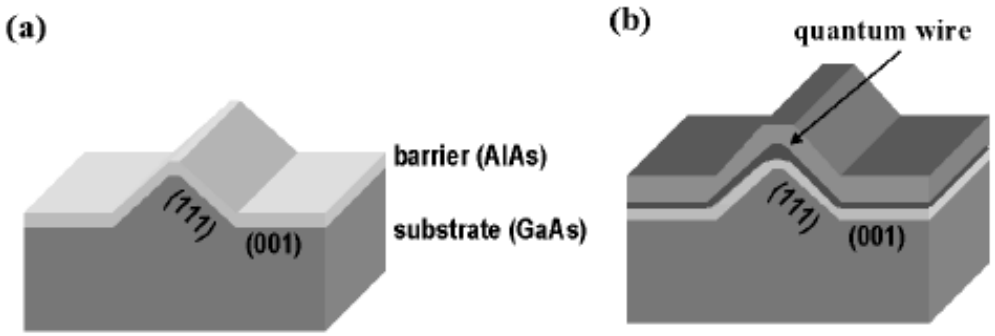


**Figure 14** Formation of one-dimensional T-intersection quantum wire structure by cleaved-edge overgrowth

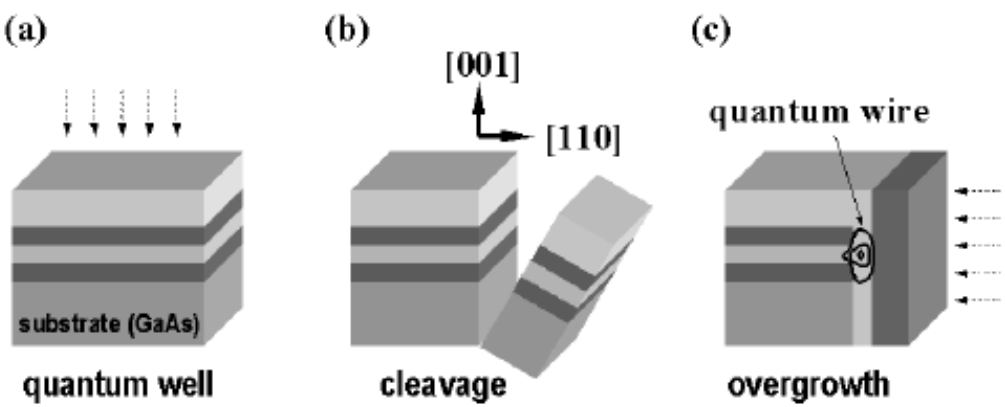

# Quantum wires

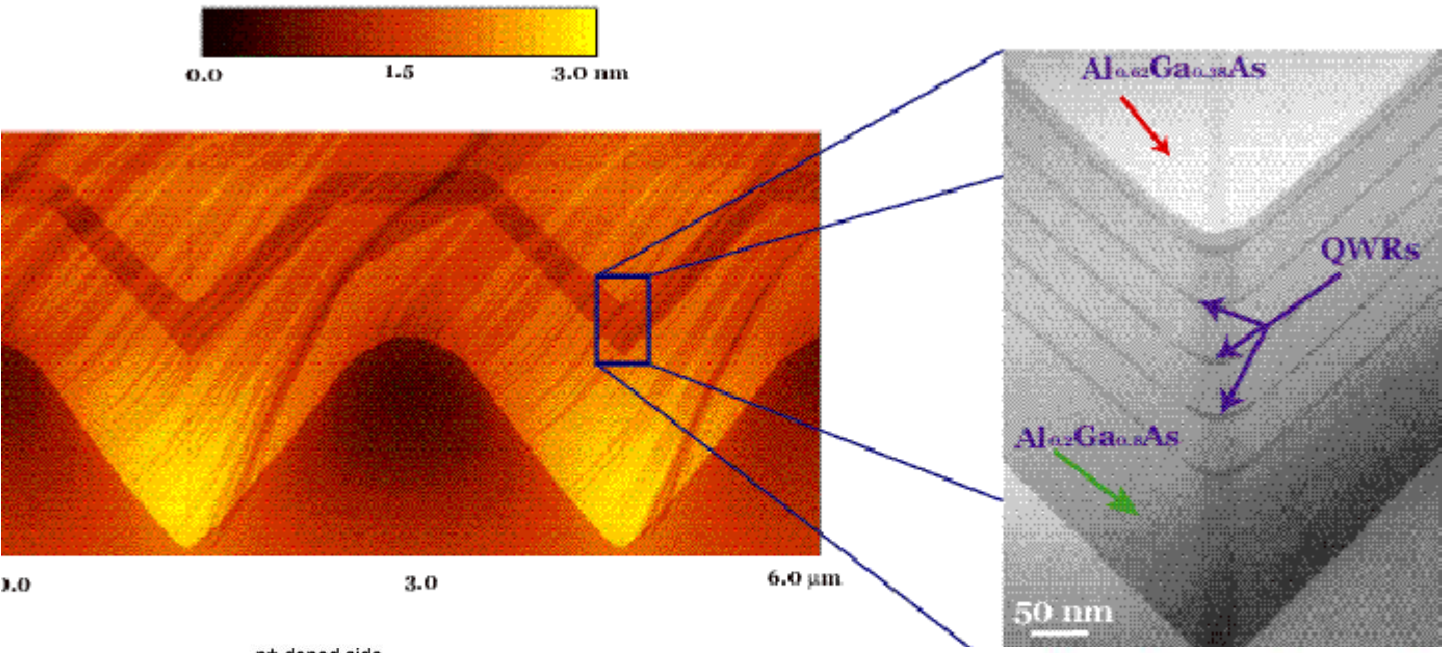


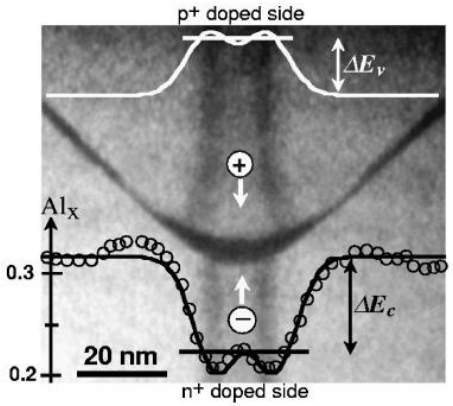


FIG. 1. TEM cross section of the V-groove QWR LED schematically showing the vertical electron and hole injection via the self-ordered VQW. Measured Al composition (open circles) and calculated conduction- (solid black curve) and valence-band potential (solid white curve) of the triple-branch VQW, is shown as a function of lateral distance.

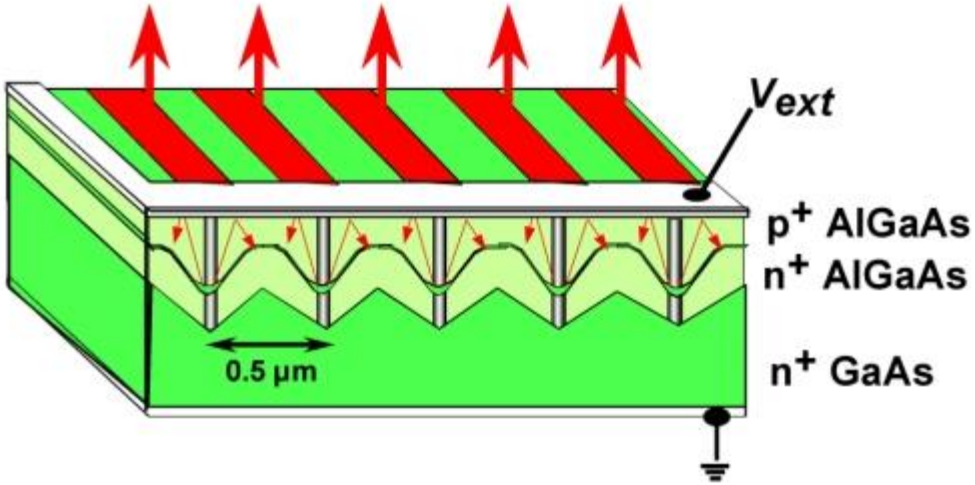

# Quantum wires

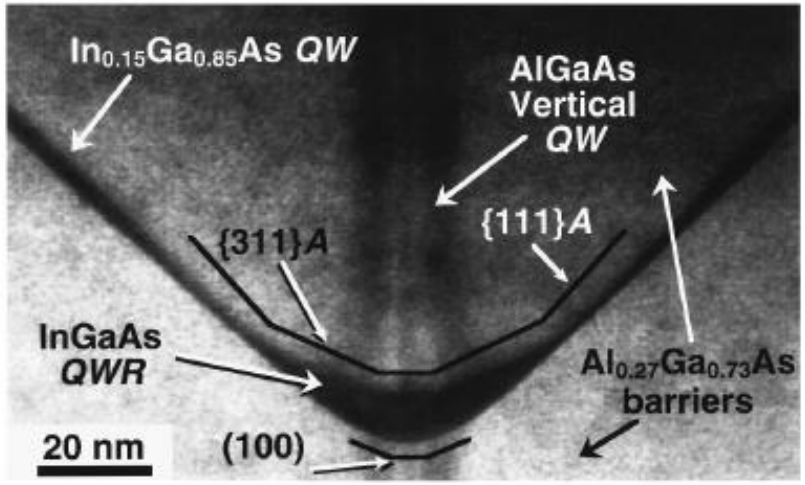


FIG. 1. Dark field TEM micrograph showing a cross-sectional view of an $In_yGa_{1-y}As/Al_xGa_{1-x}As$ QWR (sample $In_{0.15}$).

APPLIED PHYSICS LETTERS VOLUME 72, NUMBER 6 9 FEBRUARY 1998

**Self-ordering and confinement in strained InGaAs/AlGaAs V-groove quantum wires grown by low-pressure organometallic chemical vapor deposition**

E. Martinet,[a] F. Reinhardt,[b] A. Gustafsson,[c] G. Biasiol, and E. Kapon
*Department of Physics, Swiss Federal Institute of Technology (EPFL), 1015 Lausanne, Switzerland*

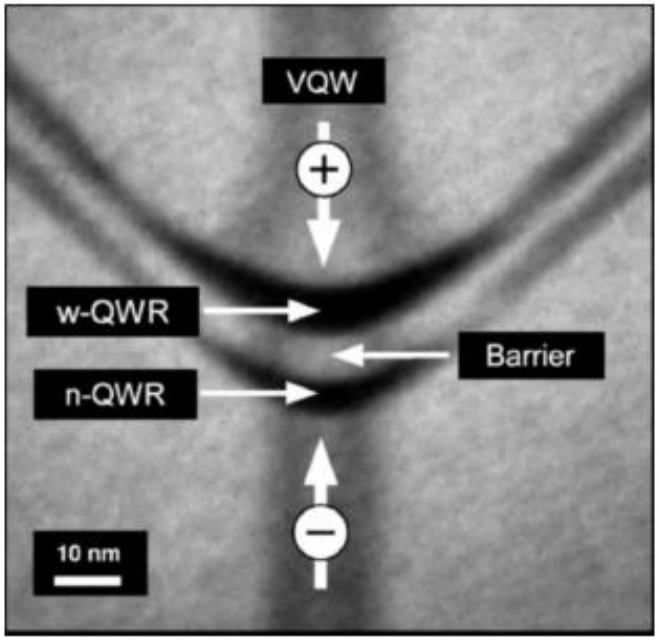


FIG. 1. Cross-sectional TEM micrograph of the QWR region in sample A with a schematic illustration of the electron and hole injection via the VQW's.

# Quantum wires

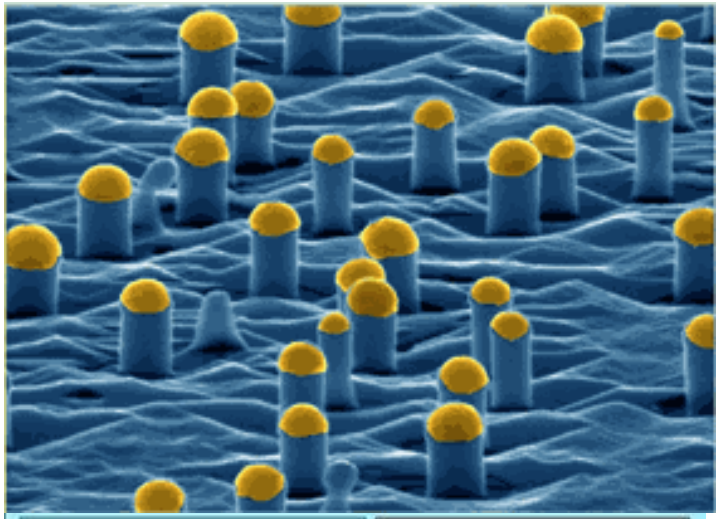

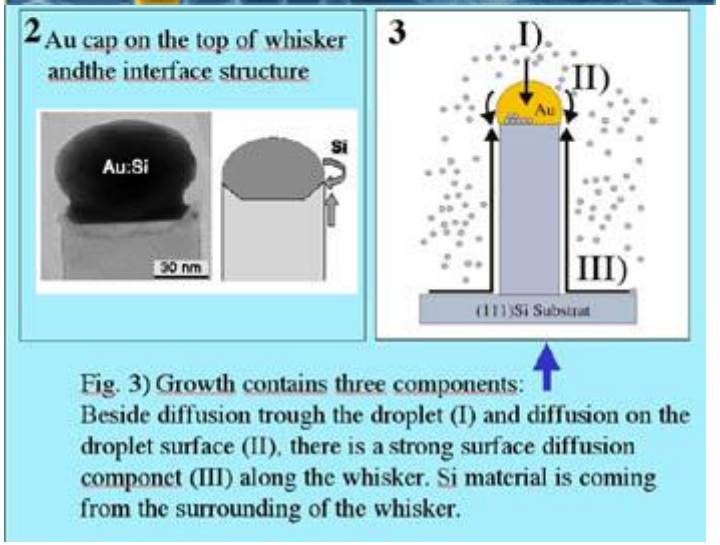


http://www.mpi-halle.mpg.de/~mbe/

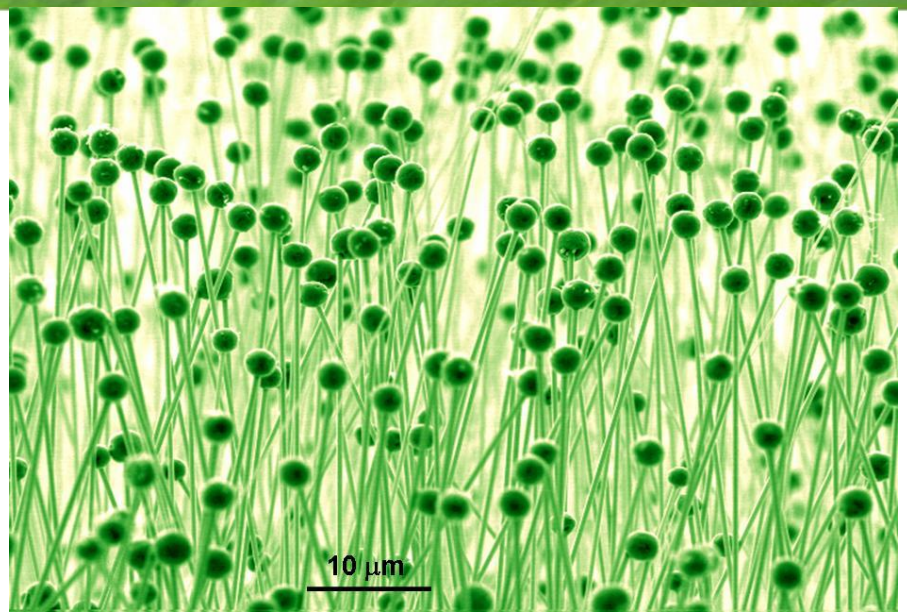


www.ece.odu.edu/g_seminar.htm

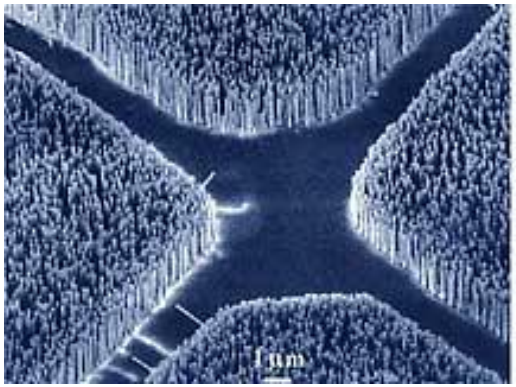


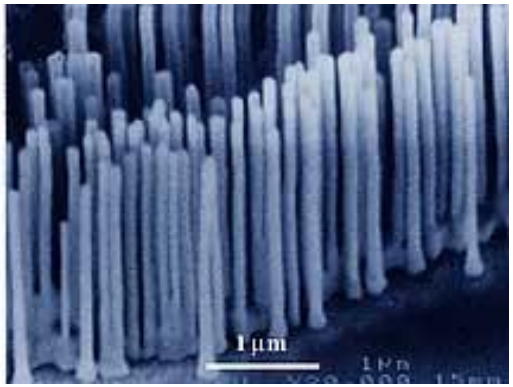


Photo by Peidong Yang/UC Berkeley, courtesy of *Science*

# Quantum wires

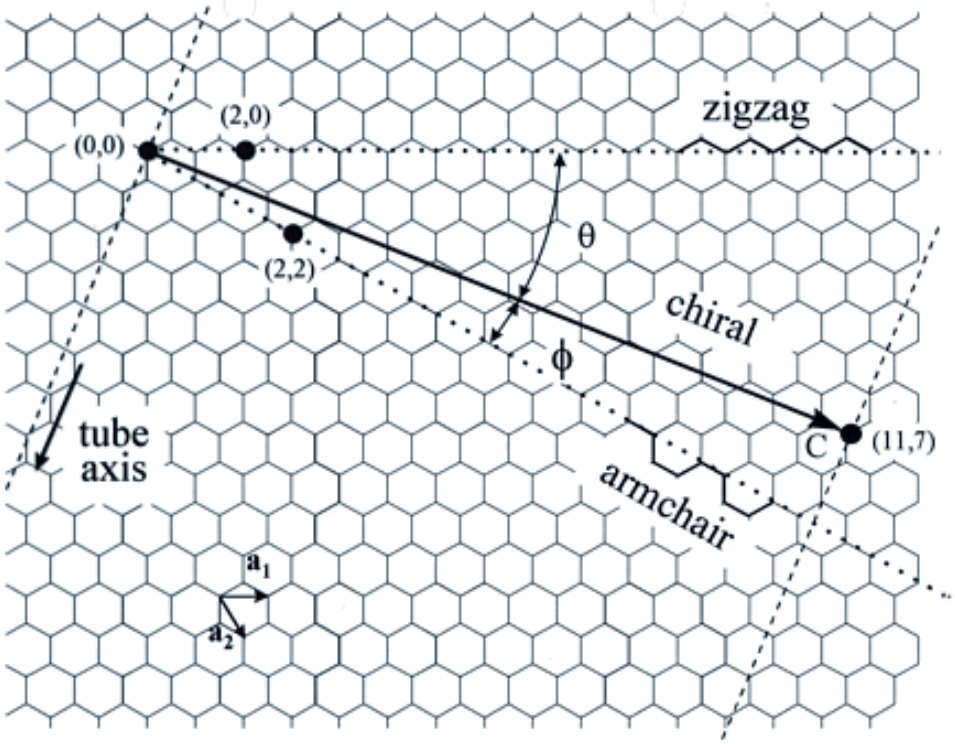


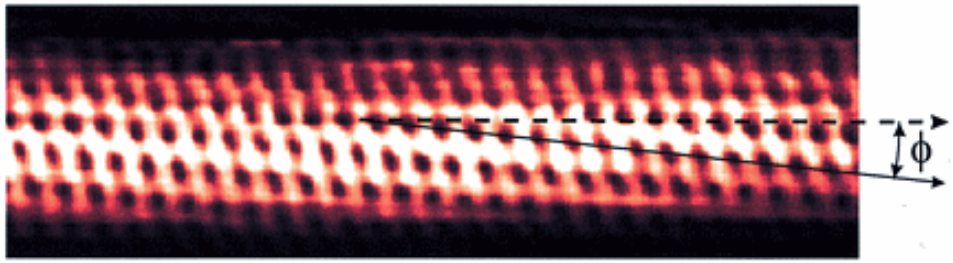


Cees Dekker

TU Delft
Technische Universiteit Delft

DIMES
Delft Institute of Microelectronics and Submicrontechnology

# Quantum wires

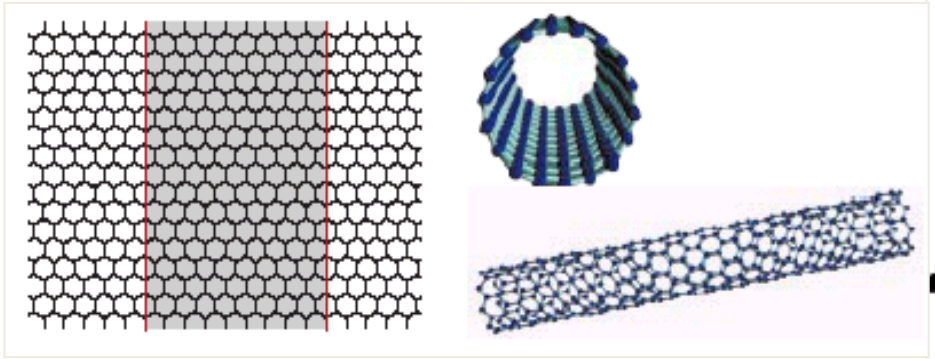

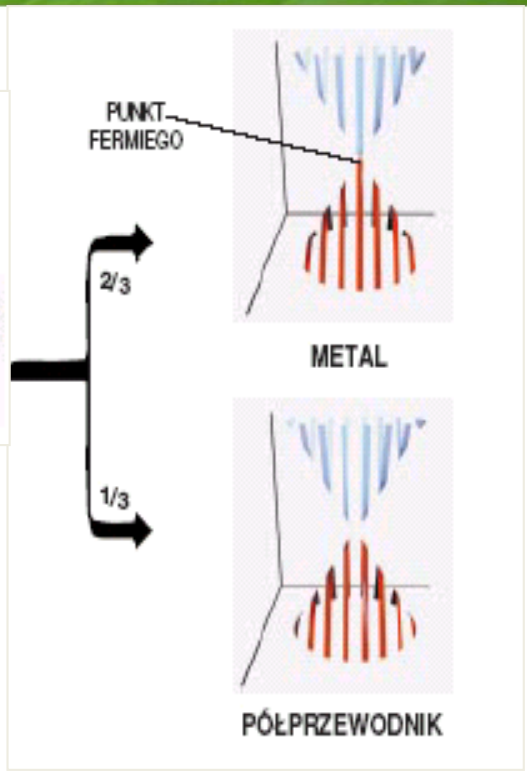


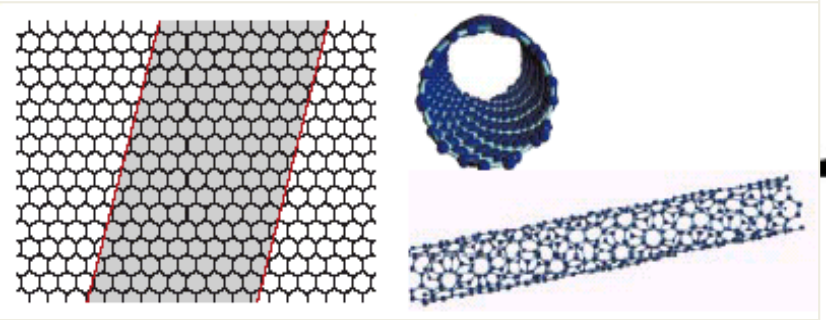

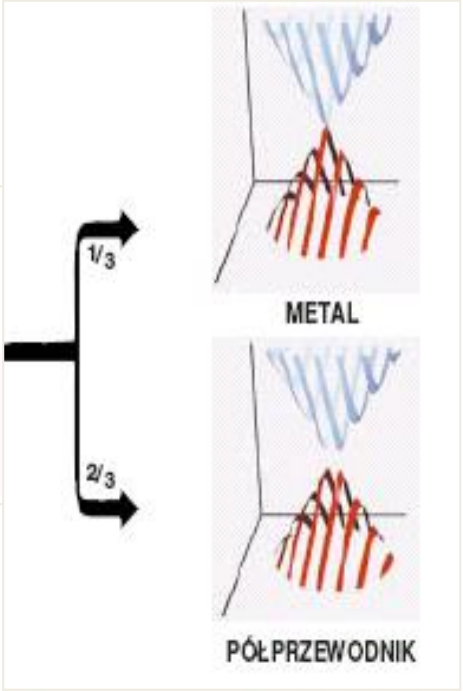


Collins P. G., Avouris P., Świat Nauki 2, 40, 2001

## AFM manipulation of single-wall carbon nanotubes on $SiO_2$

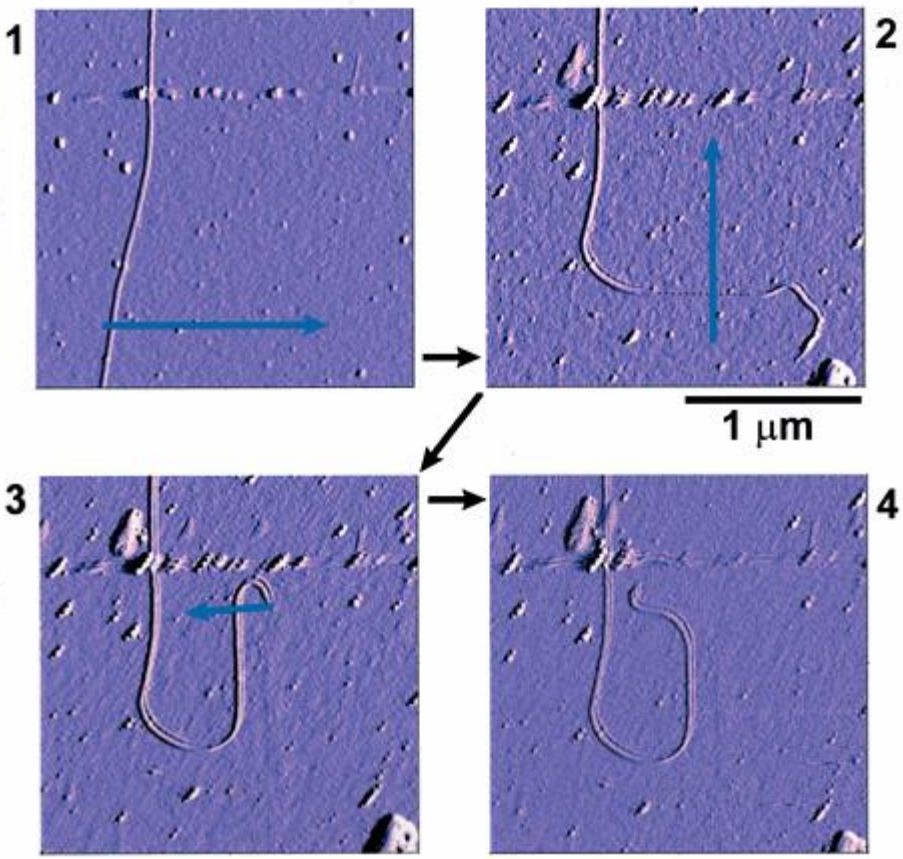


## Main method of deposition: spin coating of suspension of tubes

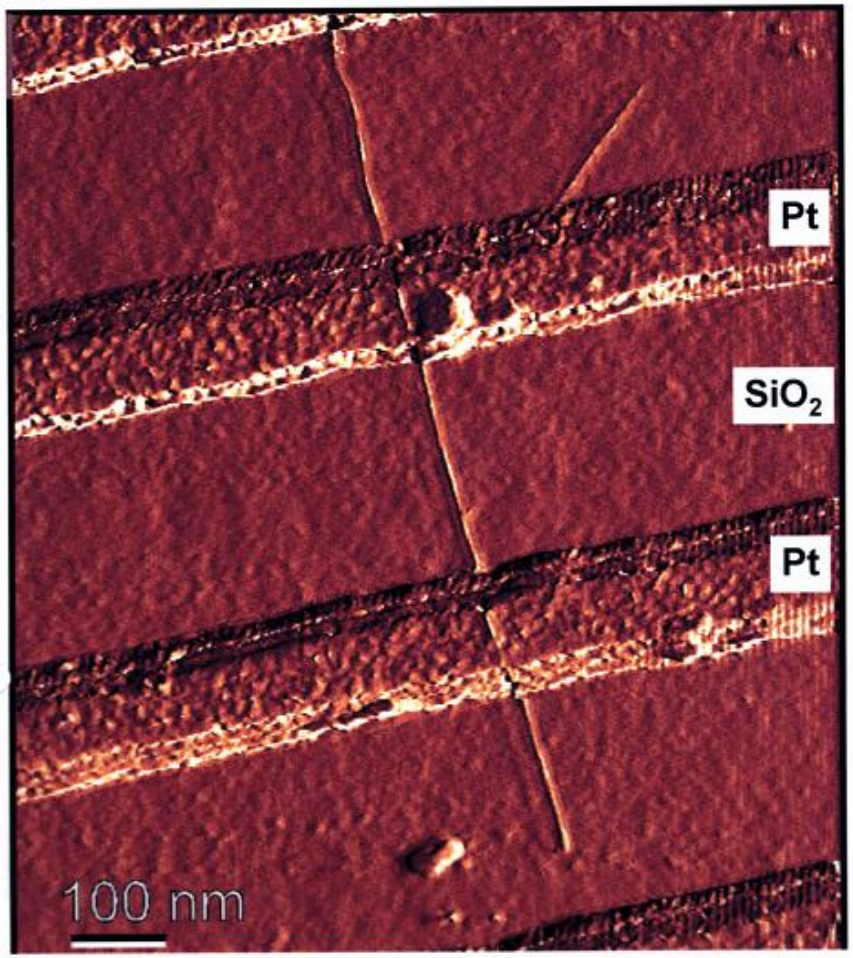


**Results in individual tubes on electrodes !**

http://online.itp.ucsb.edu/online/qhall_c98/dekker/oh/07.html

# Nano –manipulation of CNT

## STM nanostructuring: Cutting nanotubes

before cut:

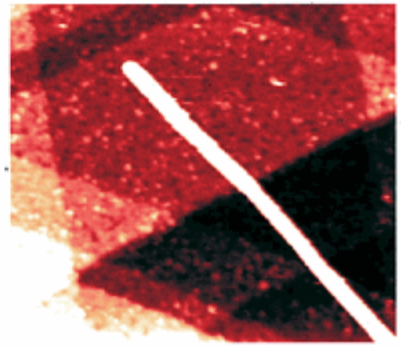

cutting occurs upon applying voltage pulse to the STM tip

after cut:

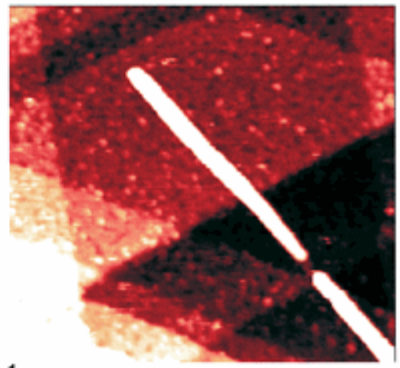

STM I-V curves show quantum size effects after cutting:

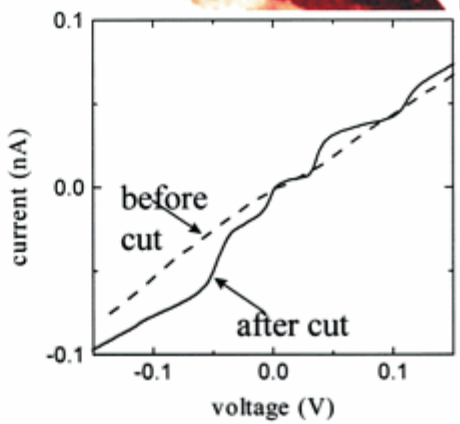


Venema, Wildoer, Tommirinde Tenasen, Dekker, Rinzler, Smalley
APL 71, 2629 ('97)

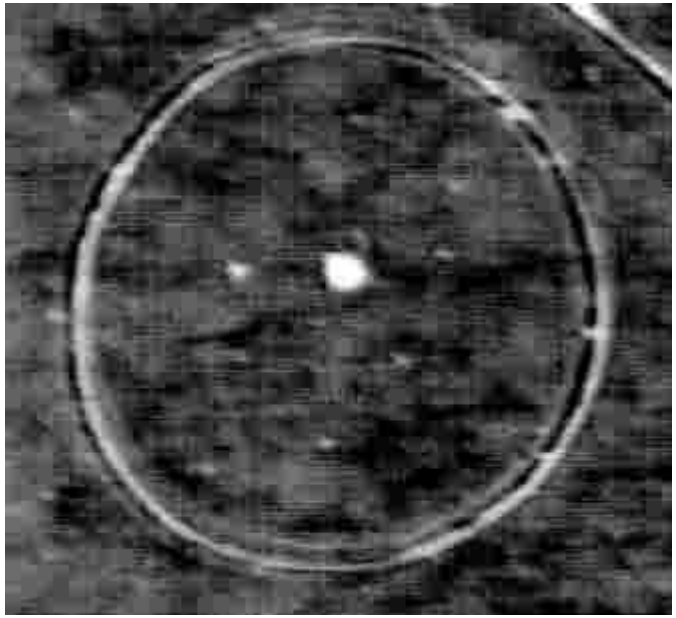

Cees Dekker, dekker@qt.tn.tudelft.nl

# Manipulation of CNT

nature materials | VOL 4 | JULY 2005 | www.nature.com/naturematerials

LETTERS

## Multifunctional brushes made from carbon nanotubes

ANYUAN CAO[1], VINOD P. VEEDU[2], XUESONG LI[1], ZHAOLING YAO[1], MEHRDAD N. GHASEMI-NEJHAD[2] AND PULICKEL M. AJAYAN[1]*

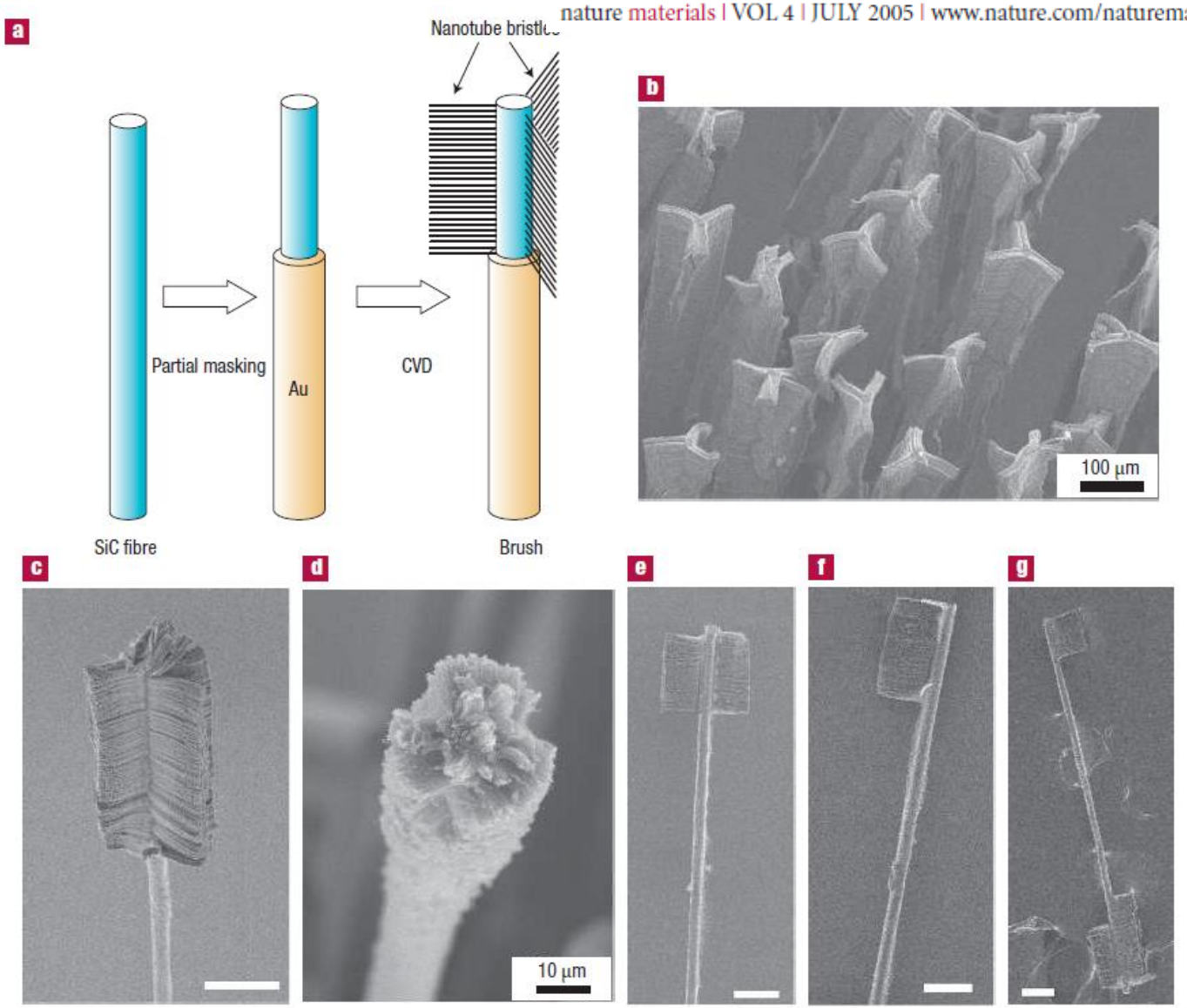

# Manipulation of CNT

nature materials | VOL 4 | JULY 2005 | www.nature.com/naturematerials

LETTERS

## Multifunctional brushes made from carbon nanotubes

ANYUAN CAO[1], VINOD P. VEEDU[2], XUESONG LI[1], ZHAOLING YAO[1], MEHRDAD N. GHASEMI-NEJHAD[2] AND PULICKEL M. AJAYAN[1]*

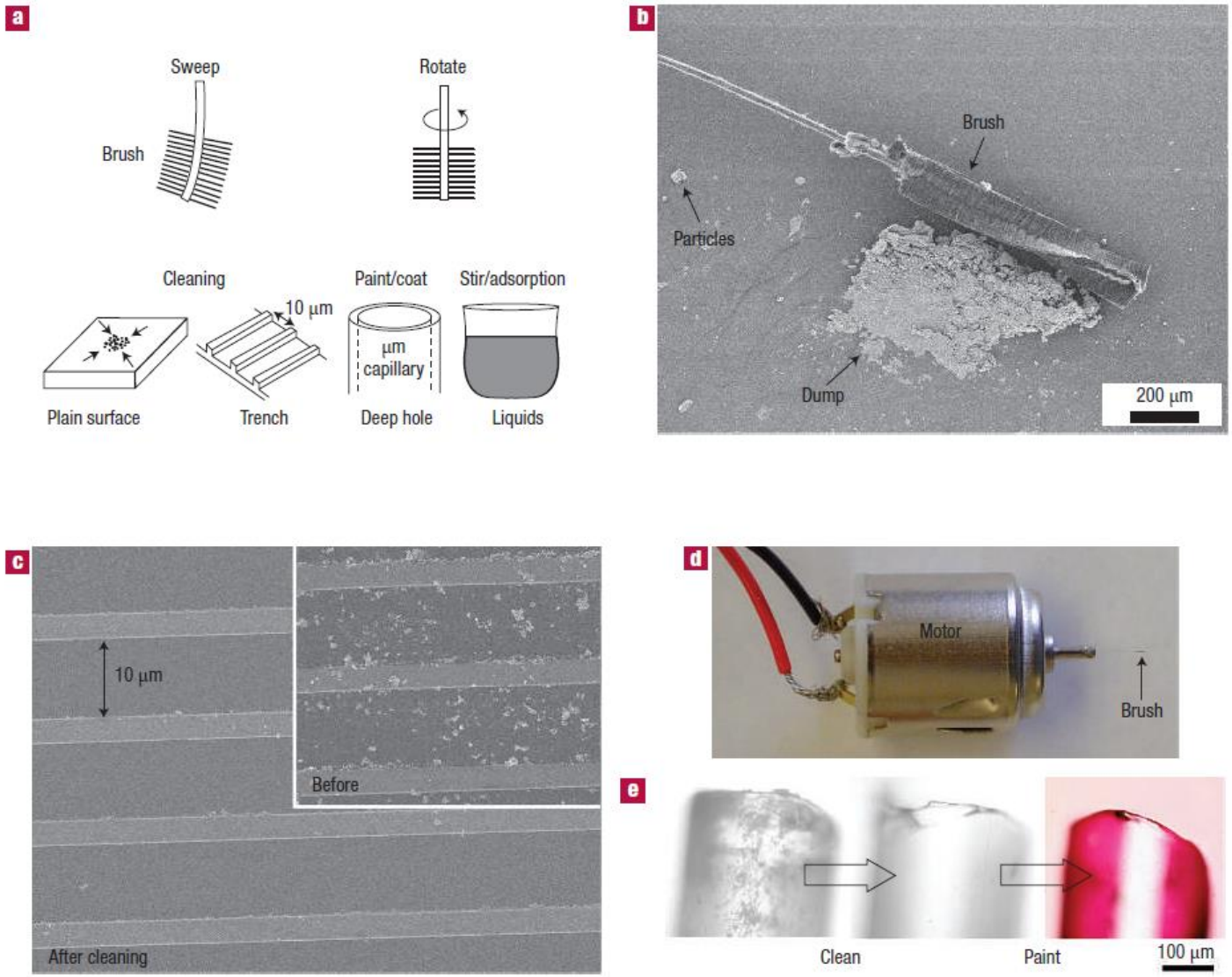

# Manipulation of CNT - nanotransistor

**“CONSTRUCTIVE DESTRUCTION”**

1. The scientists deposit ropes of “stuck together” metallic and semiconducting nanotubes on a silicon-oxide wafer,

2. Then a lithographic mask is projected onto the wafer to form electrodes (metal pads) over the nanotubes. These electrodes act as a switch to turn the semiconducting nanotubes on and off,

.3 Using the silicon wafer itself as an electrode, the scientists "switch-off" the semiconducting nanotubes, which essentially blocks any current from traveling through them,

4.. The metal nanotubes are left unprotected and an appropriate voltage is applied to the wafer, destroying only the metallic nanotubes, since the semiconducting nanotubes are now insulated,

5. The result: a dense array of unharmed, working semiconducting nanotube transistors that can be used to build logic circuits like those found in computer chips.

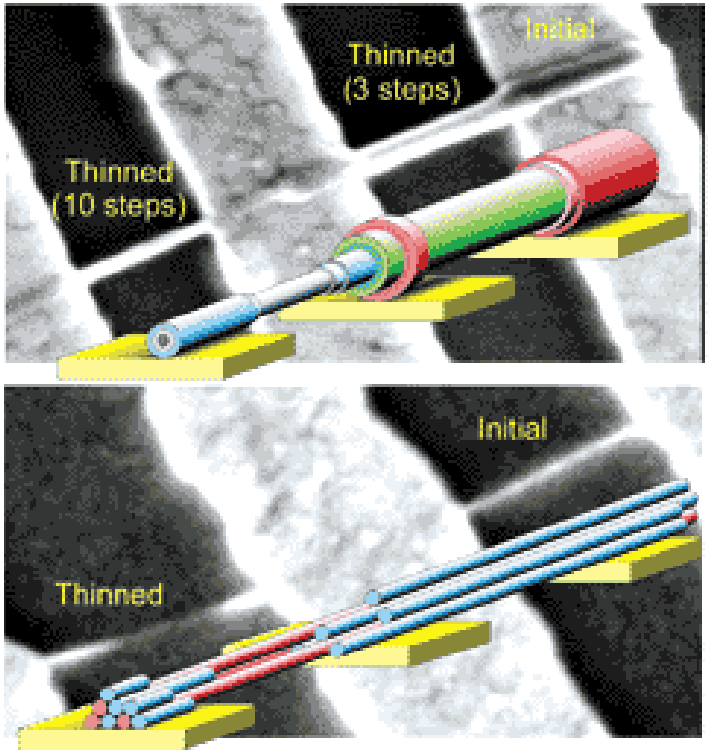


Yorktown Heights, N.Y., April 27, 2001 ... IBM scientists developed a breakthrough transistor technology that could preview how computer chips can be made smaller and faster than what is currently possible with silicon.

# Quantum wires

P.X. Gao et al. / Chemical Physics Letters 408 (2005) 174–178 175

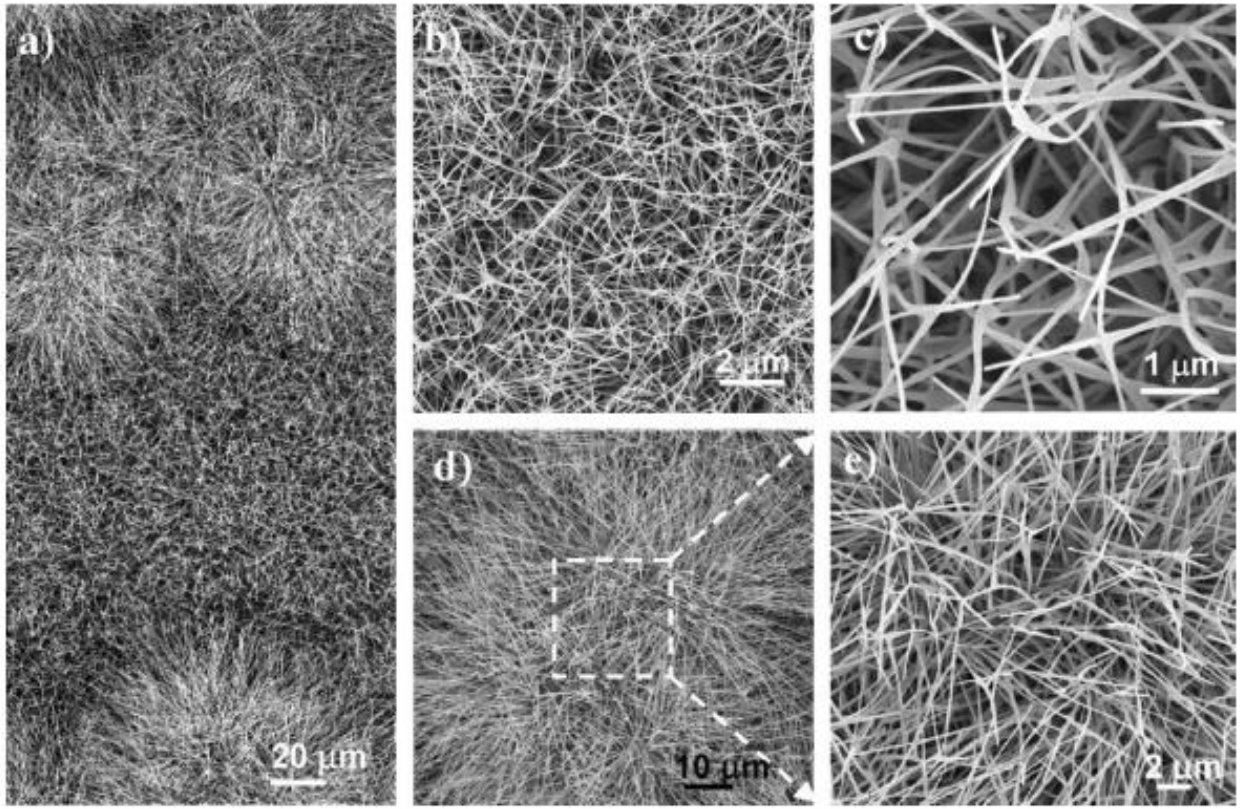


Fig. 1. (a) A typical low magnification SEM image of the as-grown networks of ZnO nanowires and nanorods consisting two types of morphologies, as indicated by area b (b,c) and c (d,e). (b,c) Enlarged SEM images of uniform networks of ZnO nanowires and nanorods. (d,e) Enlarged SEM images of clumps of nanowires showing the interconnected nanowires and nanorods.

# Quantum wires

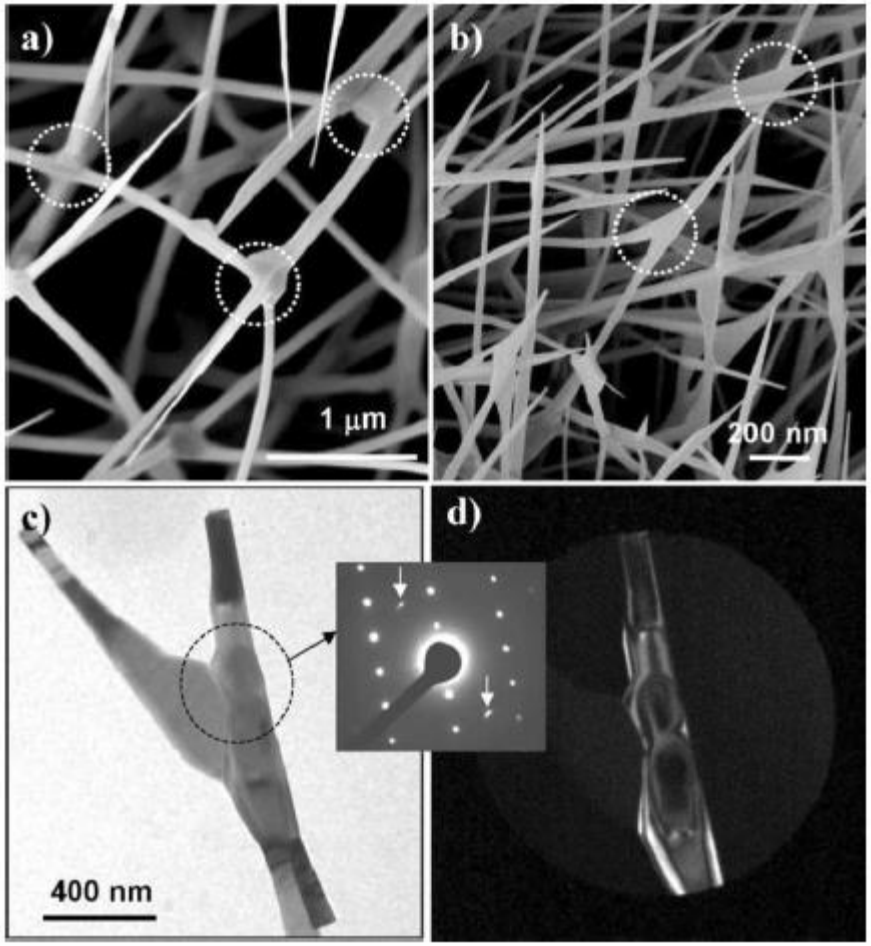


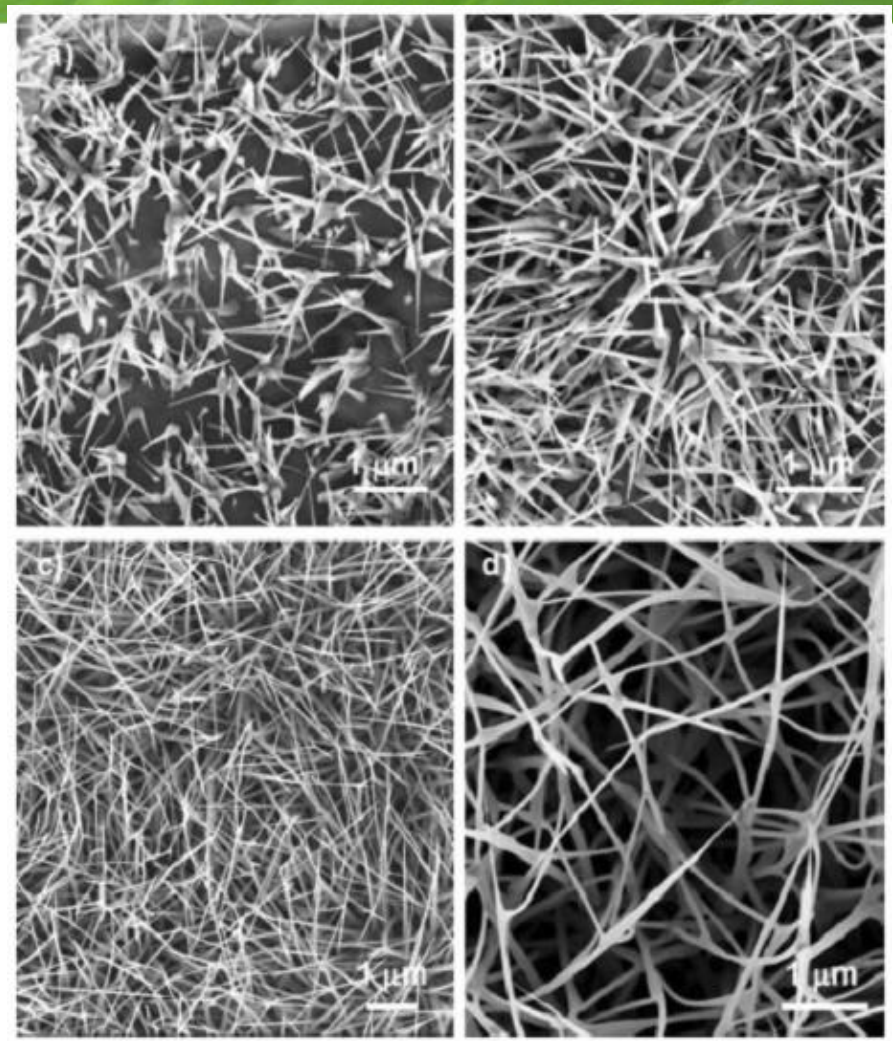


Fig. 5. Formation process of the 3D network. (a) The initial stage of interconnected nanorods growth. (b) The first layer of networking between short nanowires and nanorods. (c) The beginning of the second layer of networking. (d) Highly magnified SEM image giving a clear description about the 3D ZnO networks with mesh space around 2×2×2 (μm).

Fig. 4. (a,b) Interconnection types of ZnO nanowires in the nano-network. (c,d) Bright-field and dark-field TEM images of two nanowires interconnected with each other, indicating that the two nanowires are single crystals but they have no orientation relationship. The circle area is used for recording the selected area electron diffraction pattern (inset).

# Quantum wires

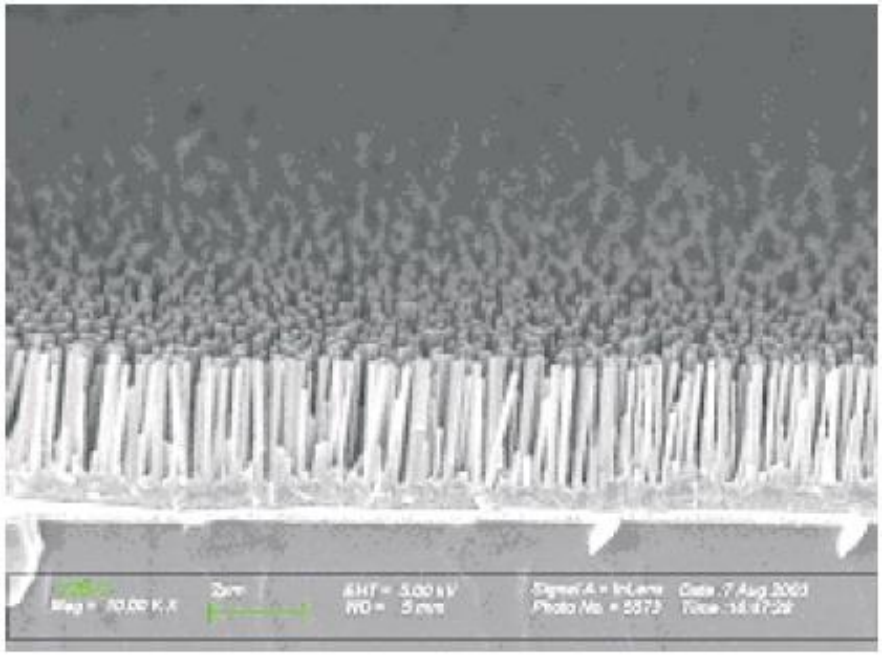

**Figure 3.** Si/$SiO_2$/Ti/Pt/ZnO/Nanowire.

*Tamkang Journal of Science and Engineering, Vol. 7, No 3, pp. 135–138 (2004)* *135*

**Growth and Patterning of ZnO Nanowires on Silicon and $LiNbO_3$ Substrates**

T. K. Shing*, H. H. Pan, I.-C Chen and C. I. Kuo

# Quantum wires

42 *Int. J. of Nanotechnology, Vol. 1, Nos. 1/2, 2004*

**Nanolasers: Lasing from nanoscale quantum wires**

Samuel S. Mao

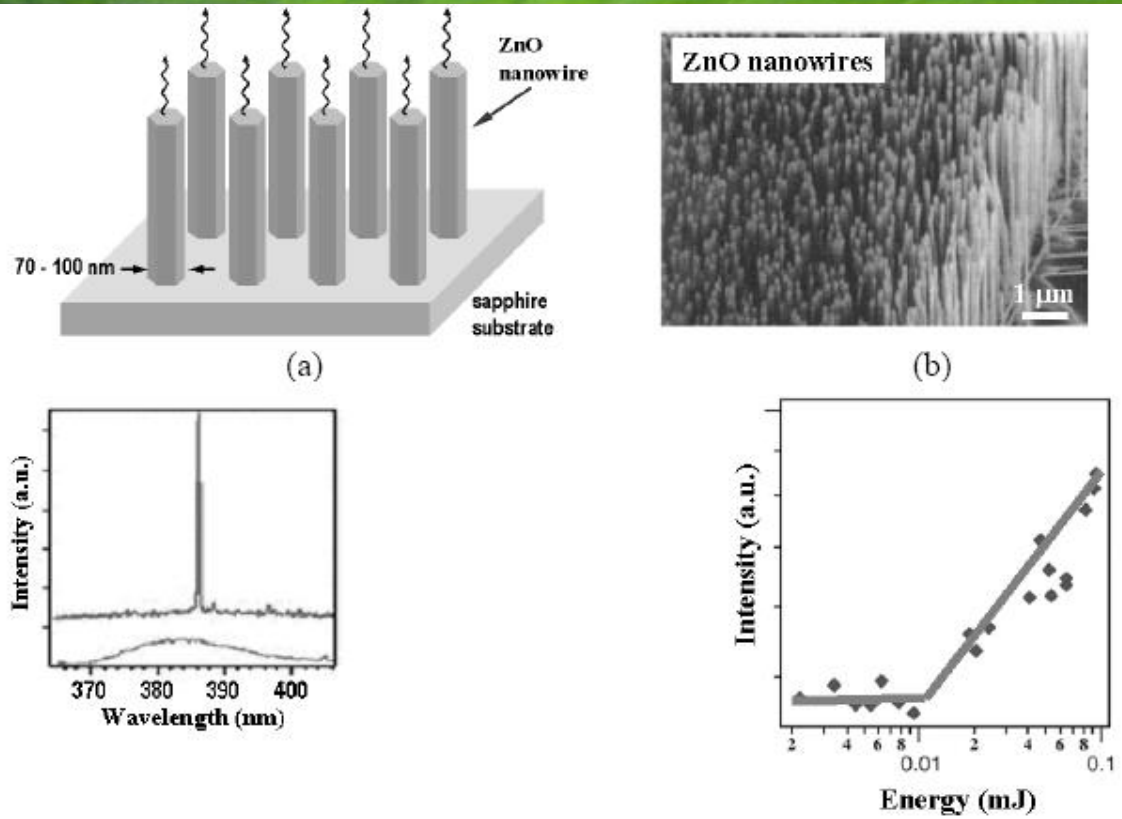


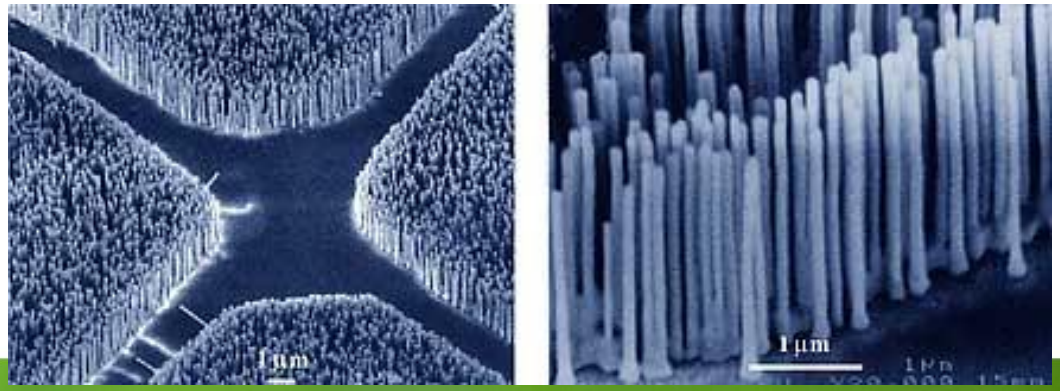


Laserowanie bez wnęki (t.j. sam nanodrut jest dla siebie wnęką!)

Photo by Peidong Yang/UC Berkeley, courtesy of *Science*

# Quantum wires

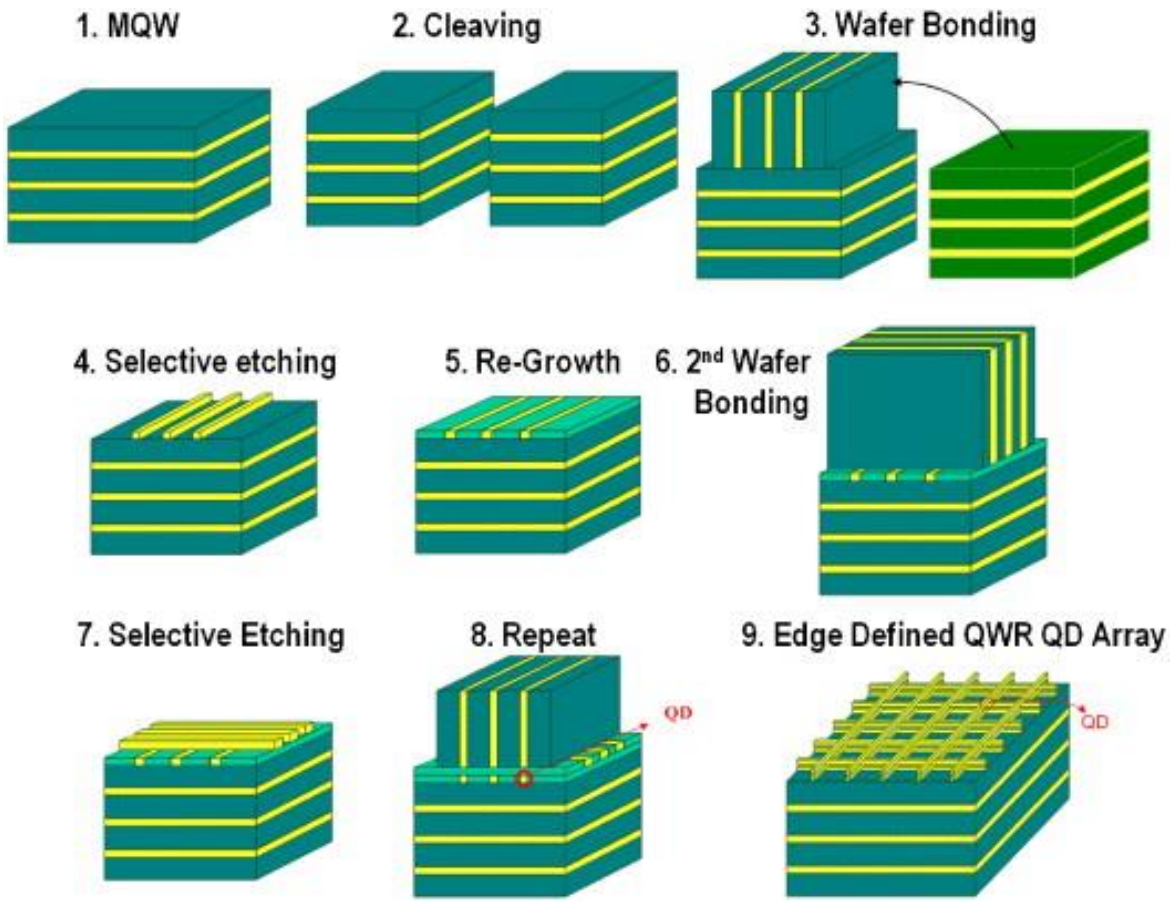


Microelectronics Journal 39, 2008, 369–374

# Quantum wires

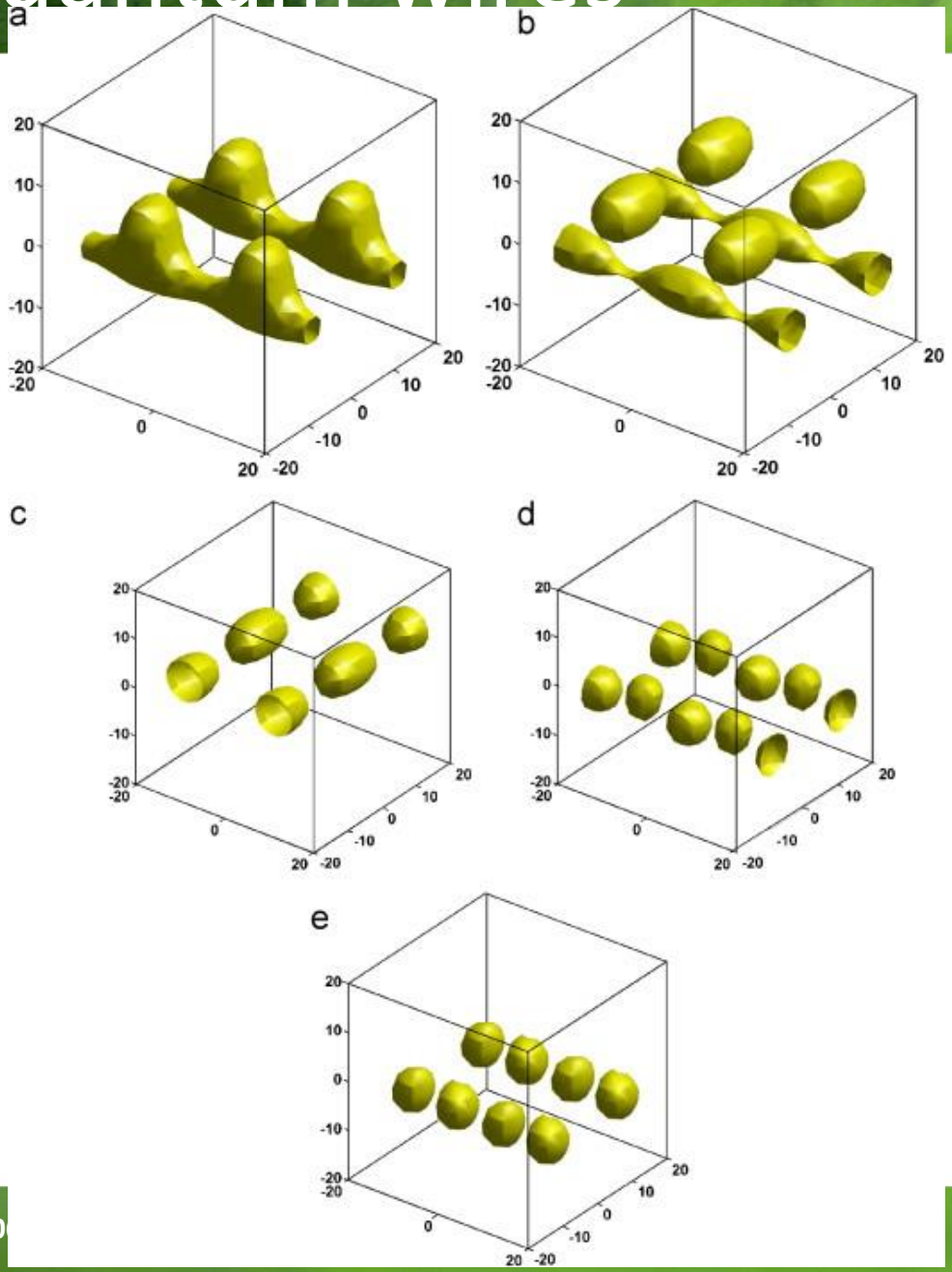


Miniband properties of superlattice quantum dot arrays fabricated by the edge-defined nanowires

Microelectronics Journal 39, 2008, 369–374

# Quantum wires

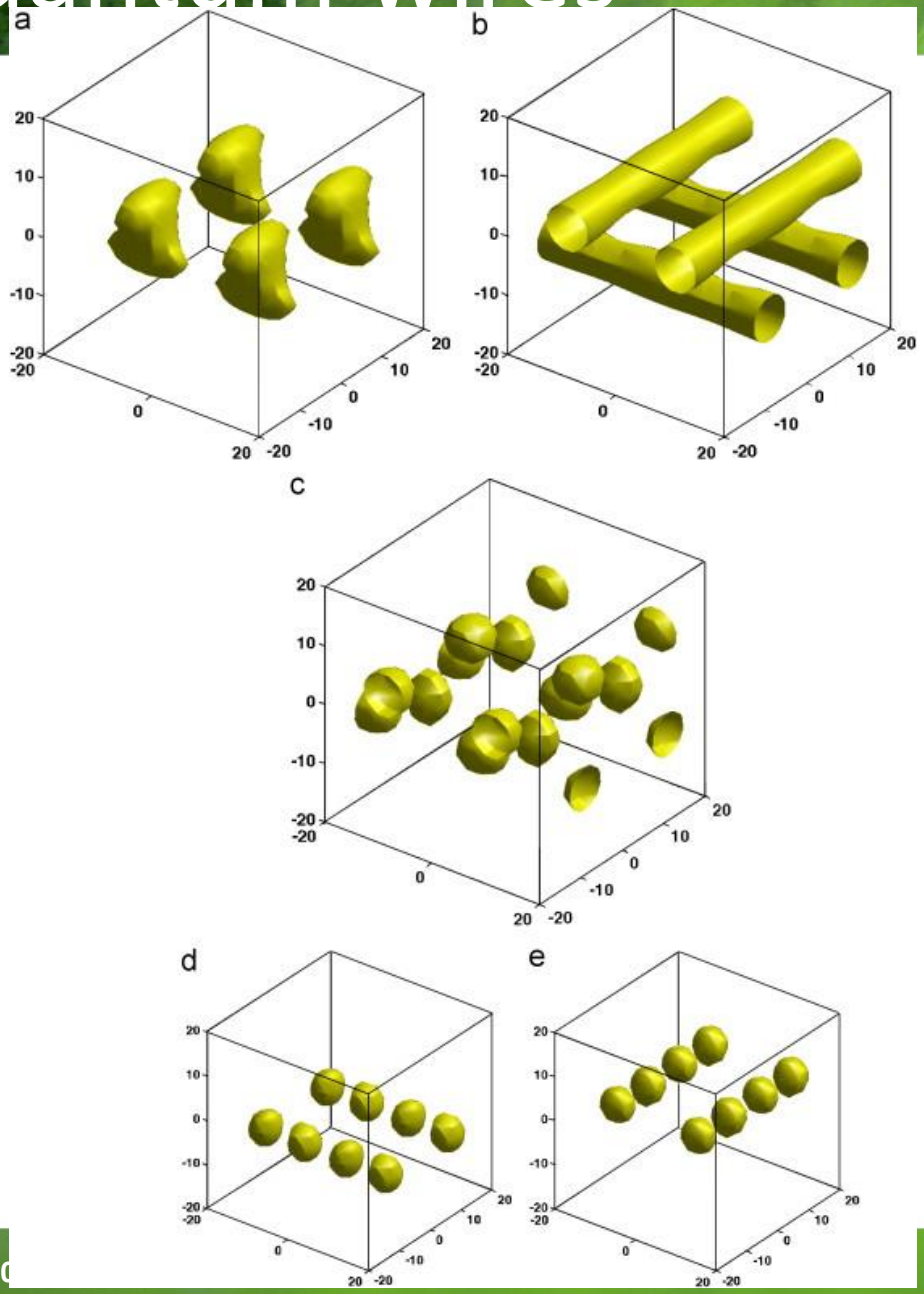


Miniband properties of superlattice quantum dot arrays fabricated by the edge-defined nanowires

Microelectronics Journal 39, 2008, 369–374

# Quantum dots

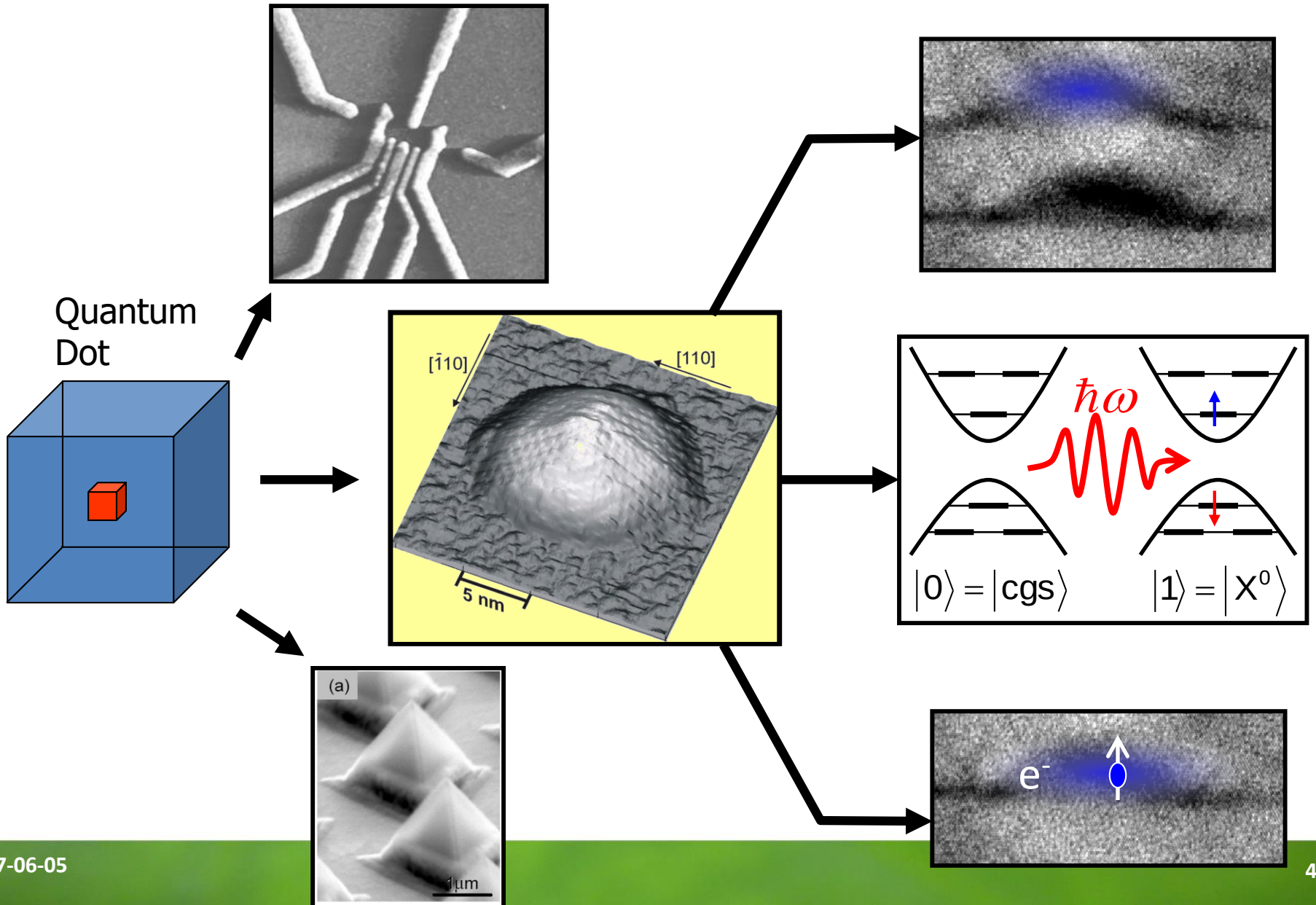

# Harmonic potential

$$\left[-\frac{\hbar^2}{2m}\frac{d^2}{dx^2}+\frac{1}{2}m\omega_0^2x^2\right]\psi(x)=E\psi(x)$$

$$\boxed{E_n=\hbar\omega_0\left(n+\frac{1}{2}\right)}$$

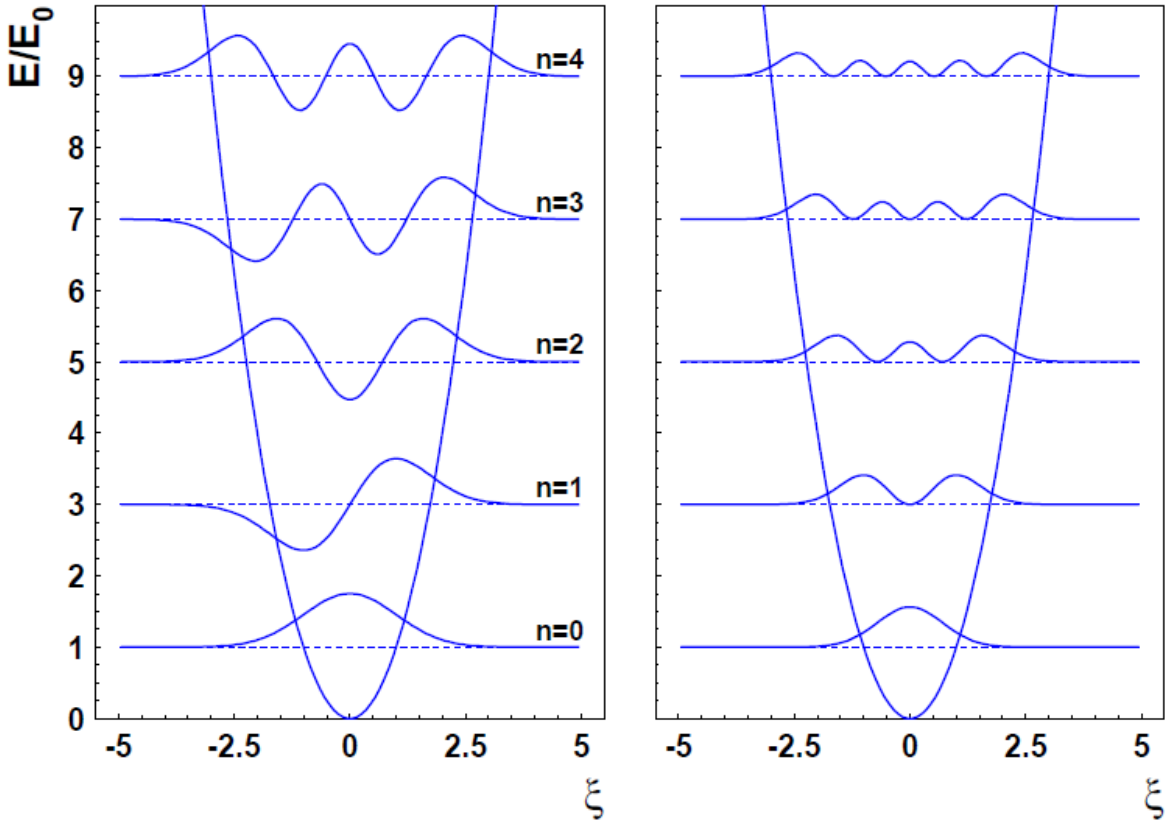


http://phoebe.ifj.edu.pl/wykłady/mk.pdf

Rysunek 10.3: Funkcje własne i gęstości prawdopodobieństwa oscylatora harmonicznego.

# Semiconductor heterostructures

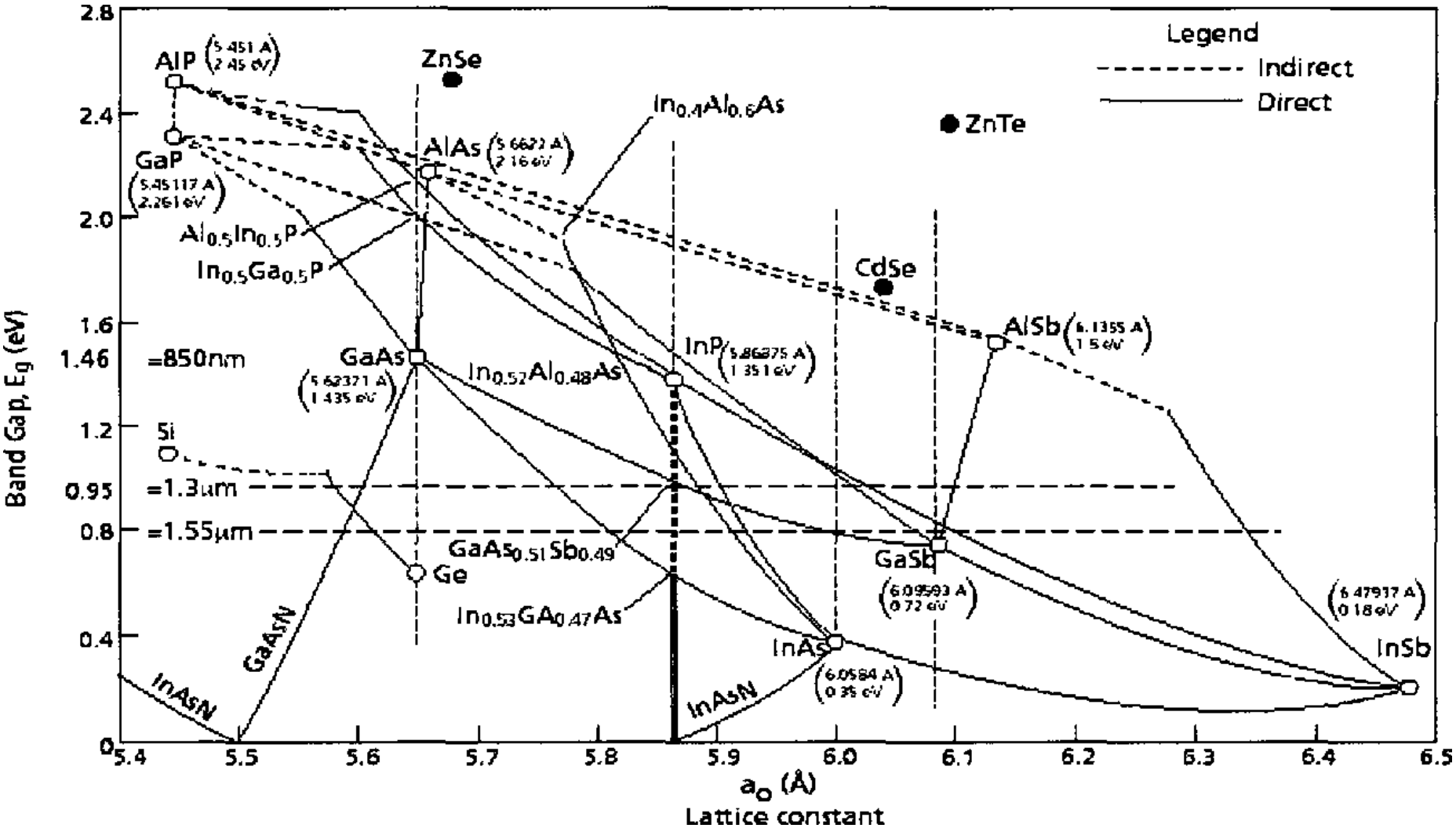


Investigation of high antimony-content gallium arsenic nitride-gallium arsenic antimonide heterostructures for long wavelength application

# The band theory of solids.

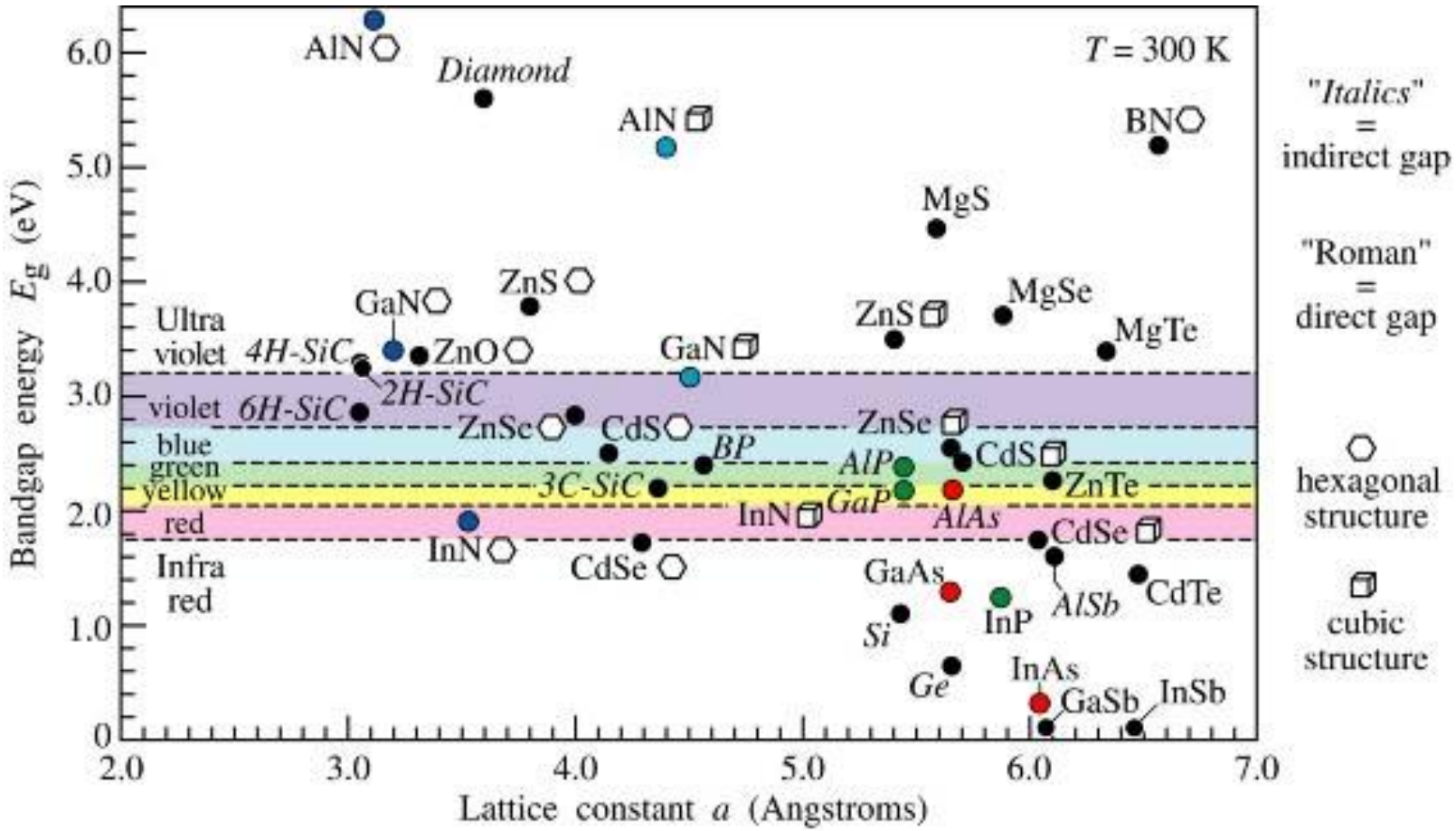


Fig. 11.4. Room-temperature bandgap energy versus lattice constant of common elemental and binary compound semiconductors.

# Harmonic potential

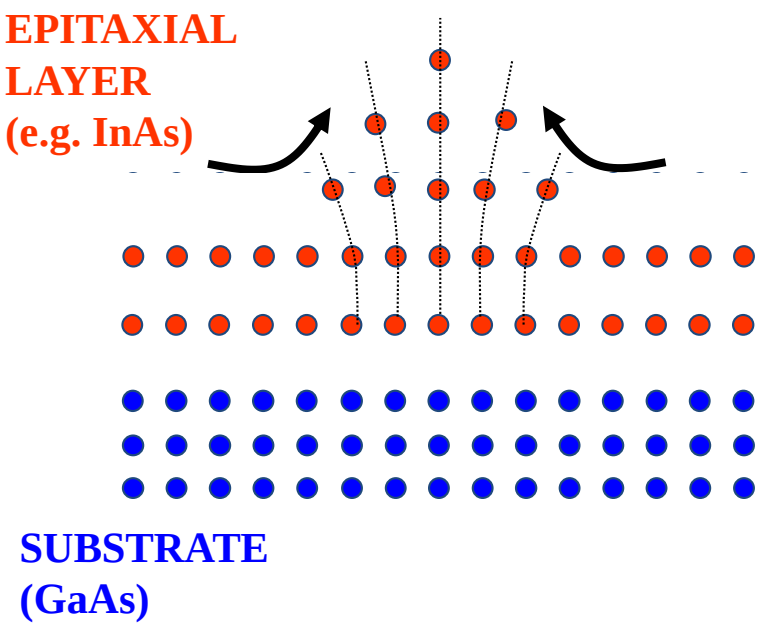


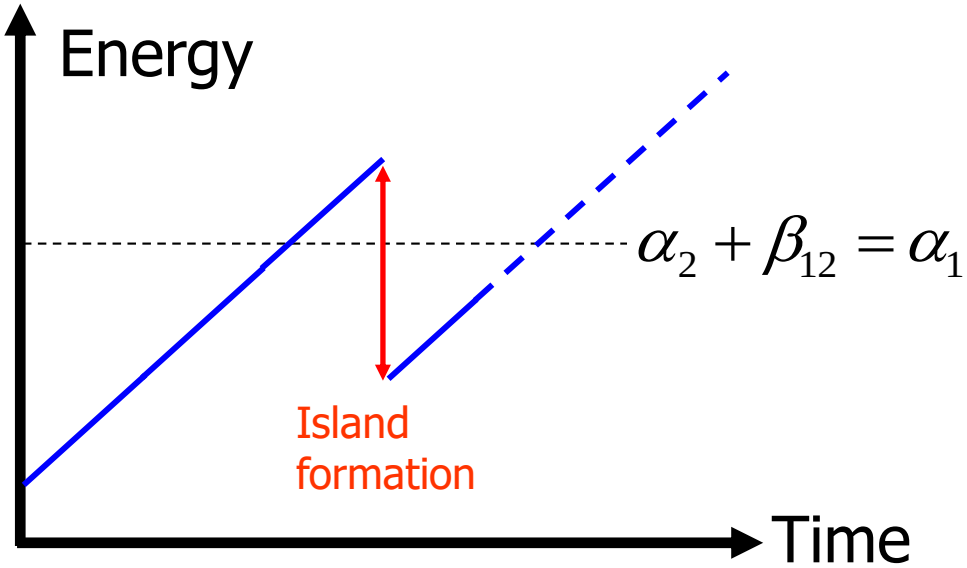


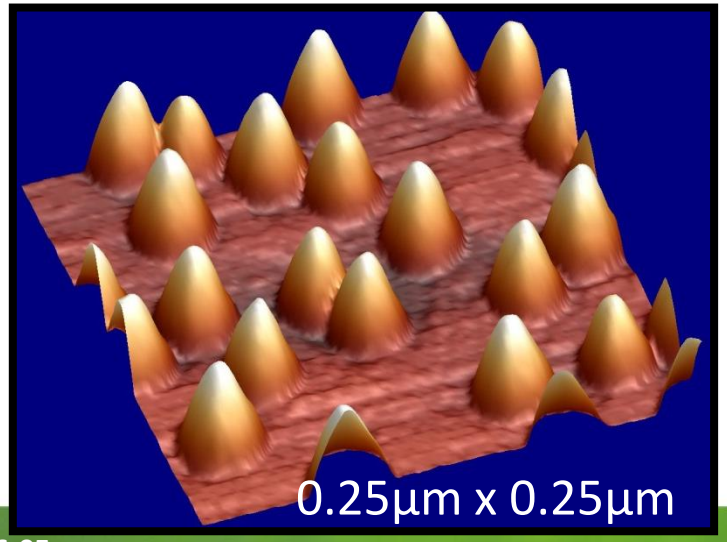


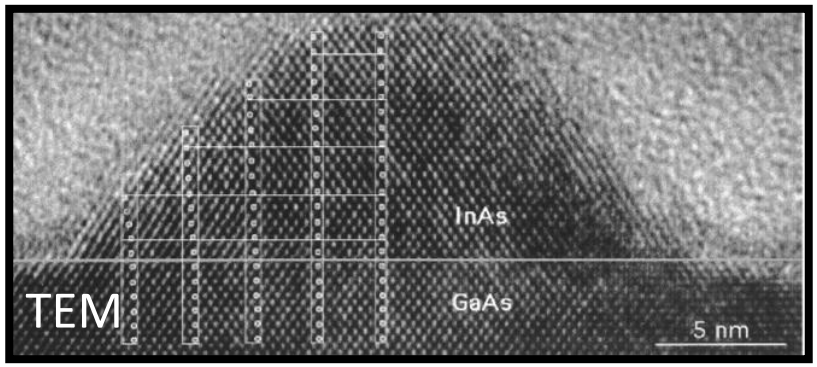


- Defect-free semiconductor "clusters" on a 2D quantum well wetting layer

# Harmonic potential 2D


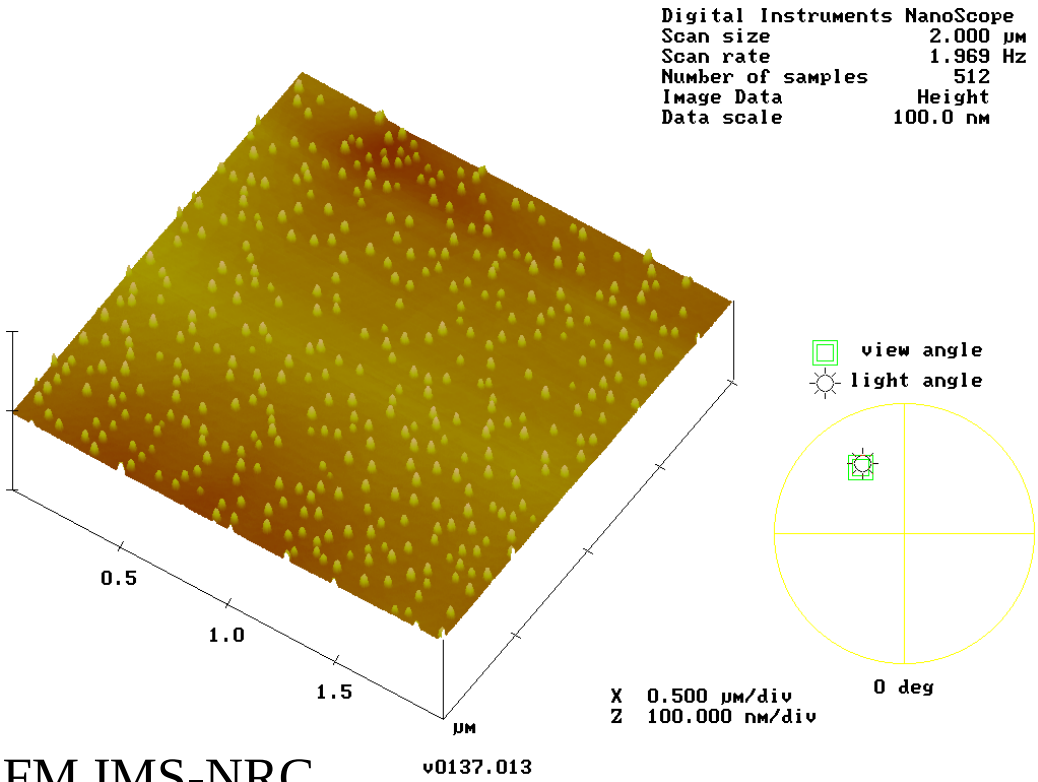


AFM IMS-NRC

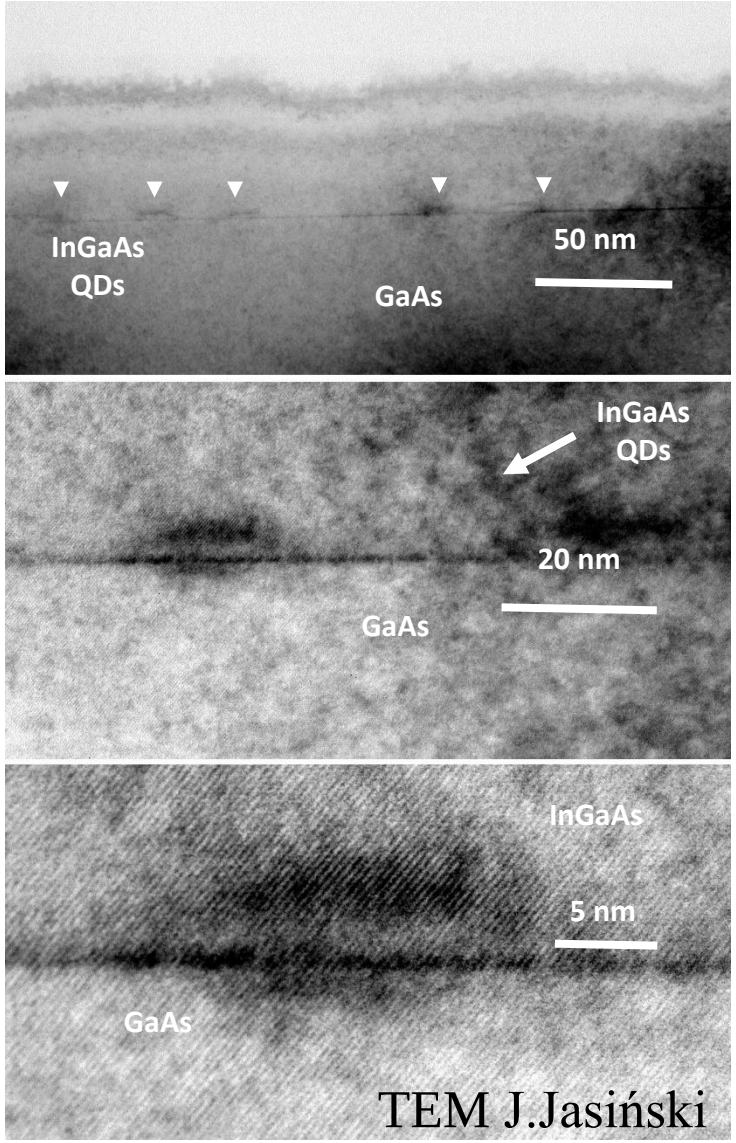


TEM J.Jasiński

# Harmonic potential 2D

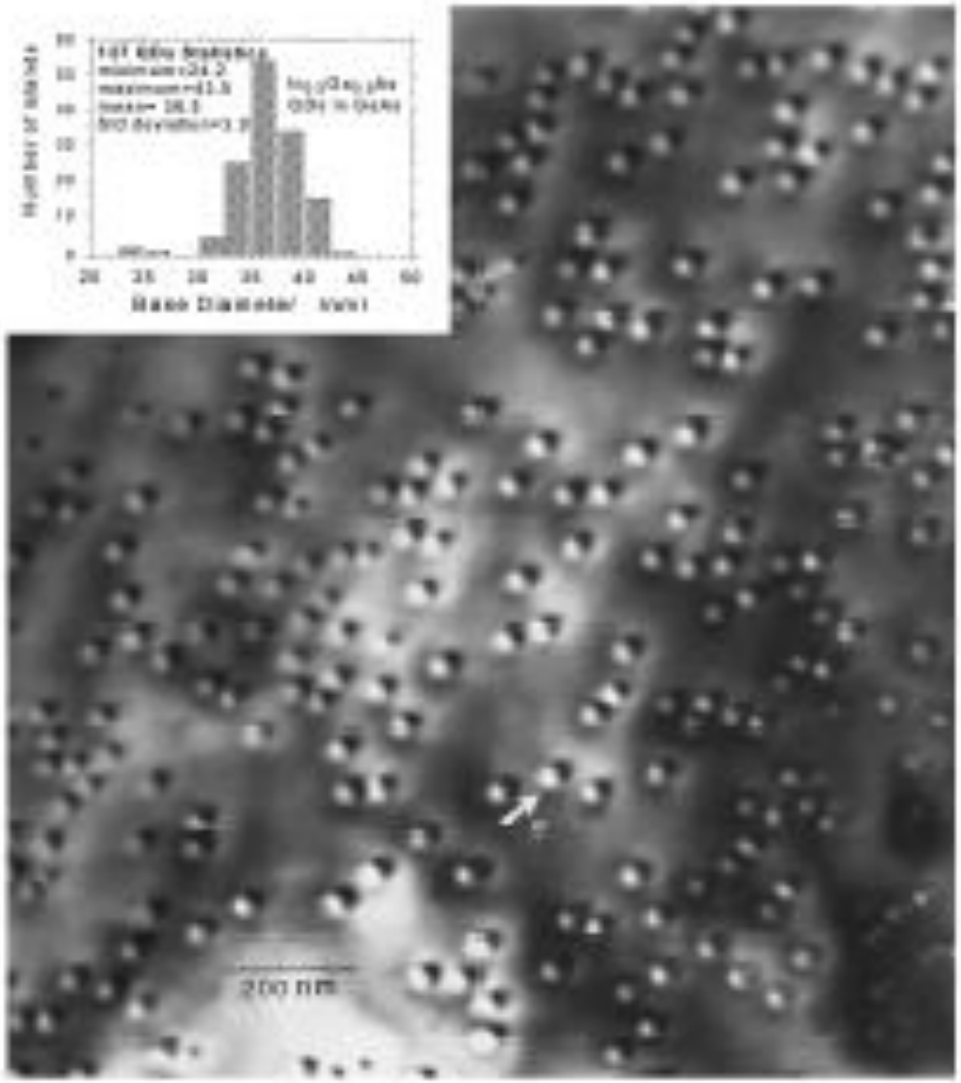


**Kropki kwantowe InGaAs/GaAs**

S.Raymond et al *Phys. Rev. B* **54**; 11548 (1995)

# Harmonic potential 2D

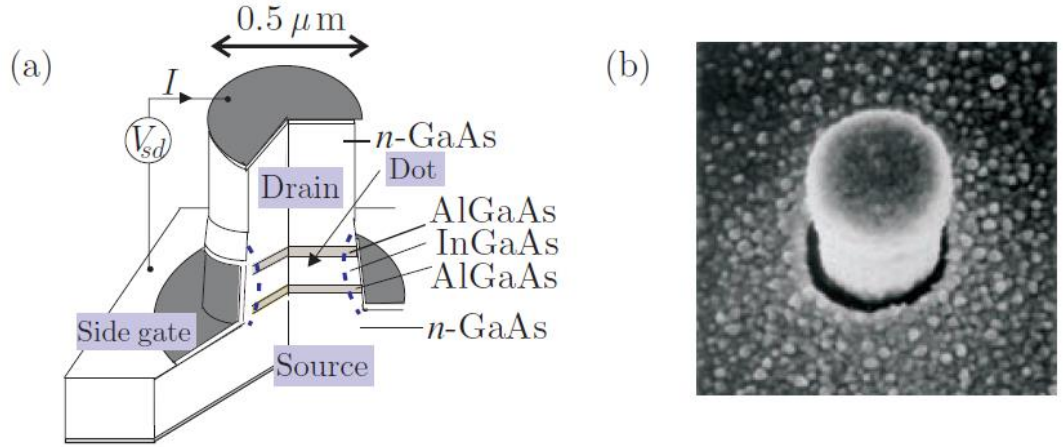


Figure 1.4: (a) Schematic diagram of a semiconductor heterostructure. The dot is located between the two AlGaAs tunnel barriers. A negative voltage applied to the side gate squeezes the dot thus reducing the effective diameter of the dot (dashed curves). (b) Scanning electron micrographs of a circular quantum dot pillar. The pillar has width of about 0.5 $\mu$m. After Kouwenhoven *et al.* [2001].

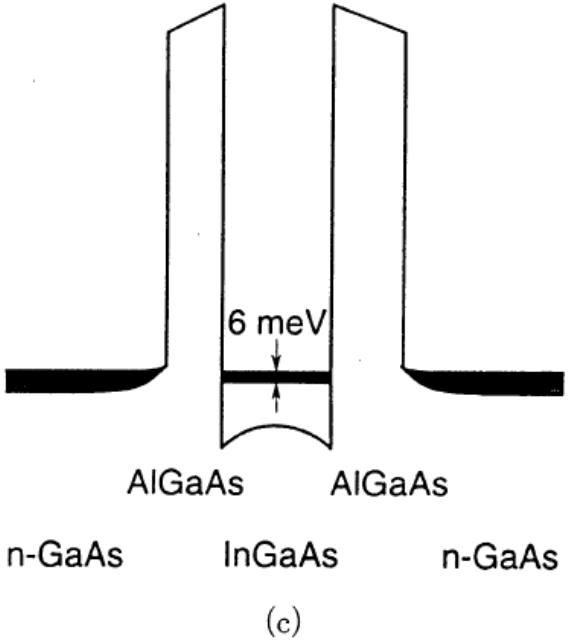


**Fig. 1. (a) Schematic diagram of the gated DBH. (b) Scanning electron micrograph image of a typical section of part of a wire test mesa. There is no short between the metal on the top (A), and the gate metal on the etched surface (B). The two white parallel markers show the position of the DBH. (c) One-dimensional self-consistent band diagram calculated for the DBH with no lateral confinement.**

Jpn. J. Appl. Phys. Vol. 36 (1997) pp. 3917–3923
Part 1, No. 6B, June 1997

# Harmonic potential 2D

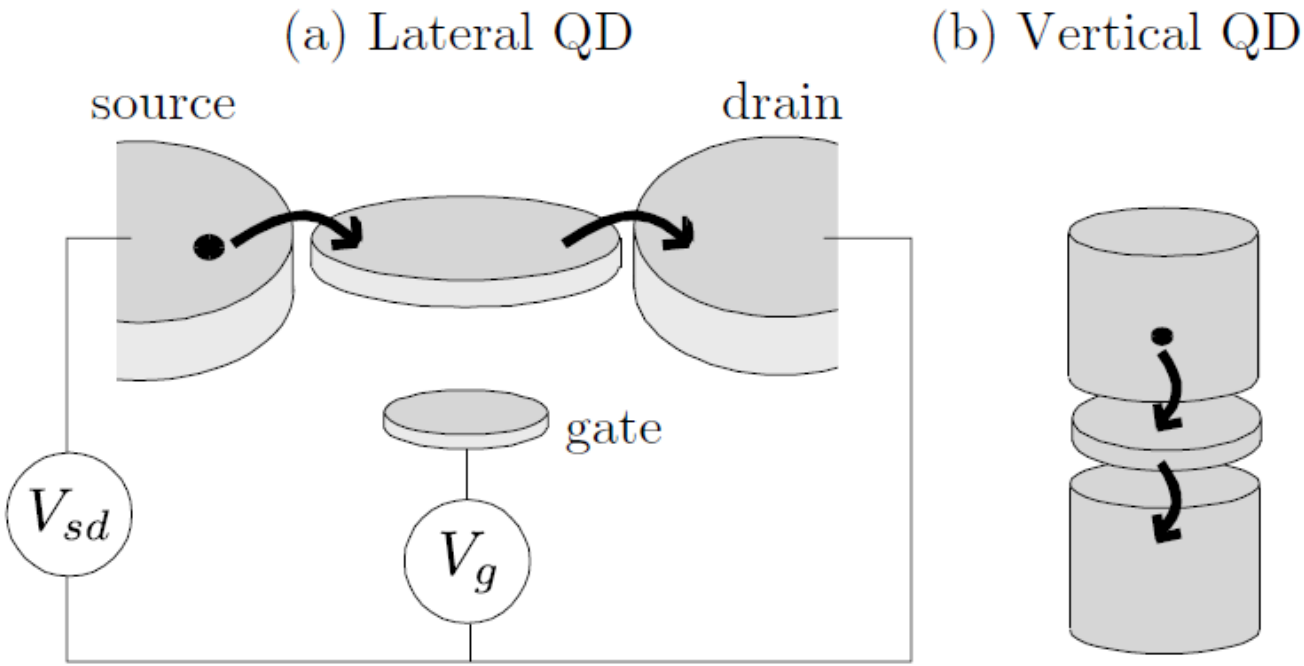


Figure 1.5: Electron flow in planar (a) and vertical (b) QD setup.

# Harmonic potential 2D

$$E_n^x = \hbar\omega_0\left(n_x + \frac{1}{2}\right)$$ in the $x$-direction and the same in $y$

$$E_n^y = \hbar\omega_0\left(n_y + \frac{1}{2}\right)$$

$$\boxed{E_n = E_n^x + E_n^y = \hbar\omega_0(N+1)}$$

Degeneracy? $N = n_x + n_y$

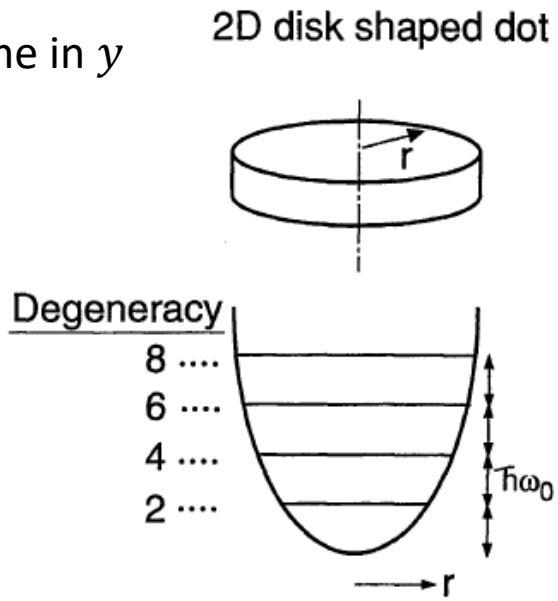


Fig. 5. Schematic model for the vertical dot with a harmonic lateral potential. The single-particle states are laterally confined into discrete equidistant 0D levels whose degeneracies are 2, 4, 6, 8, $\cdots$ including spin degeneracy from the lowest level.

Jpn. J. Appl. Phys. Vol. 36 (1997) pp. 3917–3923
Part 1, No. 6B, June 1997

# Harmonic potential 2D

$$E_n^x = \hbar\omega_0\left(n_x + \frac{1}{2}\right)$$ in the $x$-direction and the same in $y$

$$E_n^y = \hbar\omega_0\left(n_y + \frac{1}{2}\right)$$

$$\boxed{E_n = E_n^x + E_n^y = \hbar\omega_0(N+1)}$$

Degeneracy? $N = n_x + n_y$

$g_N = N + 1$

| $N$ | $(n_x, n_y)$ |
|---|---|
| 0 | (0,0) |
| 1 | (1,0) (0,1) |
| 2 | (2,0) (1,1) (0,2) |
| 3 | (3,0) (2,1) (1,2) (0,3) |

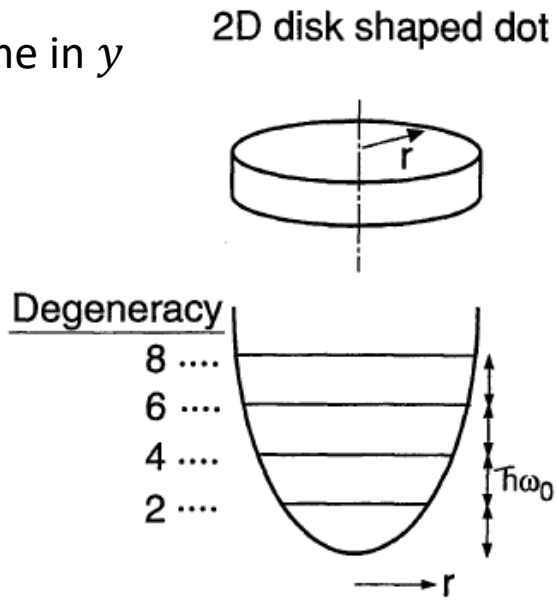


Fig. 5. Schematic model for the vertical dot with a harmonic lateral potential. The single-particle states are laterally confined into discrete equidistant 0D levels whose degeneracies are 2, 4, 6, 8, $\cdots$ including spin degeneracy from the lowest level.

Jpn. J. Appl. Phys. Vol. 36 (1997) pp. 3917–3923
Part 1, No. 6B, June 1997

# Spectroscopy of Quantum Dots

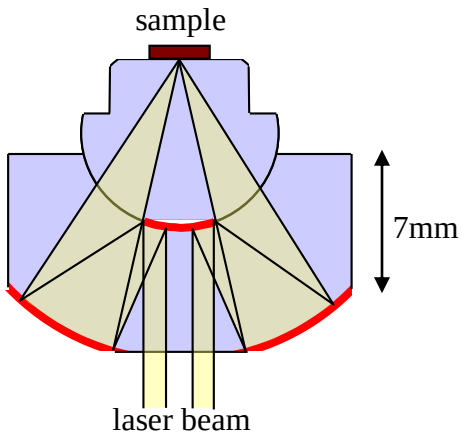


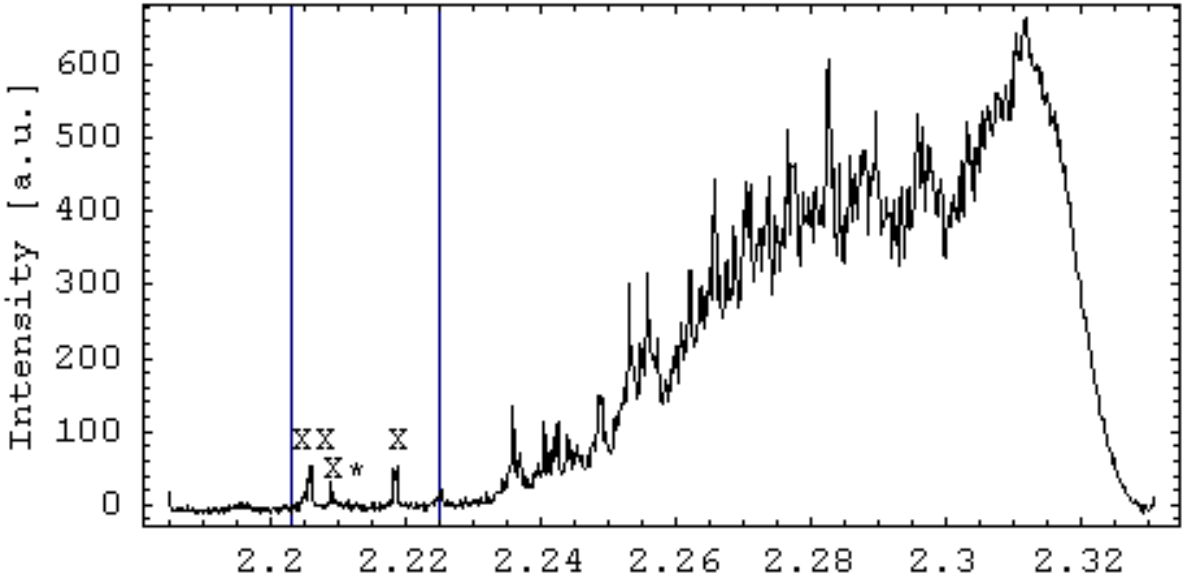

# Spectroscopy of Quantum Dots

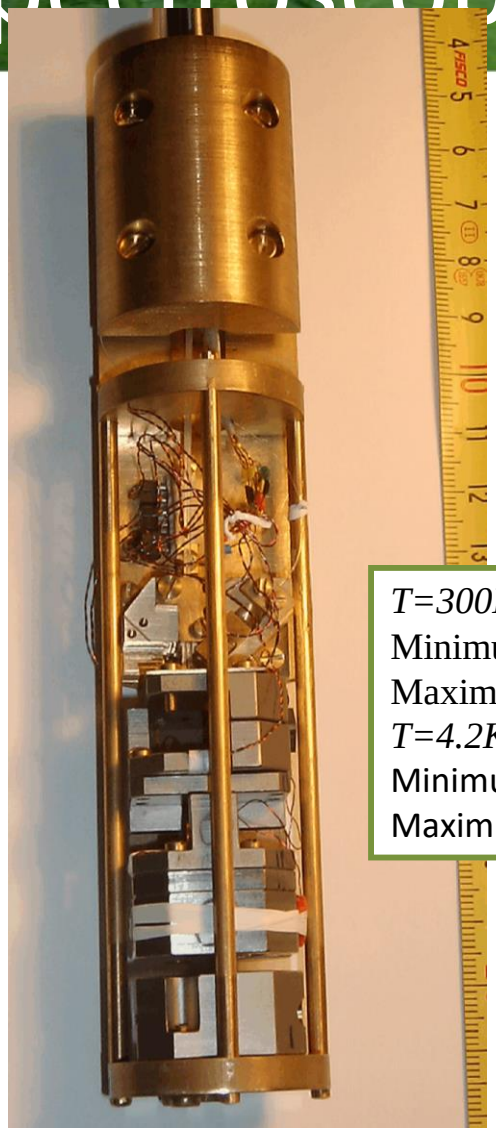

WYDZIAŁ FIZYKI
UNIWERSYTET WARSZAWSKI

*T=300K*
Minimum step~50 nm
Maximum step ~1 μm
*T=4.2K*
Minimum step~5 nm
Maximum step ~100 nm


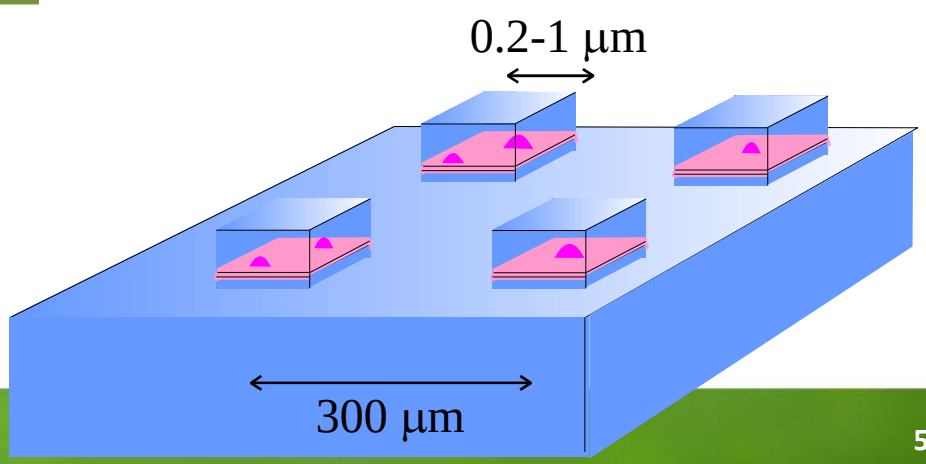


A.Babinski, et al. Physica E 26 (2005) 190

# Spectroscopy of Quantum Dots

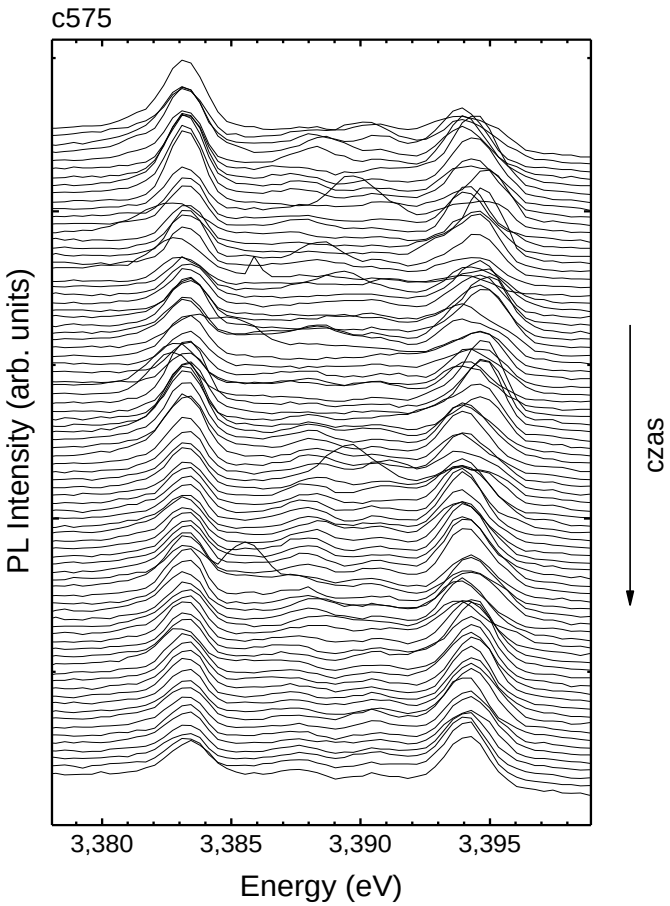


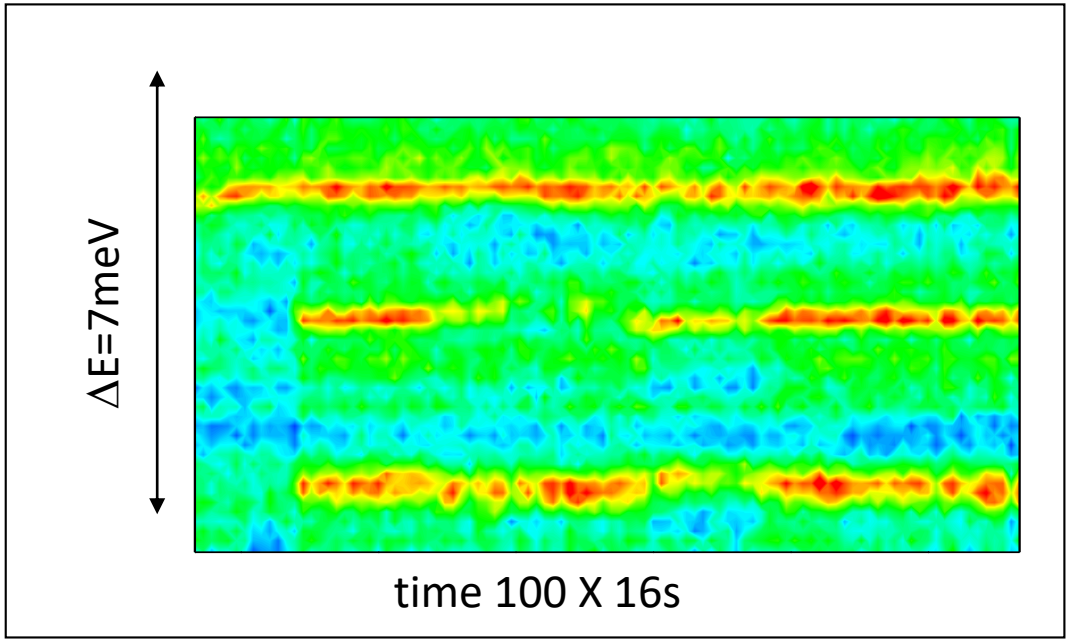


**FUW**
**Hoża 69**

$\mu PL$- Katarzyna Surowiecka et al.

# Harmonic potential 2D

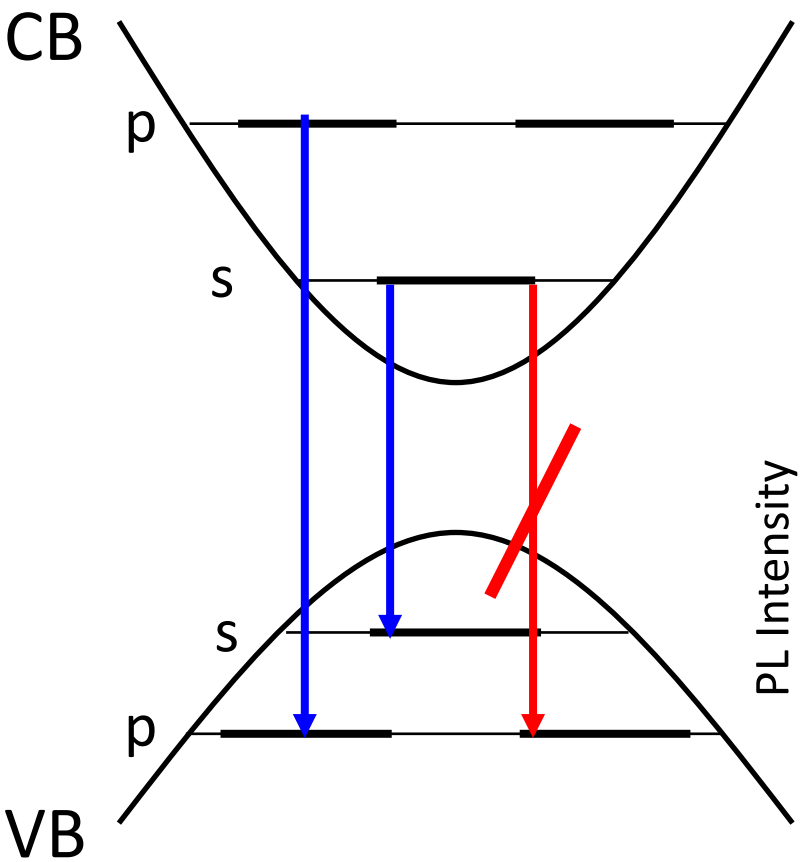


Harmonic oscillator model:

- s-, p-, d-,… shells
- Allowed interband transition

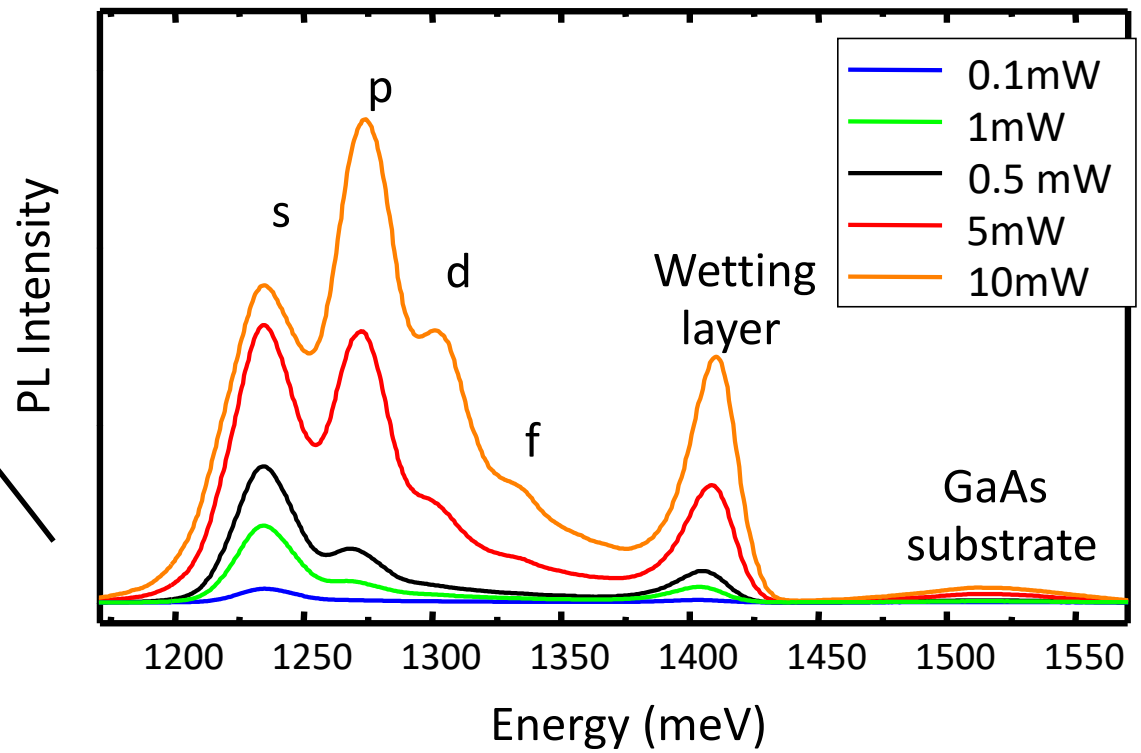

# Harmonic potential 2D

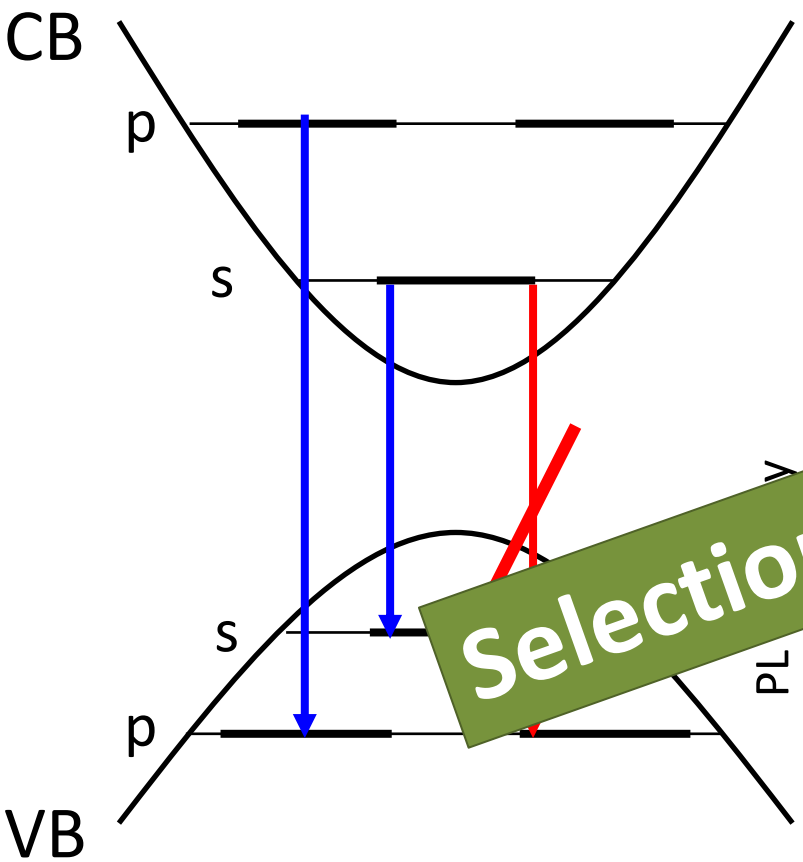


Harmonic oscillator model:

- s-, p-, d-,… shells
- Allowed interband transition

Selection rules?

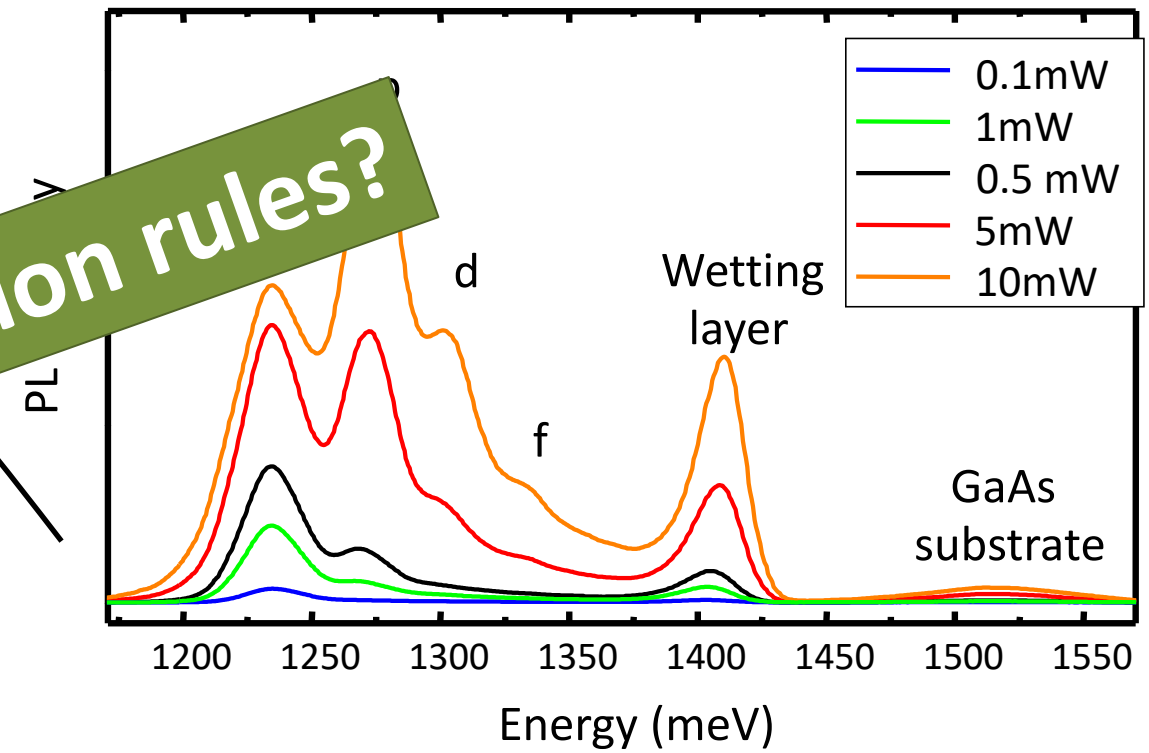

# Harmonic potential 2D

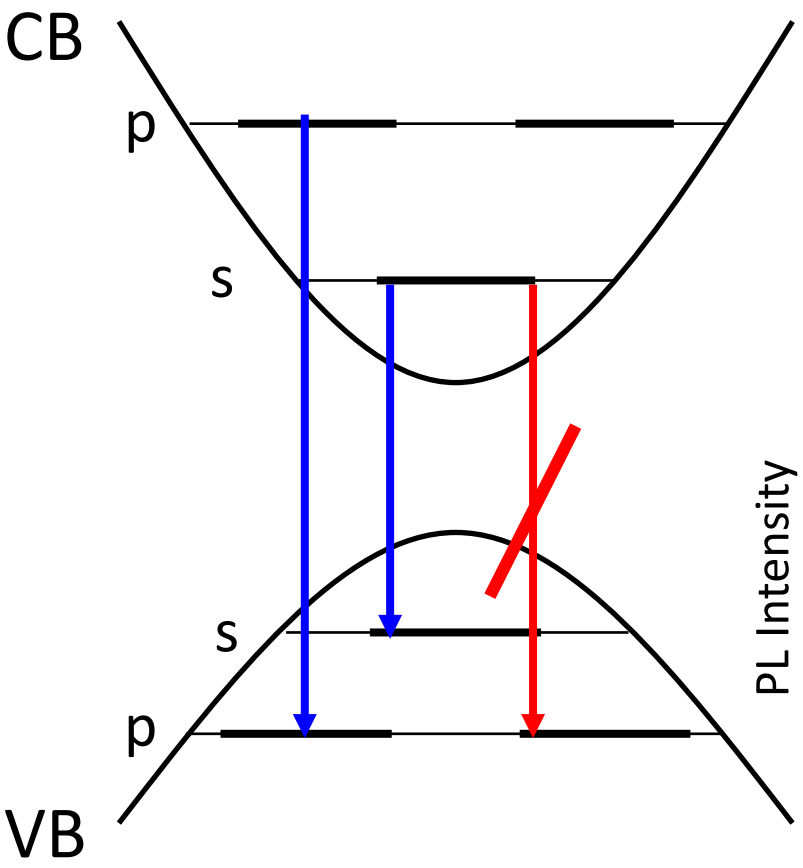


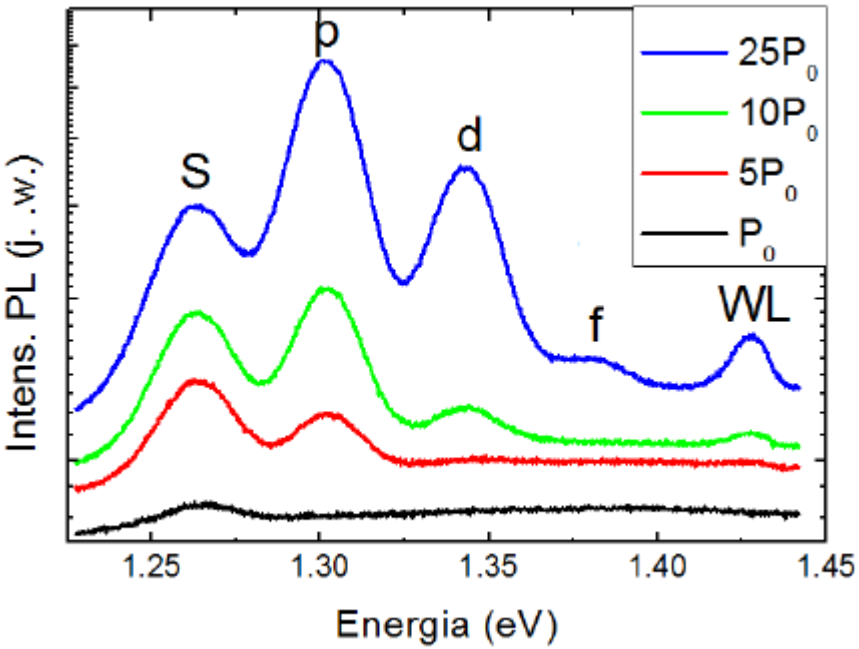


Zależność od mocy pobudzania widm fotoluminescencji otrzymanych w temperaturze bliskiej temperatury ciekłego helu (ok. 5 K) dla licznego (wielomilionowego) zbioru kropek kwantowych InAs/GaAs.

# Harmonic potential 2D

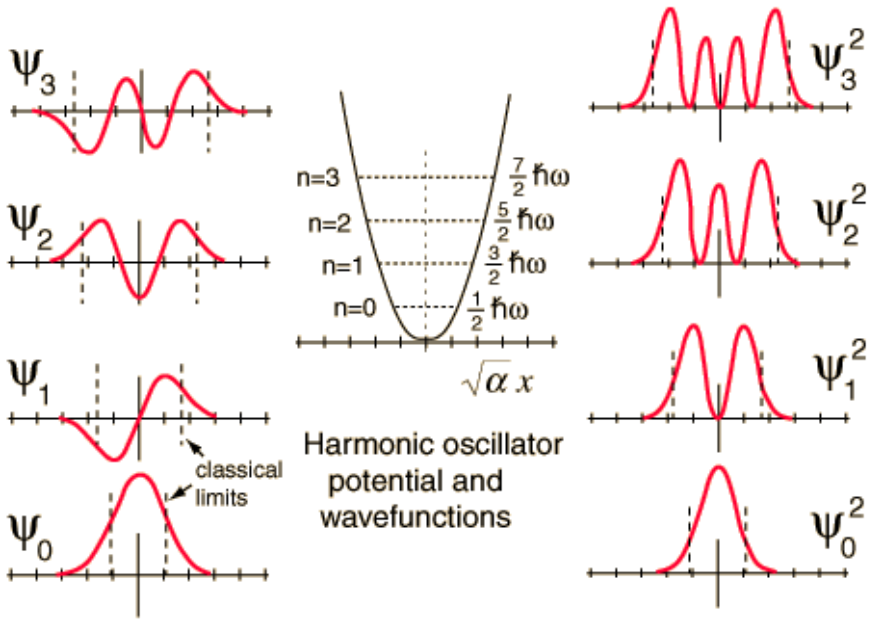


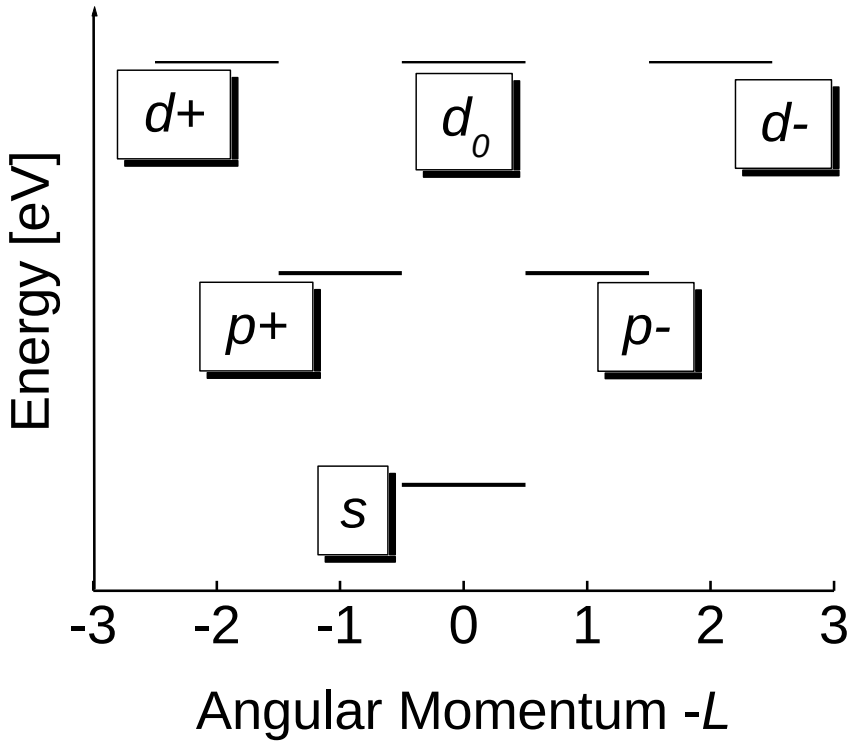


$n, m = 0,1,2...$

$L = n - m$ (elektron)

Adam Babiński

# Harmonic potential 2D

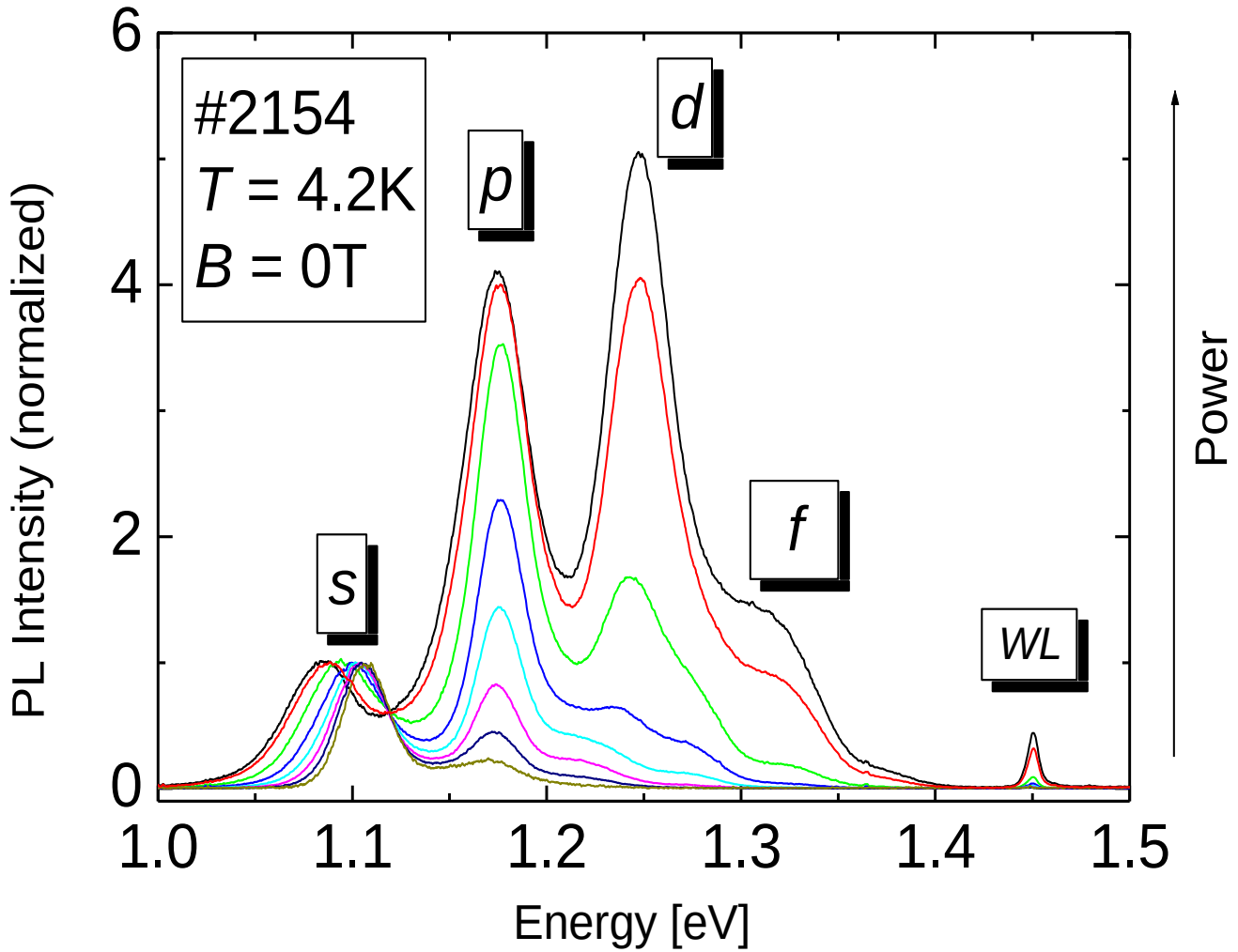


Adam Babiński

# Harmonic potential 2D

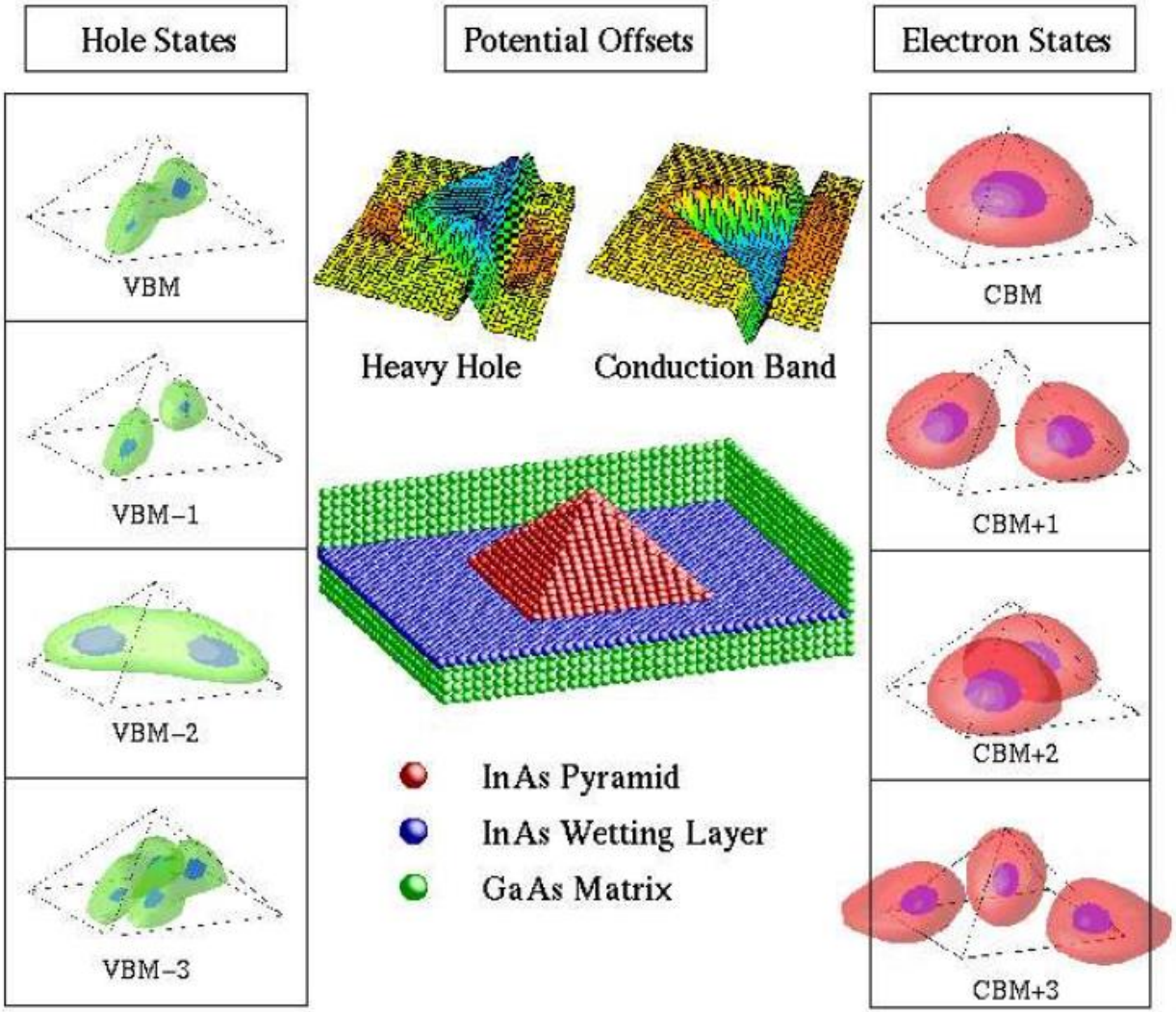


*The electronic structure of a strained InAs (110) pyramidal quantum dot embedded within GaAs. The strain-modified band offsets are shown above the atomic structure. They exhibit a well for both heavy holes and electrons.*
*Isosurface plots of the four highest hole states and four lowest electron states, as obtained from pseudopotential calculations, appear on the left and right. CBM means conduction band minimum and VBM valence band minimum*

MRS Bulletin Vol. 23 No. 2, p. 35 (1998).

# Harmonic potential 2D

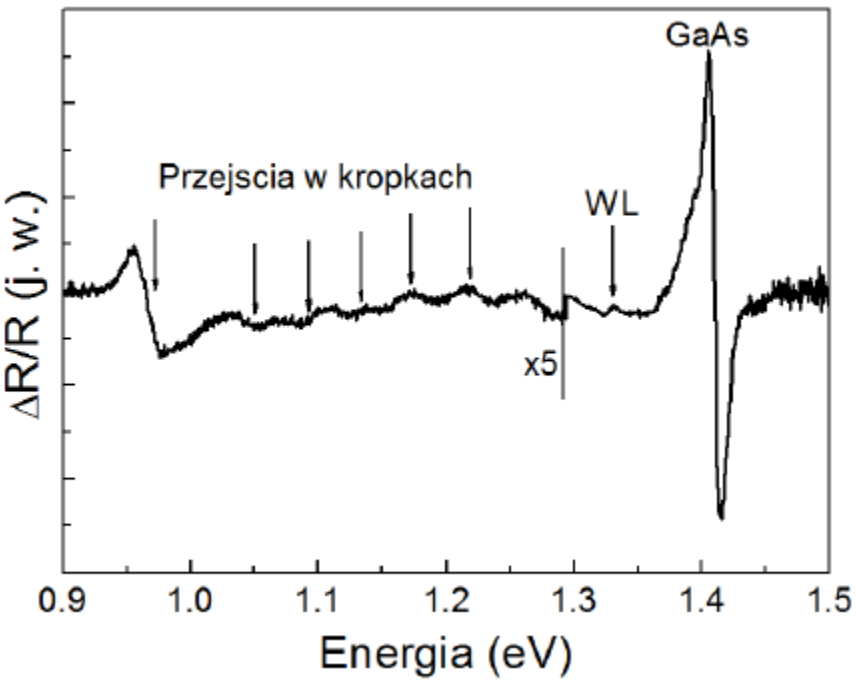


The spectrum of photo reflections at room temperature of the quantum dots In-As / GaAs structure [W. Rudno-Rudziński, et al. Solid State Commun. 135, 232 (2005)]

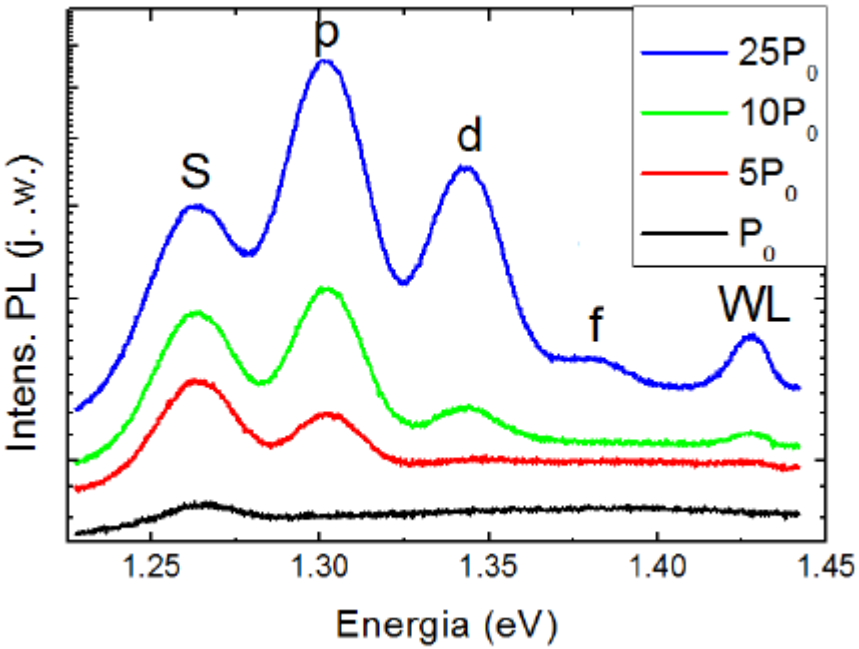


The dependence of photoluminescence spectra of the intensity of stimulation at temperatures close to liquid helium temperature (approx. 5 K) for a large number (several million) of quantum dots InAs / GaAs.

# Harmonic potential 3D

$E_n^x = \hbar\omega_0\left(n_x + \frac{1}{2}\right)$ in the $x$-direction and the same in $y$

$$\boxed{E_n = E_n^x + E_n^y + E_n^z = \hbar\omega_0\left(N + \frac{3}{2}\right)}$$

Degeneracy? $N = n_x + n_y + n_z$

$$g_N = \frac{(N+1)(N+2)}{2}$$

| $N$ | $(n_x, n_y, n_z)$ |
|---|---|
| 0 | (0,0,0) |
| 1 | (1,0,0) (0,1,0) (0,0,1) |
| 2 | (2,0,0) (0,2,0) (0,0,2) (1,1,0) (1,0,1) (0,1,1) |
| 3 | 3x(3,0,0) 1x(1,1,1) 6x(2,0,1) |

# THE ARTICLE

## ARTIFICIAL ATOMS

The charge and energy of a sufficiently small particle of metal or semiconductor are quantized just like those of an atom. The current through such a quantum dot or one-electron transistor reveals atom-like features in a spectacular way.

Marc A. Kastner

M A Kastner, *Phys. Today* , **46**, 24 (1993)

REVIEW ARTICLE

## Electrons in artificial atoms

**R. C. Ashoori**

**Progress in semiconductor technology has enabled the fabrication of structures so small that they can contain just one mobile electron. By varying controllably the number of electrons in these 'artificial atoms' and measuring the energy required to add successive electrons, one can conduct atomic physics experiments in a regime that is inaccessible to experiments on real atoms.**

R C Ashoori, *Nature* , **379**, 413 (1996)

# THE ARTICLE

NATURE | VOL 405 | 22 JUNE 2000 | www.nature.com

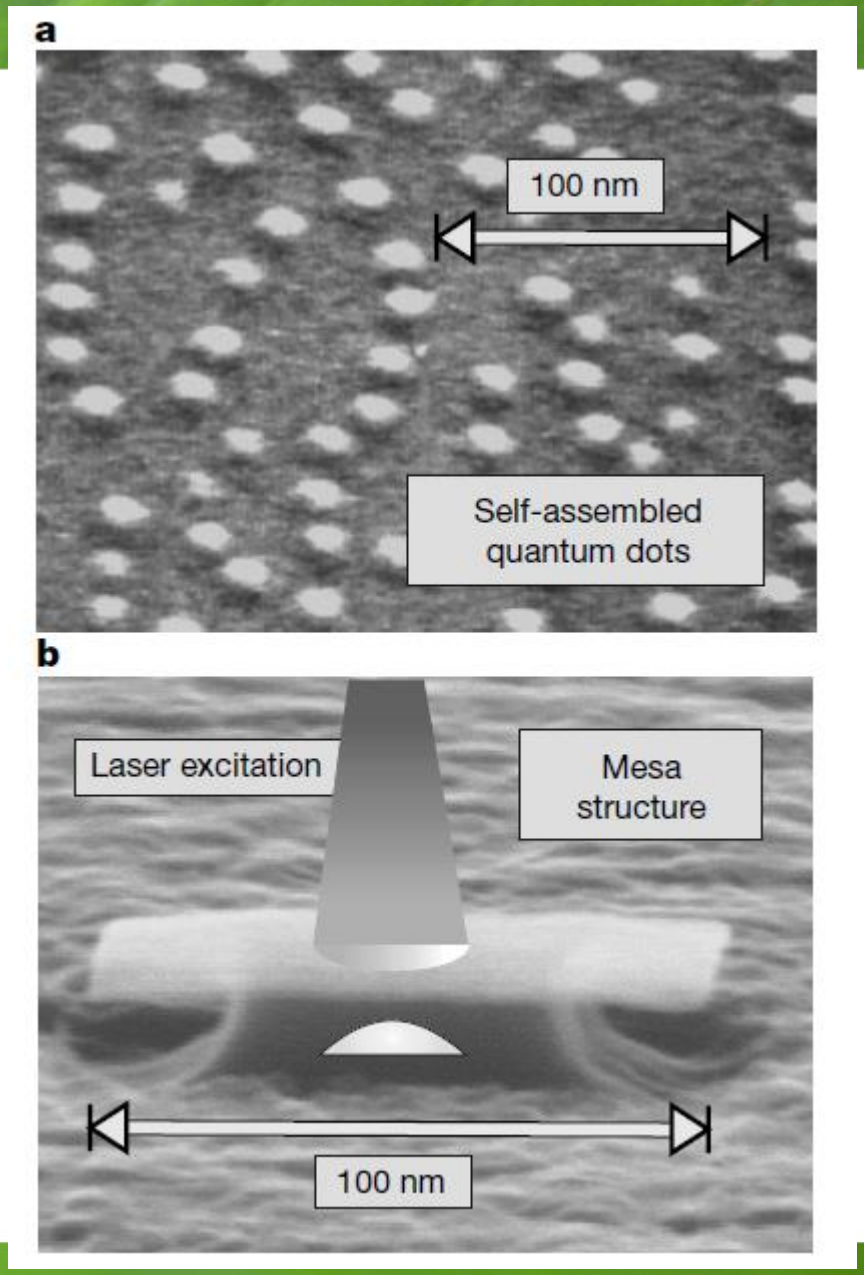


**Figure 1** Scanning electron micrographs illustrating the experimental technique used for studying single self-assembled quantum dots. **a**, Scanning electron micrograph of a GaAs semiconductor layer on which $In_{0.60}Ga_{0.40}As$ self-assembled quantum dots with a density of about $10^{10}$ $cm^{-2}$ have been grown by molecular beam epitaxy. To permit their microscopic observation these dots—unlike those used for spectroscopy—have not been covered by a GaAs cap layer. To a good approximation, all quantum dots have the same shape exhibiting rotational symmetry. However, their size varies by a few nanometres around an average diameter of 15 nm. This inhomogeneity results in a considerable broadening of the emission lines in spectroscopic studies. **b**, To avoid this broadening we have studied the emission of a single quantum dot. Lithographic techniques were used to fabricate small mesa structures on samples capped by a GaAs layer. The lateral mesa size was reduced to such an extent (<100 nm) that only a single dot is contained in it. These mesa structures have been studied by photoluminescence spectroscopy at low temperature. A laser beam (shown schematically as a truncated cone above the mesa) injects a controlled number of electrons and holes into the dot indicated by the lens shape, and the emission spectrum of this complex is recorded. To reduce sample heating under optical excitation, the structures are held in superfluid helium at about 1.2 K. After dispersion by a monochromator, the emission is detected by a CCD (charge-coupled device) camera.

# THE ARTICLE

NATURE | VOL 405 | 22 JUNE 2000 | www.nature.com

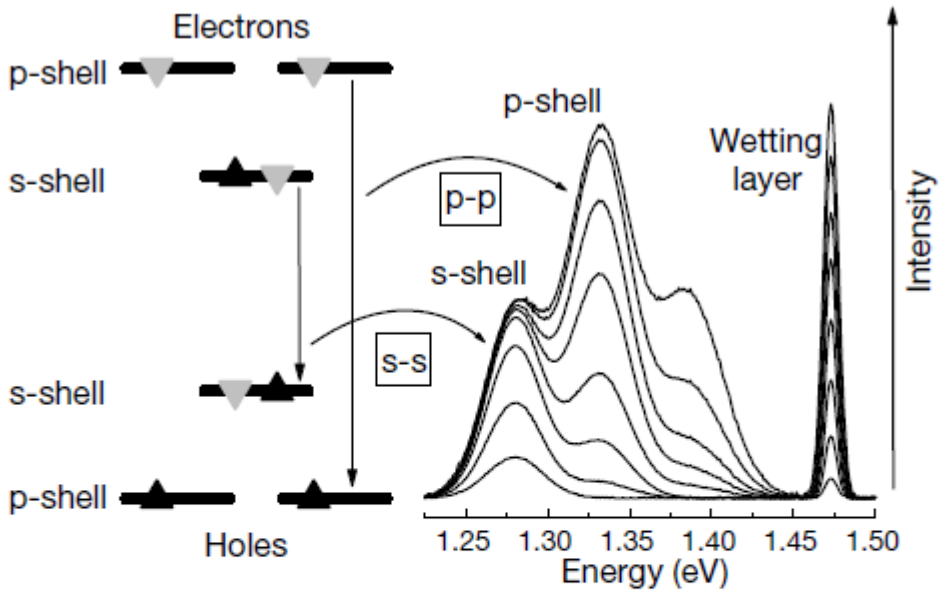


**Figure 2** State filling spectroscopy on quantum dots. On the left is a scheme of the dot energy levels, their occupation by carriers and the radiative transitions. Spin orientations of electrons and holes: grey triangles, spin-down; black triangles, spin-up. On the right are typical emission spectra resulting from these transitions for an ensemble of $In_{0.60}Ga_{0.40}As$ quantum dots; these spectra were recorded at different excitation powers (an Ar-ion laser was used).

# THE ARTICLE

NATURE | VOL 405 | 22 JUNE 2000 | www.nature.com

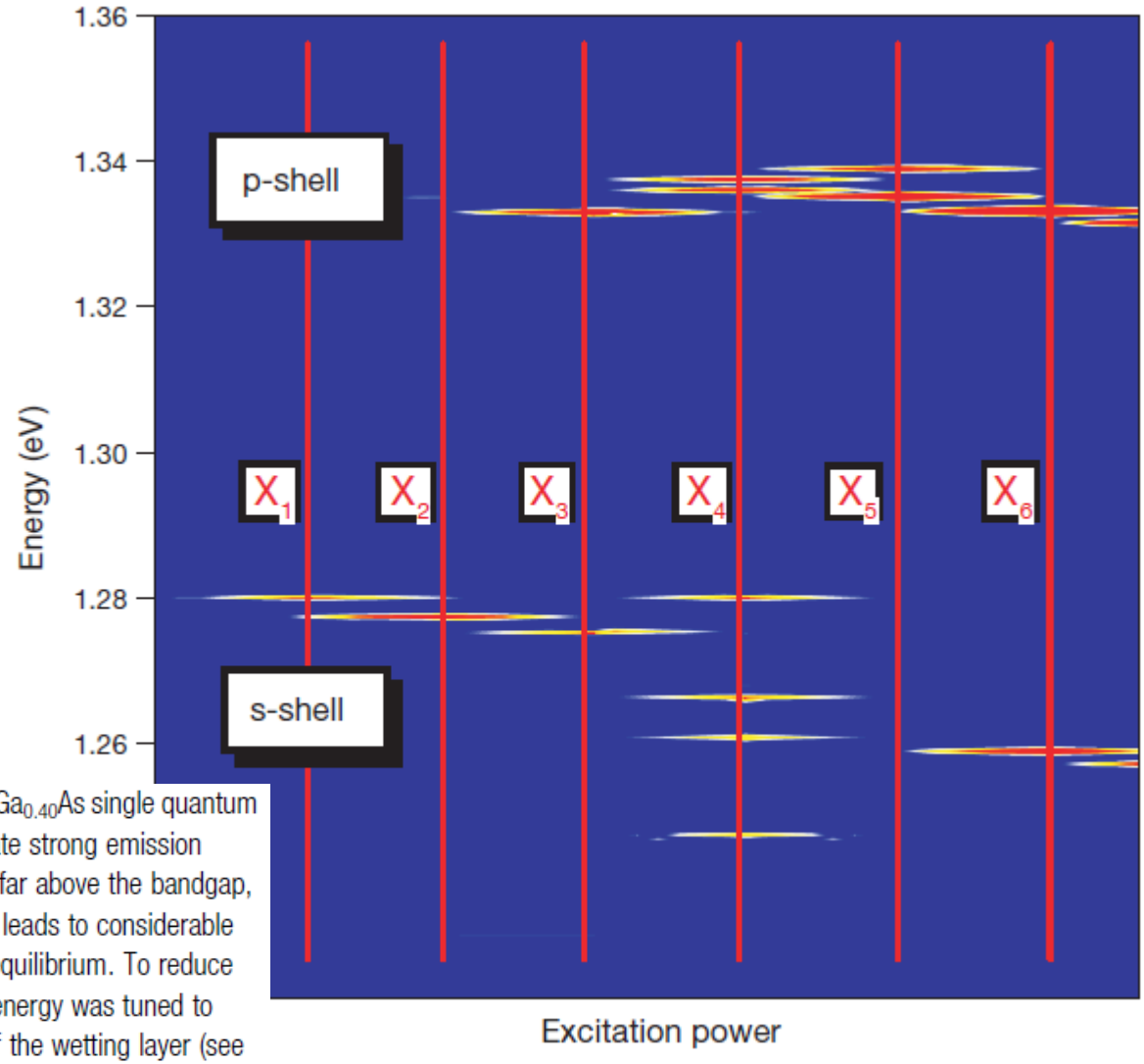


**Figure 3** Contour plot of the variation of the emission of an $In_{0.60}Ga_{0.40}As$ single quantum dot with excitation power and with energy. Bright regions indicate strong emission intensities, blue regions low intensities. When optically exciting far above the bandgap, carrier relaxation involving multiple phonon emission processes leads to considerable sample heating, which causes the system to be in strong non-equilibrium. To reduce heating, a Ti-sapphire laser was used as excitation source. Its energy was tuned to $E = 1.470$ eV, corresponding to emission close to the bottom of the wetting layer (see Fig. 2). The excitation power $P_{ex}$ was varied between 50 nW and 5 mW.

# THE ARTICLE

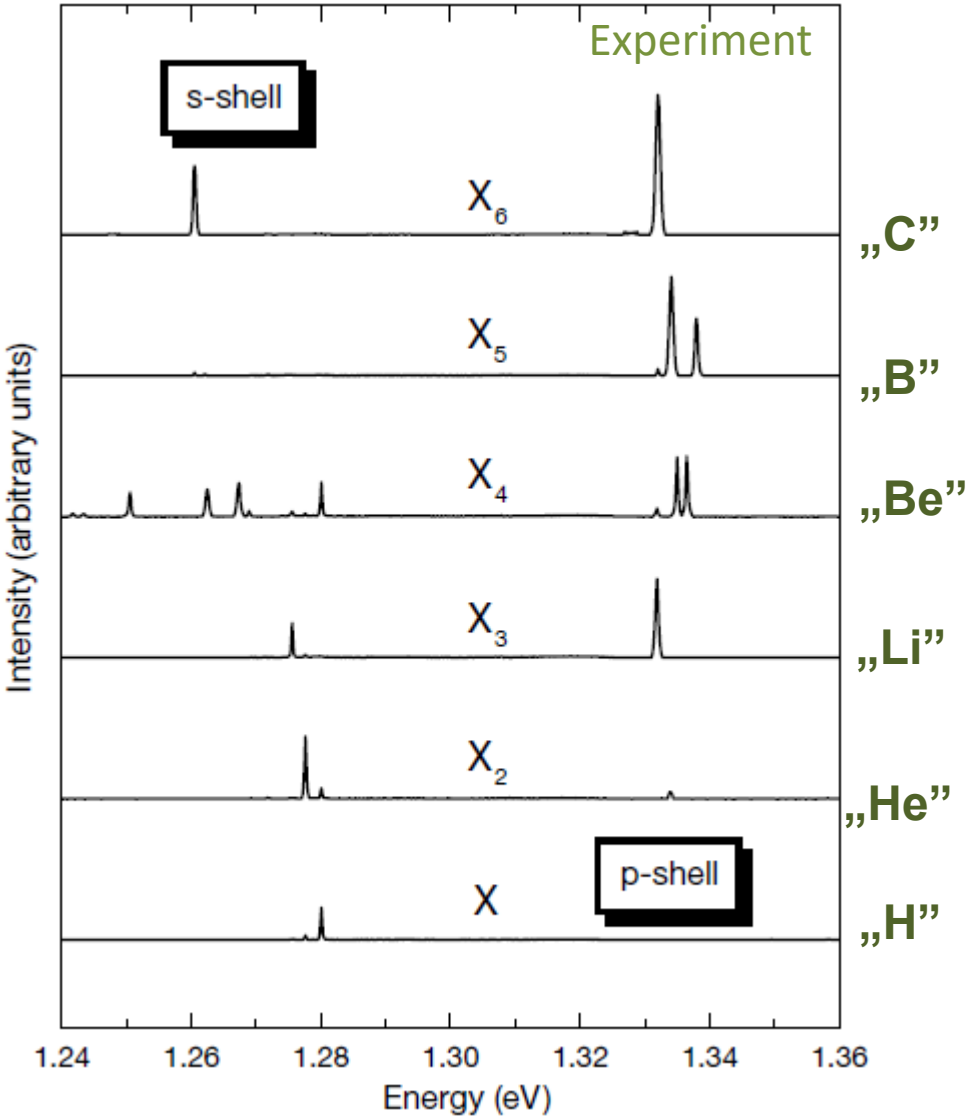
Experiment
s-shell
p-shell
X6
X5
X4
X3
X2
X
„C”
„B”
„Be”
„Li”
„He”
„H”
Intensity (arbitrary units)
1.24
1.26
1.28
1.30
1.32
1.34
1.36
Energy (eV)

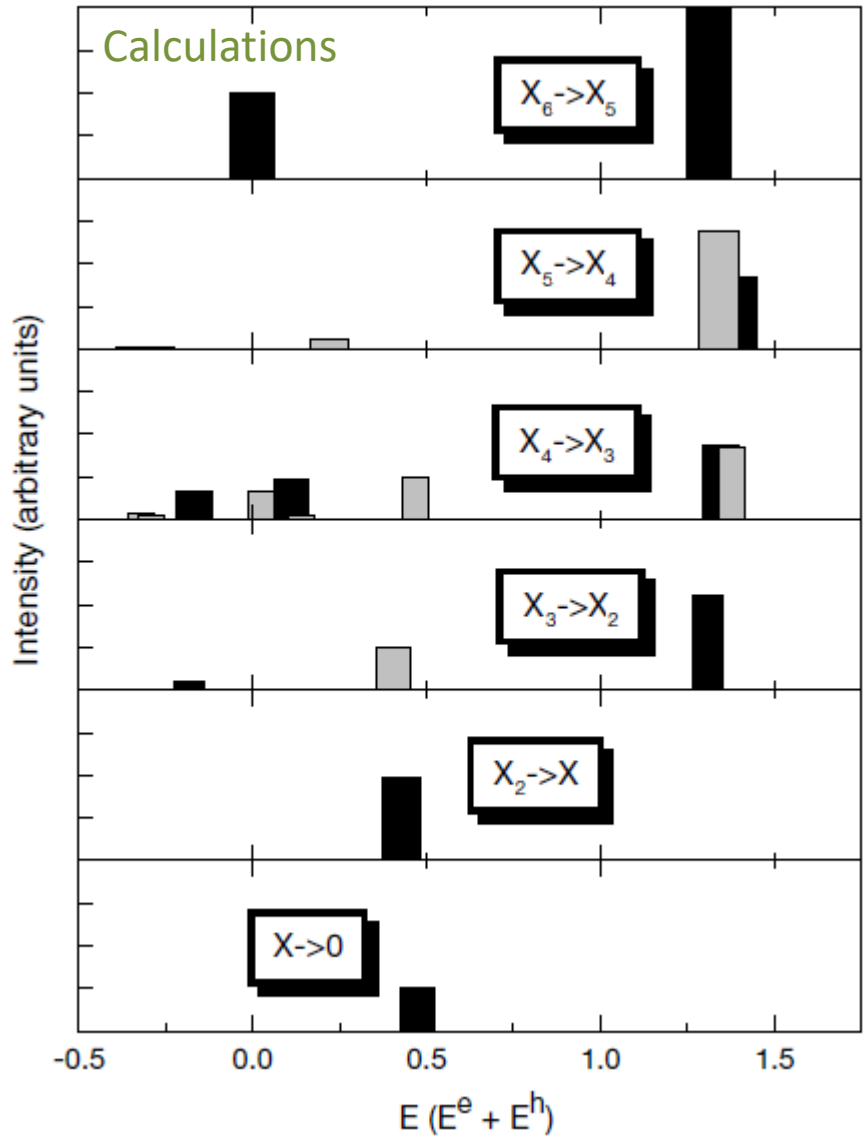
Calculations
X6->X5
X5->X4
X4->X3
X3->X2
X2->X
X->0
Intensity (arbitrary units)
-0.5
0.0
0.5
1.0
1.5
E (Ee + Eh)

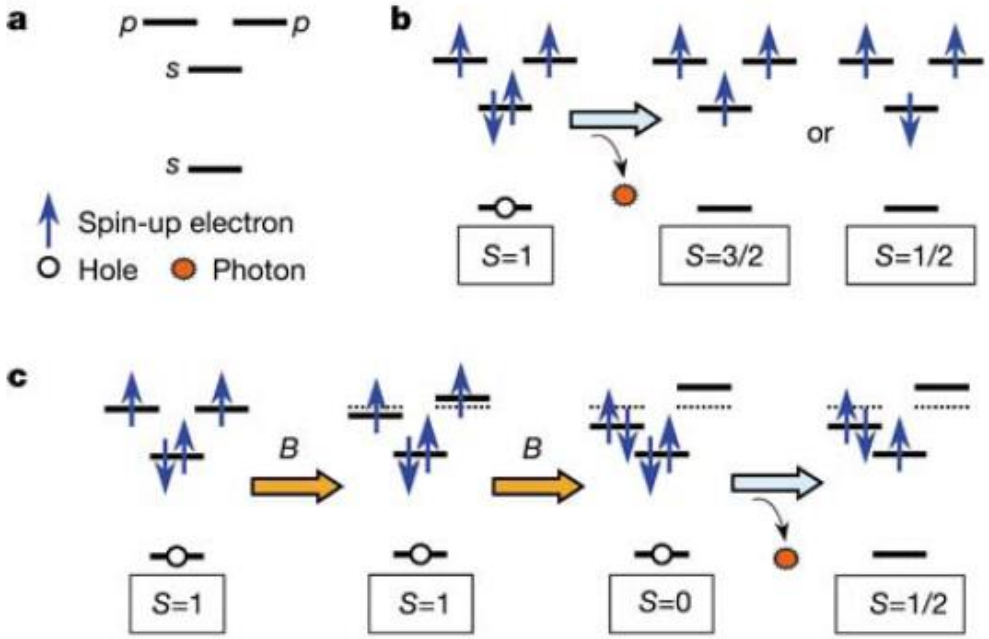


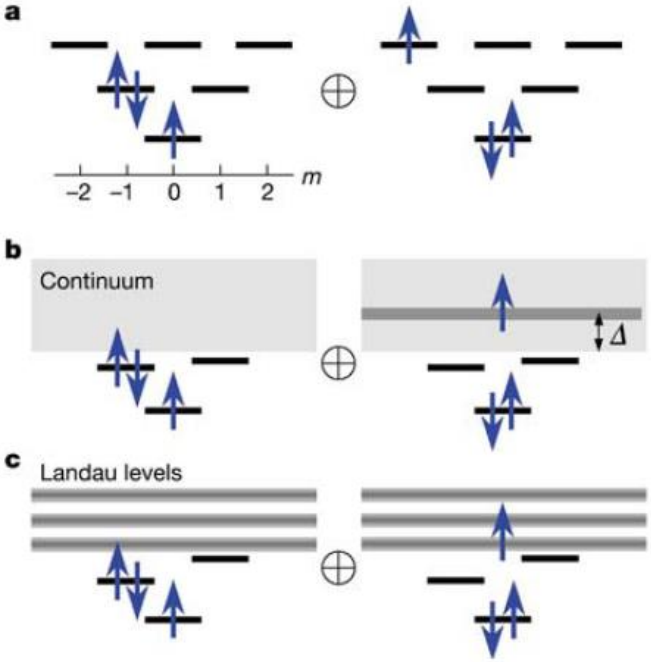


K.Karrai et al., *Nature* **427,** 135 (2004)

# Spherical quantum dots

The energy gap in spherical quantum dots [Brus, L. E. J. Phys. Chem. 1986, **90**, 2555, Brus. L. E. J. Chem. Phys. 1984, **80**, 4403]

$$E_g^*(R) = E_g^{bulk} + \frac{\hbar^2\pi^2}{2R^2 m_0}\left(\frac{1}{m_e} + \frac{1}{m_h}\right) - \frac{1.8e^2}{4\pi\varepsilon\varepsilon_0 R}$$

$R$ – diameter

Quantum localization: the smaller the particle - more vectors $k$ needed to describe the state of the carrier. So the particle is in the well! INCREASES the energy

Part of the Coulomb $e - h$ interaction reduces energy. Calculated for the hydrogen-like state $\Psi_n(r)$ $(n = 1)$ :

$$\varepsilon_n = \frac{\hbar^2 k_n^2}{2m} = \frac{\hbar^2 n^2 \pi^2}{2mL^2}$$

$$\Psi_n(r) = \frac{C_n}{r}\sin\left(\frac{n\pi r}{R}\right)$$

# Spherical quantum dots

The energy gap in spherical quantum dots [Brus, L. E. J. Phys. Chem. 1986, **90**, 2555, Brus. L. E. J. Chem. Phys. 1984, **80**, 4403]

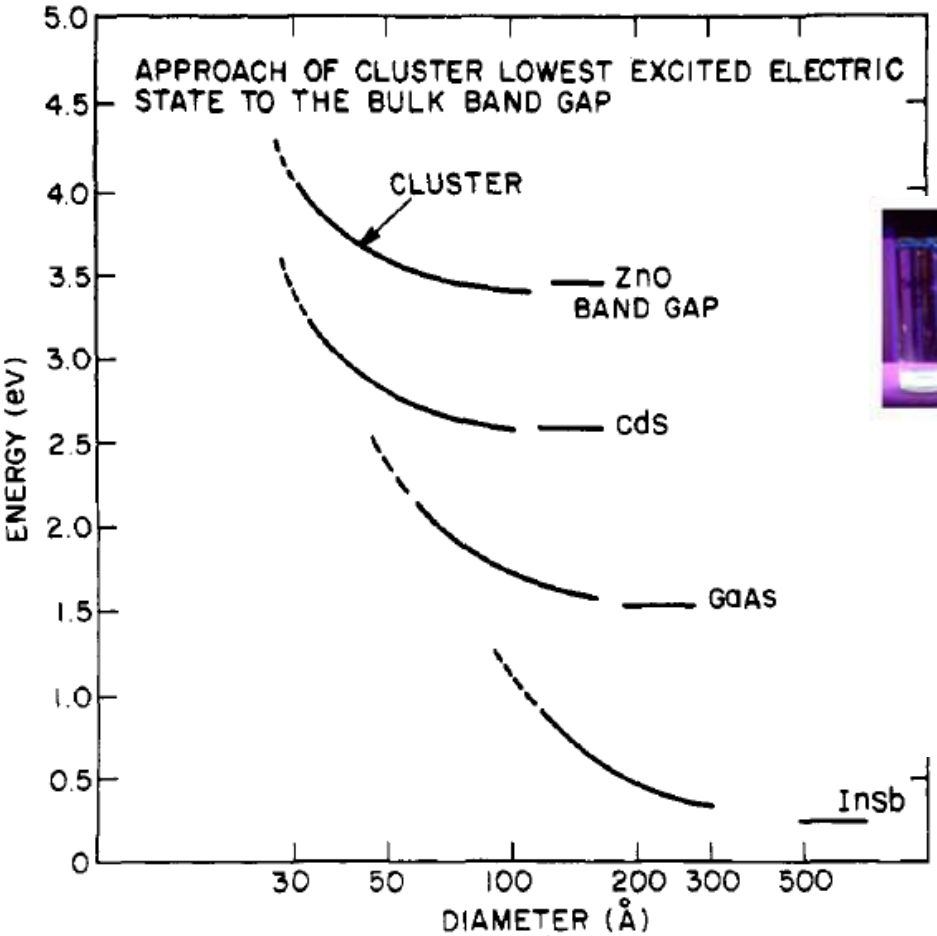


**Figure 5.** Calculated energy of the cluster lowest excited electronic state in relation to the bulk band gap. Adapted from ref 31.

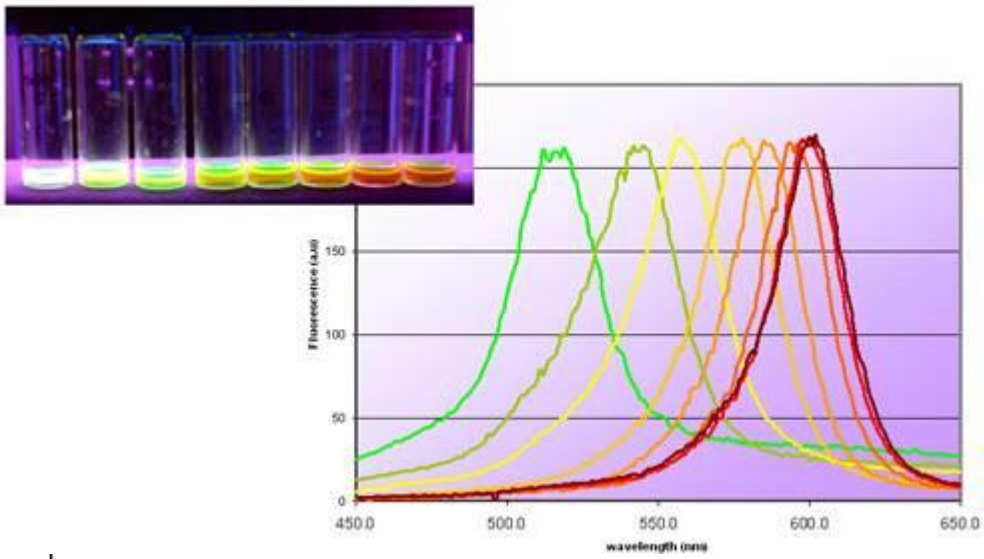


http://www.sussex.ac.uk/Users/kaf18/QDSpectra.jpg

# Spherical quantum dots

Current Opinion in Chemical Biology 2006, 10:423–429 *Nanoscale controlled self-assembled monolayers and quantum dots*

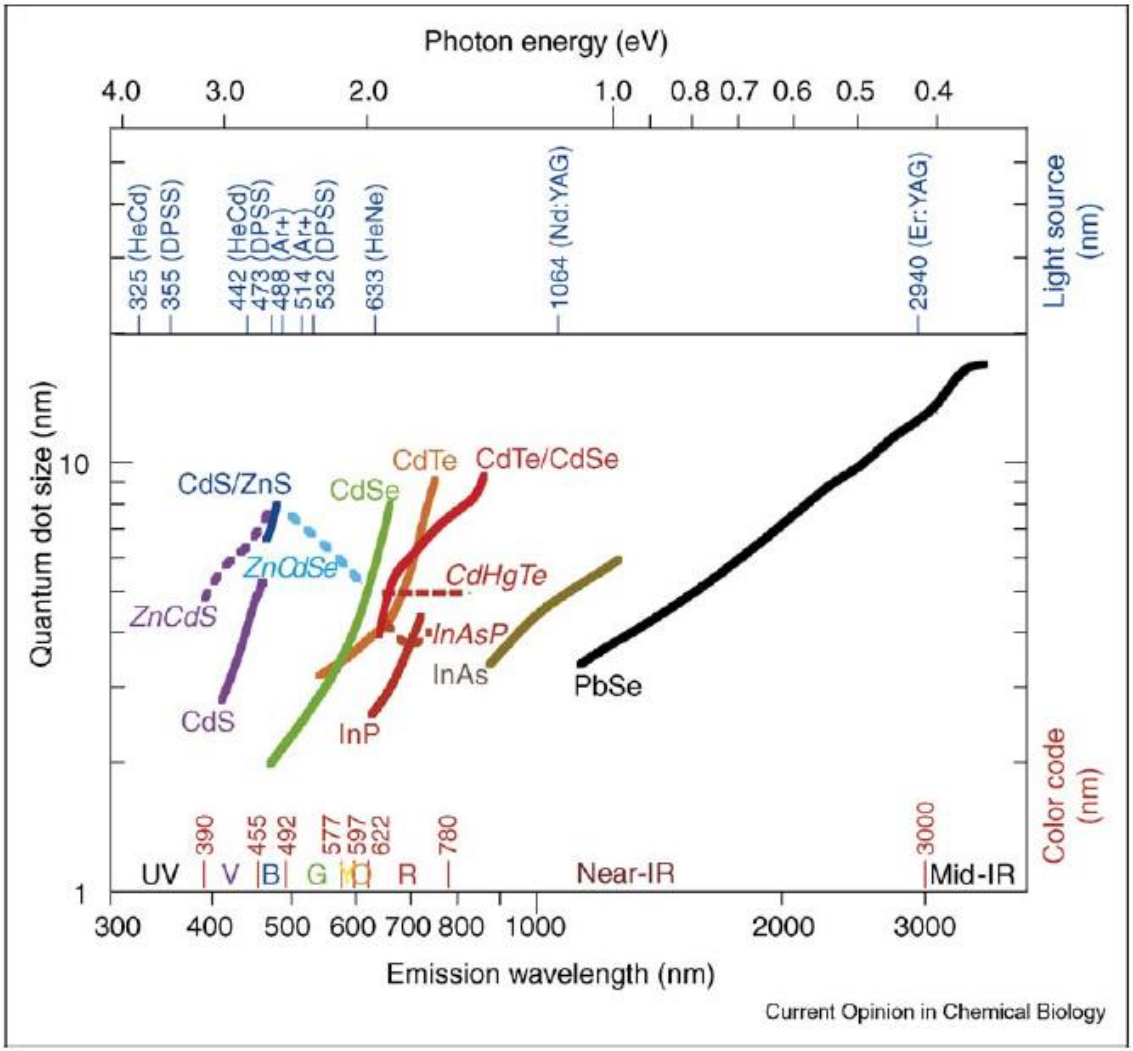

# Spherical quantum dots

The energy gap in spherical quantum dots [Brus, L. E. J. Phys. Chem. 1986, **90**, 2555, Brus. L. E. J. Chem. Phys. 1984, **80**, 4403]

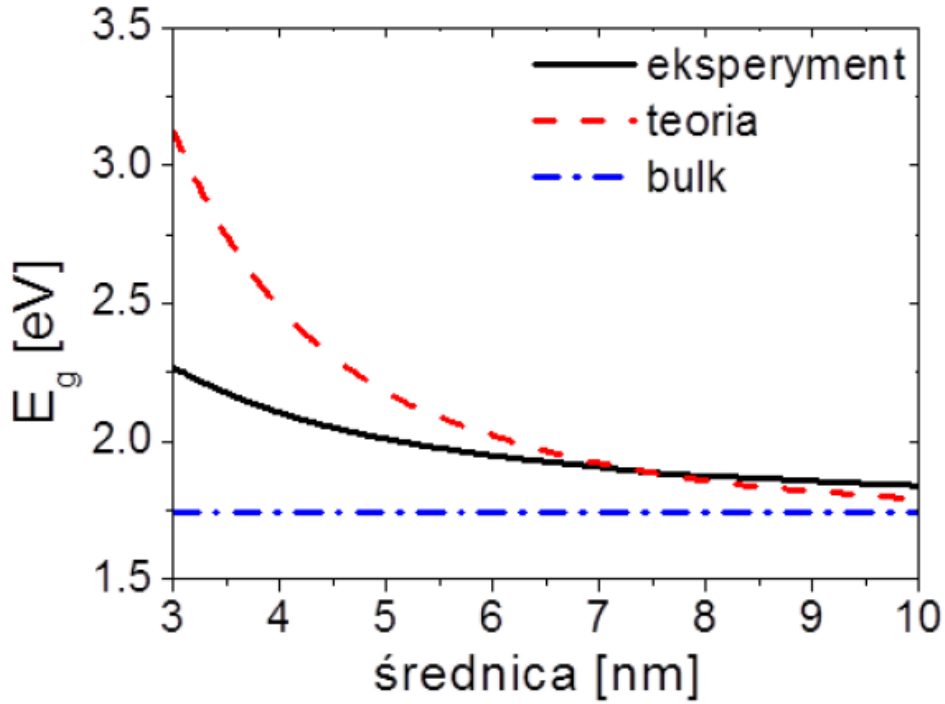


Przerwa energetyczna CdSe

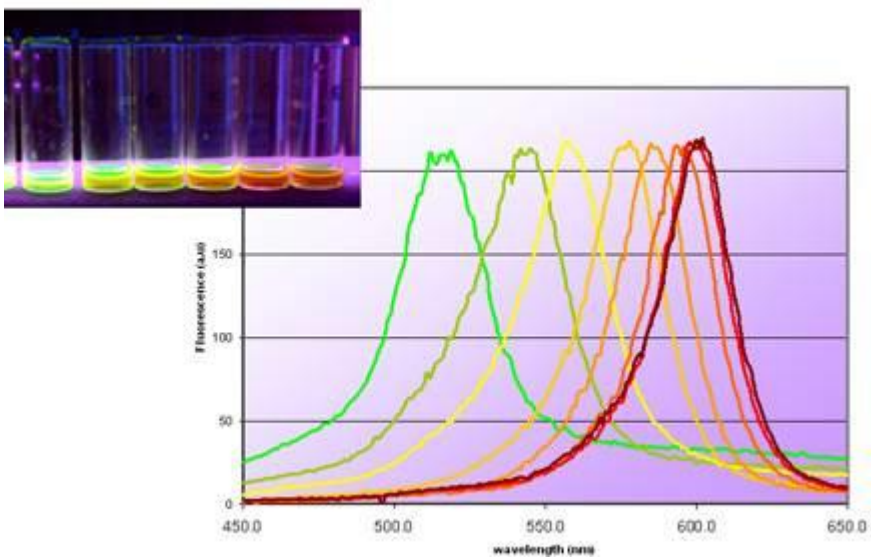


http://www.sussex.ac.uk/Users/kaf18/QDSpectra.jpg

# Spherical quantum dots

The energy gap in spherical quantum dots [Brus, L. E. J. Phys. Chem. 1986, **90**, 2555, Brus. L. E. J. Chem. Phys. 1984, **80**, 4403]

$$E_g^*(R) = E_g^{bulk} + \frac{\hbar^2\pi^2}{2R^2 m_0}\left(\frac{1}{m_e} + \frac{1}{m_h}\right) - \frac{1.8e^2}{4\pi\varepsilon\varepsilon_0 R}$$

$R$ – diameter

Quantum localization: the smaller the particle - more vectors $k$ needed to describe the state of the carrier. So the particle is in the well! INCREASES the energy

Part of the Coulomb $e - h$ interaction reduces energy. Calculated for the hydrogen-like state $\Psi_n(r)$ $(n = 1)$ :

$$\varepsilon_n = \frac{\hbar^2 k_n^2}{2m} = \frac{\hbar^2 n^2 \pi^2}{2mL^2}$$

$$\Psi_n(r) = \frac{C_n}{r}\sin\left(\frac{n\pi r}{R}\right)$$

# Optical transitions

$$\varepsilon_{e,n_e} = E_c^{GaAs} + \frac{\hbar^2\pi^2 n_e^2}{2m_0 m_e a^2}$$

$$\varepsilon_{h,n_h} = E_v^{GaAs} - \frac{\hbar^2\pi^2 n_h^2}{2m_0 m_h a^2}$$

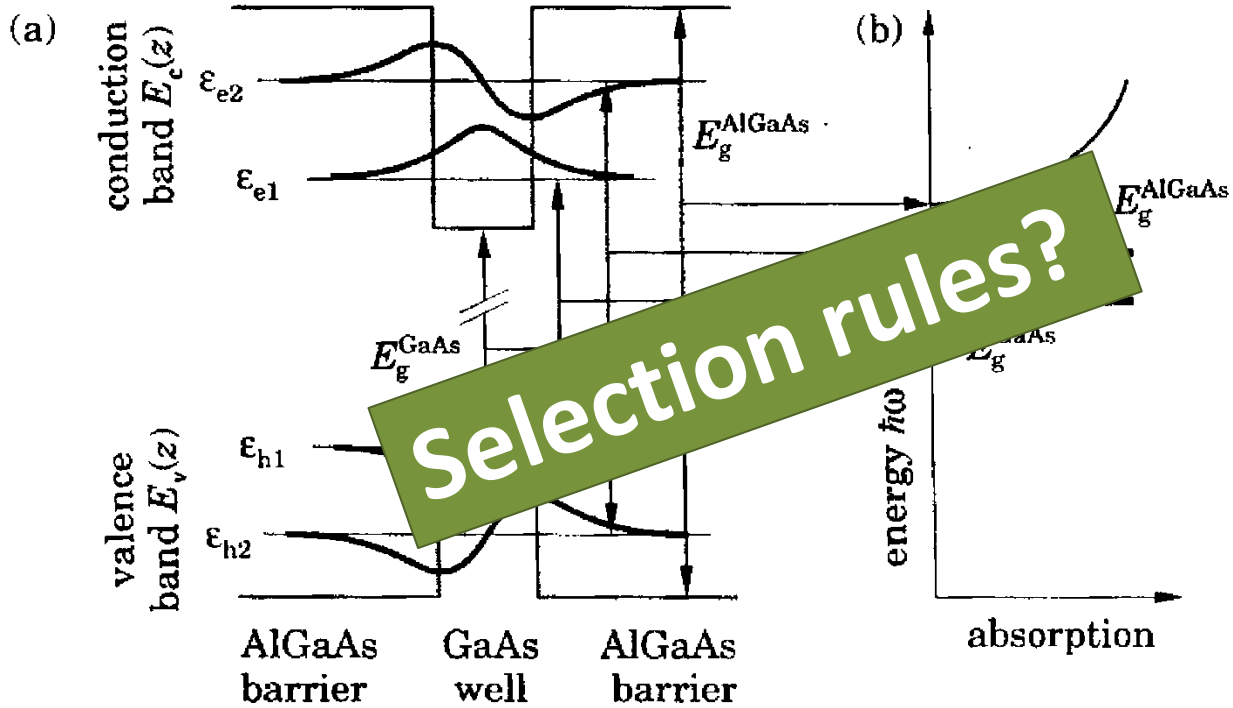


Selection rules?

$$\hbar\omega_n = \varepsilon_{e,n_e} - \varepsilon_{h,n_h} = E_g^{GaAs} + \frac{\hbar^2\pi^2 n^2}{2m_0 a^2}\left(\frac{1}{m_e} + \frac{1}{m_h}\right) = E_g^{GaAs} + \frac{\hbar^2\pi^2 n^2}{2m_0 m_{eh} a^2}$$

Optical effective mass $\frac{1}{m_{eh}} = \frac{1}{m_e} + \frac{1}{m_h}$

# Spherical quantum dots

# Spherical quantum dots

http://www.medicine.tcd.ie/molecular-medicine/gallery/pictures/scientific-pictures.php

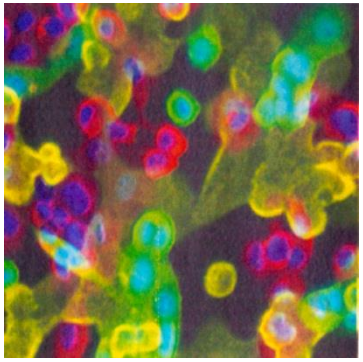

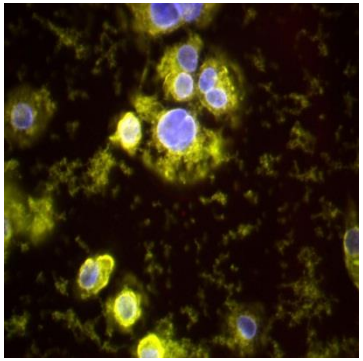

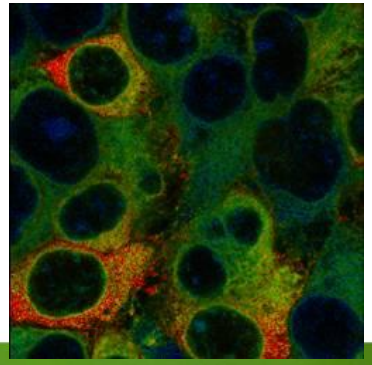

## Synthesis Techniques

- Vapor phase (molecular beams, flame synthesis etc…
- Solution phase synthesis
- Aqueous Solution
- Nonaqueous Solution
- Typically the rapid reduction of organmetallic precusors in hot organics with surfactants

## Semiconductor Nanoparticles

II-VI: CdS, CdSe, PbS, ZnS

III-V: InP, InAs

MO: $TiO_2$, ZnO, $Fe_2O_3$, PbO, $Y_2O_3$

# Spherical quantum dots

http://www.medicine.tcd.ie/molecular-medicine/gallery/pictures/scientific-pictures.php

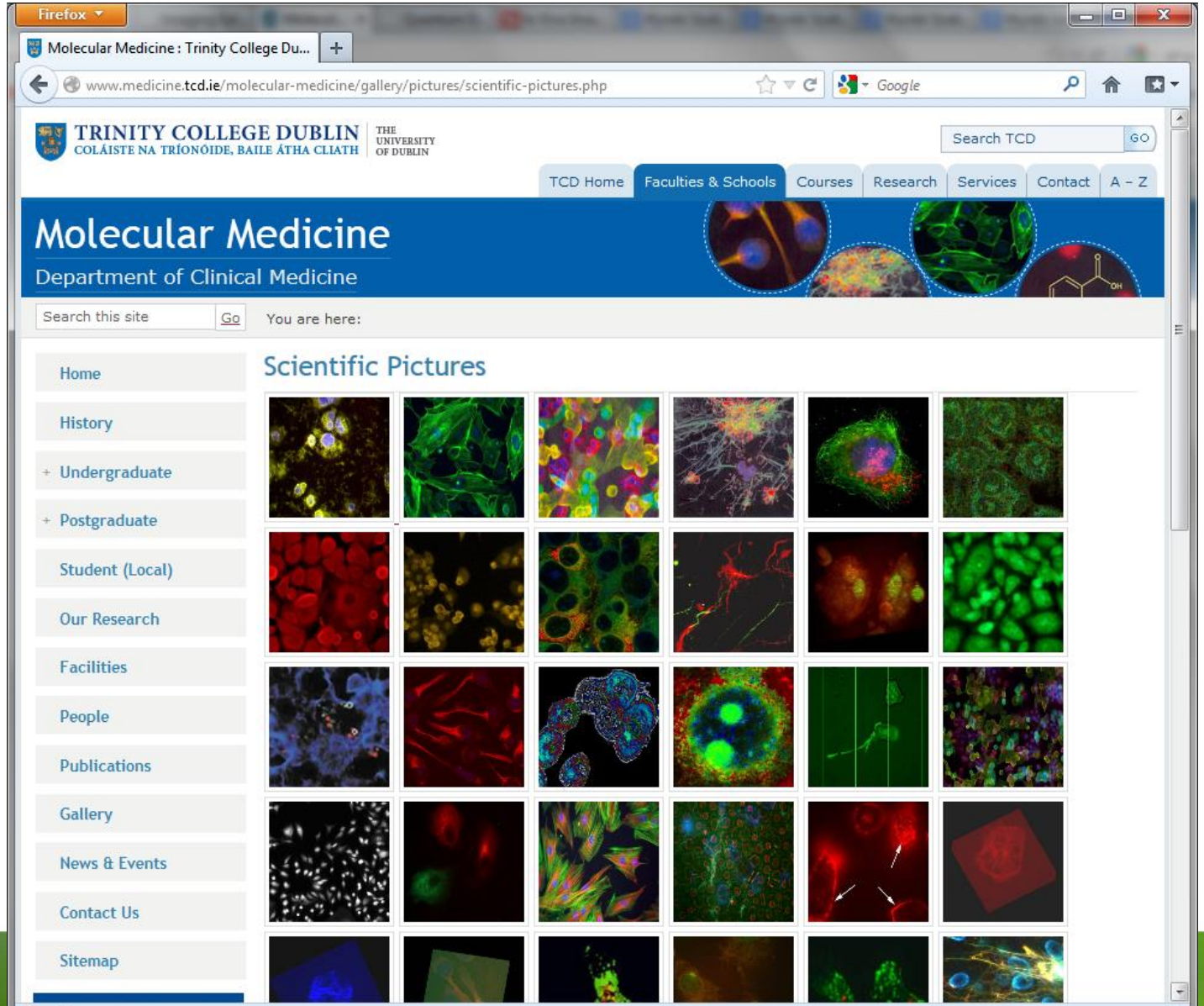


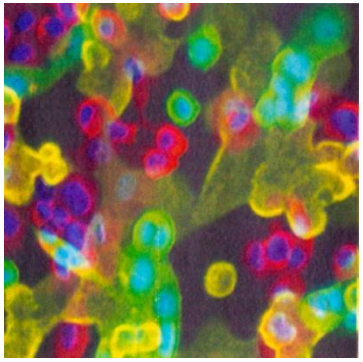

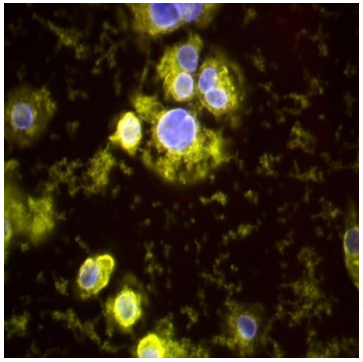

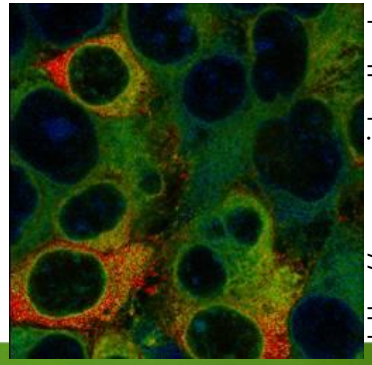

http://www.evidenttech.com/)

# Spherical quantum dots

http://www.microscopyu.com/articles/fluorescence/index.html

Firefox

Nikon MicroscopyU | Fluorescence Micr...

www.microscopyu.com/articles/fluorescence/index.html

INSTRUMENTS | NIKON EU | NIKONUSA | NIKON.COM

Nikon MICROSCOPYU
THE SOURCE FOR MICROSCOPY EDUCATION

HOME | TUTORIALS | GALLERIES | MICROSCOPY BASICS | SMALL WORLD | MUSEUM | DOWNLOADS | CONTACT

**Featured Sections**
- Live-Cell Imaging
- Fluorescence Microscopy
- Optical Systems
- Phase Contrast
- DIC Microscopy
- Confocal Microscopy
- Superresolution Microscopy
- Stereomicroscopy
- Polarized Light Microscopy
- Cell Motility Video Gallery
- Swept Field Video Gallery
- FRET Pair Combinations
- Featured Microscopists
- Microscopy Literature

CFI60 OPTICS

**Microscopy Digital Imaging**
- Digital Imaging Overview
- Basic Imaging Concepts
- Intro to CCD Cameras
- Matching Resolutions
- CCD Signal-to-Noise

Home > Fluorescence Microscopy

## Concepts in Fluorescence Microscopy

In the rapidly expanding fields of cellular and molecular biology, widefield and confocal fluorescence illumination and observation is becoming one of the techniques of choice. These techniques, which are almost universally employed in both the medical and biological sciences, have spurred the development of more sophisticated microscopes and numerous fluorescence accessories.

### Review Articles

**Introduction to Fluorescence Microscopy**
Basic equipment and techniques necessary for observing specimens in fluorescence.

**Basics of FRET Microscopy**
Using fluorescence to examine dynamic interactions between probes in living cells.

**Fluorescence *in situ* Hybridization**
Referred to as FISH, the technique is used primarily for chromosomal analysis.

**Introduction to Fluorescent Proteins**
Genetically-encoded fluorescent probes that are revolutionizing live-cell imaging.

**Stereomicroscopy Fluorescence Illumination**
Fluorescence Illuminators enable examination of large specimens in stereomicroscopy.

**Optical System and Detector Requirements**

**Total Internal Reflection Fluorescence**
TIRF restricts the excitation and detection of fluorophores to a thin region of the specimen.

**Multiphoton Microscopy**
Mode-locked pulsed lasers are used for deep tissue imaging and optical sectioning.

**Nikon Fluorescence Filter Sets**
Discussion of the properties of various fluorescence filter combinations.

**Fluorescent Protein Imaging Parameters**
Filter requirements, photobleaching, objective choice, highlighters, and multicolor imaging.

**Confocal Microscopy**
Confocal microscopy offers several advantages over conventional microscopy.

**Laser Safety Basics**

**Search MicroscopyU**
Enter Search Terms...
SEARCH

**Small World Competition**
- Enter the 2013 Contests
- 2013 Small World
- 2013 Small World In Motion
- Competition Rules
- Competition Prizes
- Small World Gallery
- 2011 Tour Schedule

**Interactive Flash Tutorial**

Matching Fluorophores with Nikon Filters

**Microscope Safety**
- Basic Ergonomics
- Laser Safety Tips

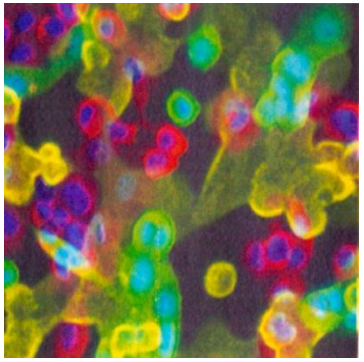

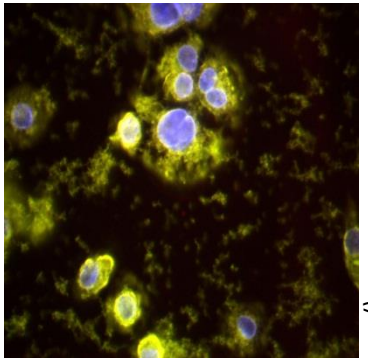

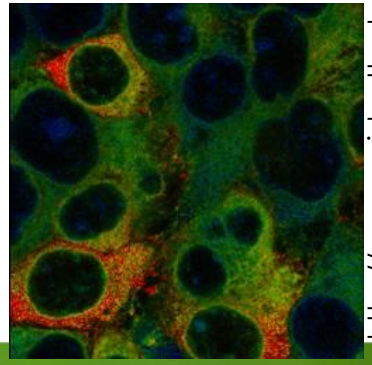

http://www.evidenttech.com/)

# Spherical quantum dots

Schematic illustration of bioconjugation methods. **(a)** Use of a bifunctional ligand such as mercaptoacetic acid for linking QDs to biomolecules [8••]. **(b)** TOPO-capped QDs bound to a modified acrylic acid polymer by hydrophobic forces. **(c)** QD solubilization and bioconjugation using a mercaptosilane compound [7••]. **(d)** Positively charged biomolecules are linked to negatively charged QDs by electrostatic attraction [9]. **(e)** Incorporation of QDs in microbeads and nanobeads [20••].

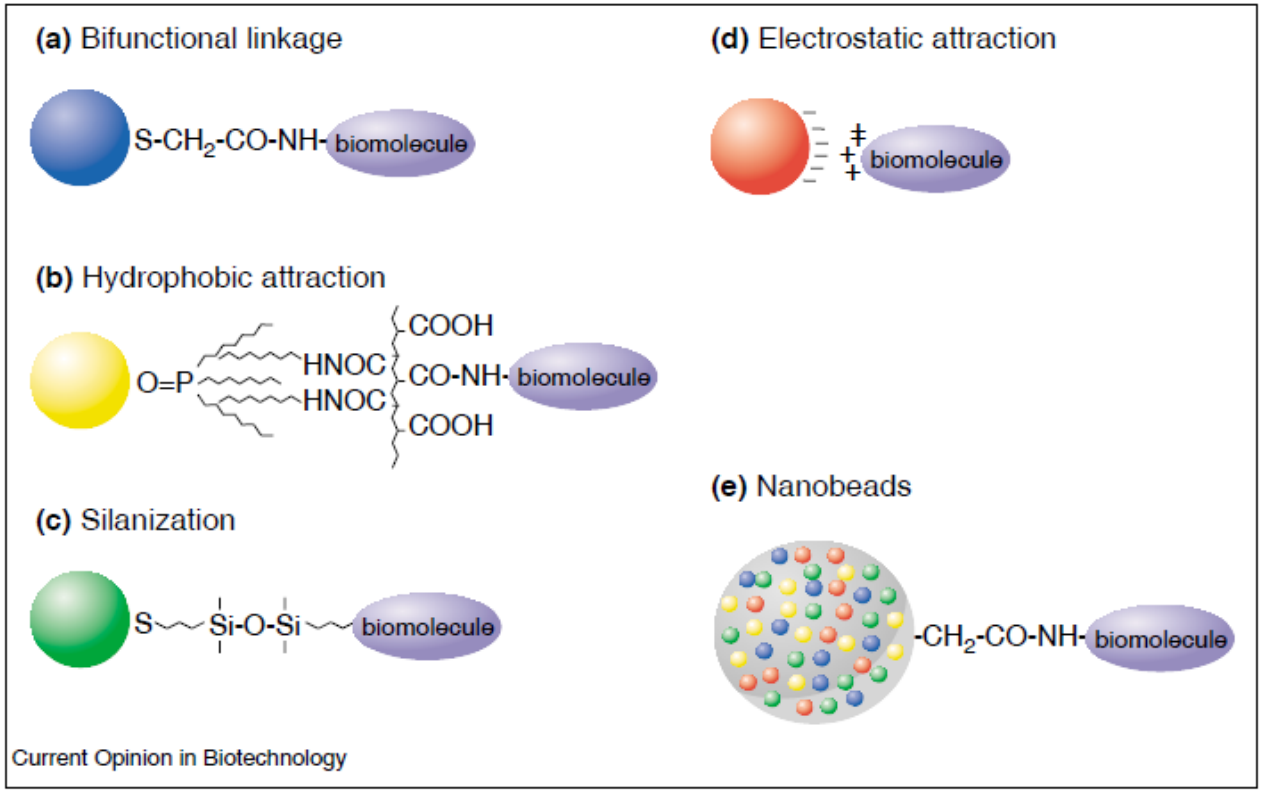


**Luminescent quantum dots for multiplexed biological detection and imaging**
W. Chan et al. Current Opinion in Biotechnology 2002, 13:40–46

# Spherical quantum dots

*In vivo molecular and cellular imaging with quantum dots* Xiaohu Gao Current Opinion in Biotechnology 2005, 16:63–72

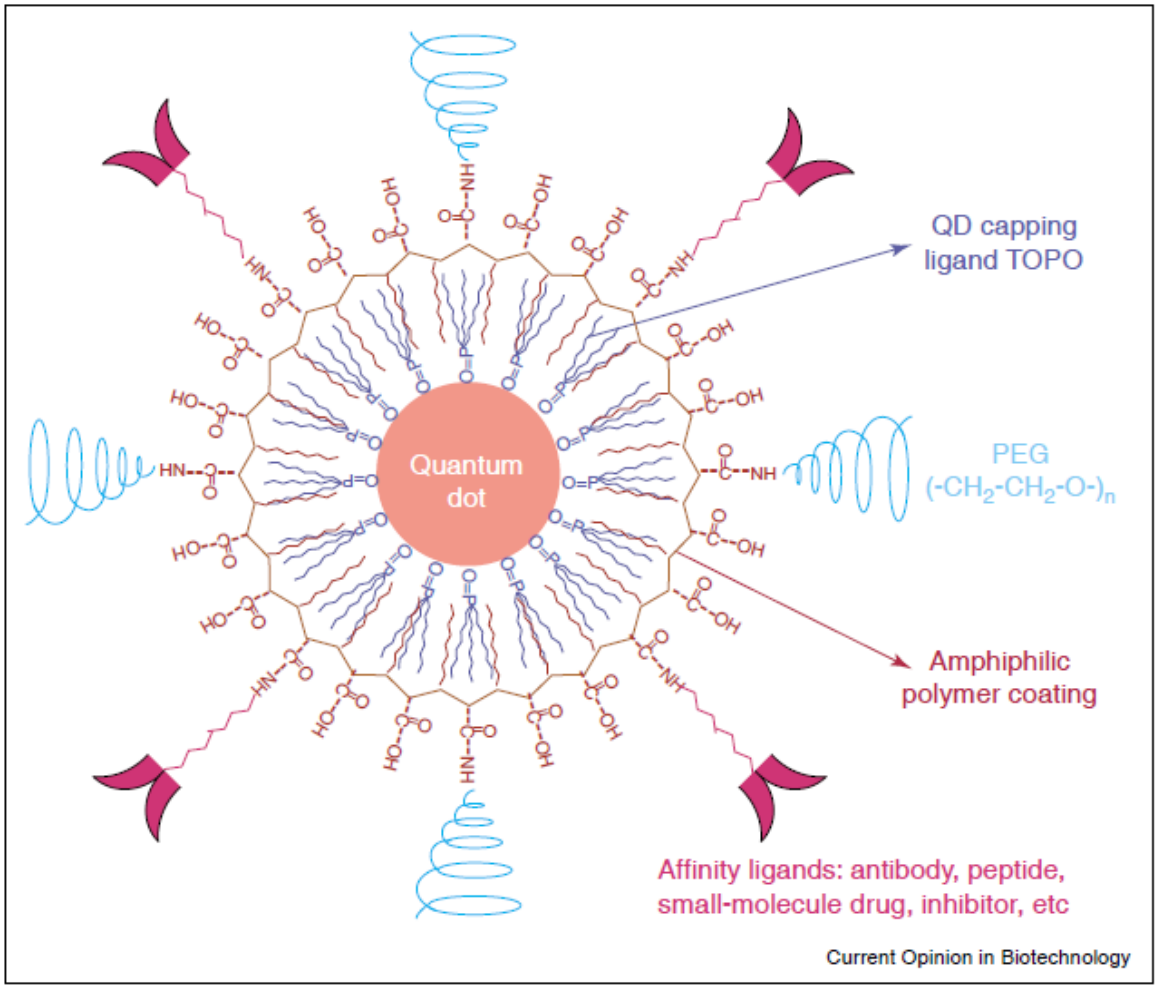


The structure of a multifunctional QD probe. Schematic illustration showing the capping ligand TOPO, an encapsulating copolymer layer, tumor-targeting ligands (such as peptides, antibodies or small-molecule inhibitors), and polyethylene glycol (PEG).

# Spherical quantum dots

*Synthesis of multi-shell nanocrystals by a single step coating process, Nanotechnology 2006*

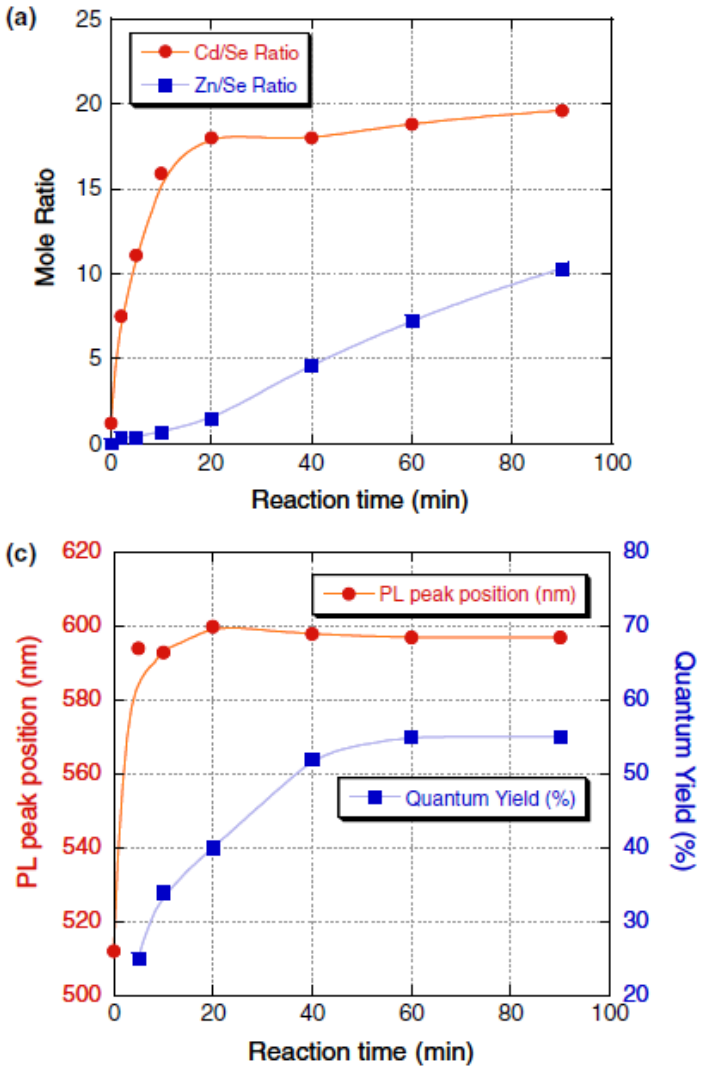


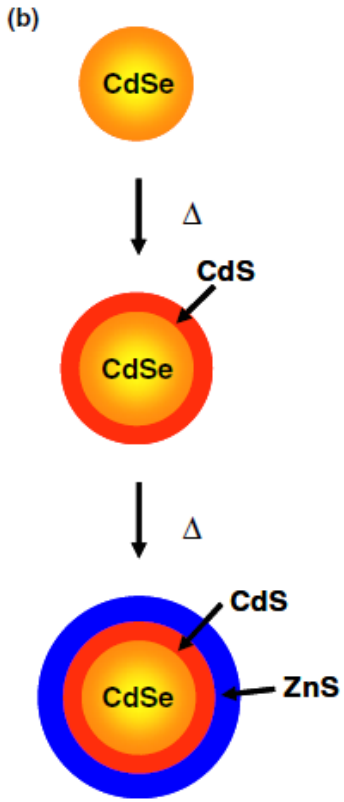


Quantum Yield = wydajność kwantowa

The **fluorescence quantum yield** is defined as the ratio of the number of emitted photons to the number of exciting photons absorbed by the substance at the same time and the same volume.

**Figure 1.** (a) Elemental ratios of Cd to Se and Zn to Se (measured by ICP), (b) a conceptual drawing of the CdSe core → CdSe/CdS core/shell → CdSe/CdS/ZnS core/multi-shell structure, and (c) PL peak positions, and QYs of CdSe/CdS/ZnS nanocrystals taken at different time intervals during the reaction.

# Spherical quantum dots

*In vivo molecular and cellular imaging with quantum dots* Xiaohu Gao Current Opinion in Biotechnology 2005, 16:63–72

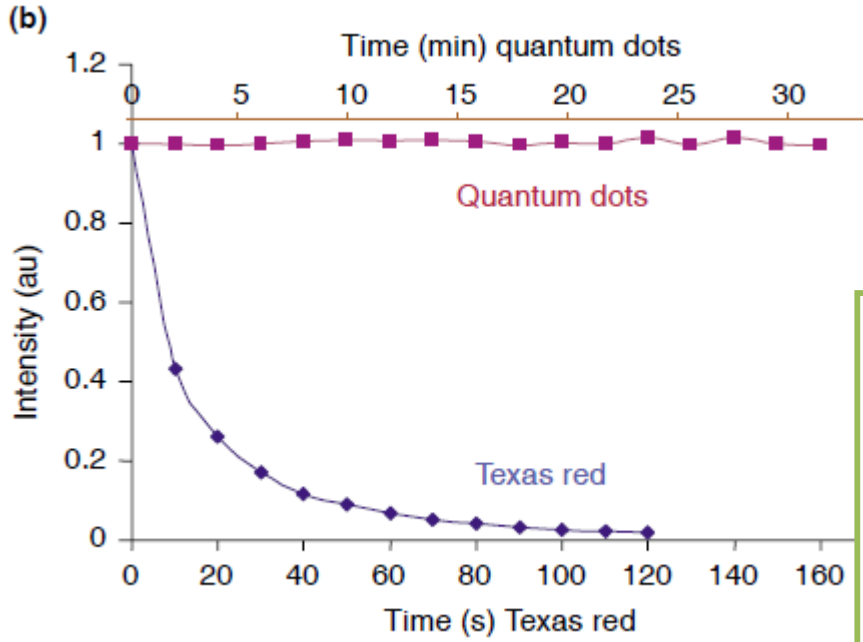


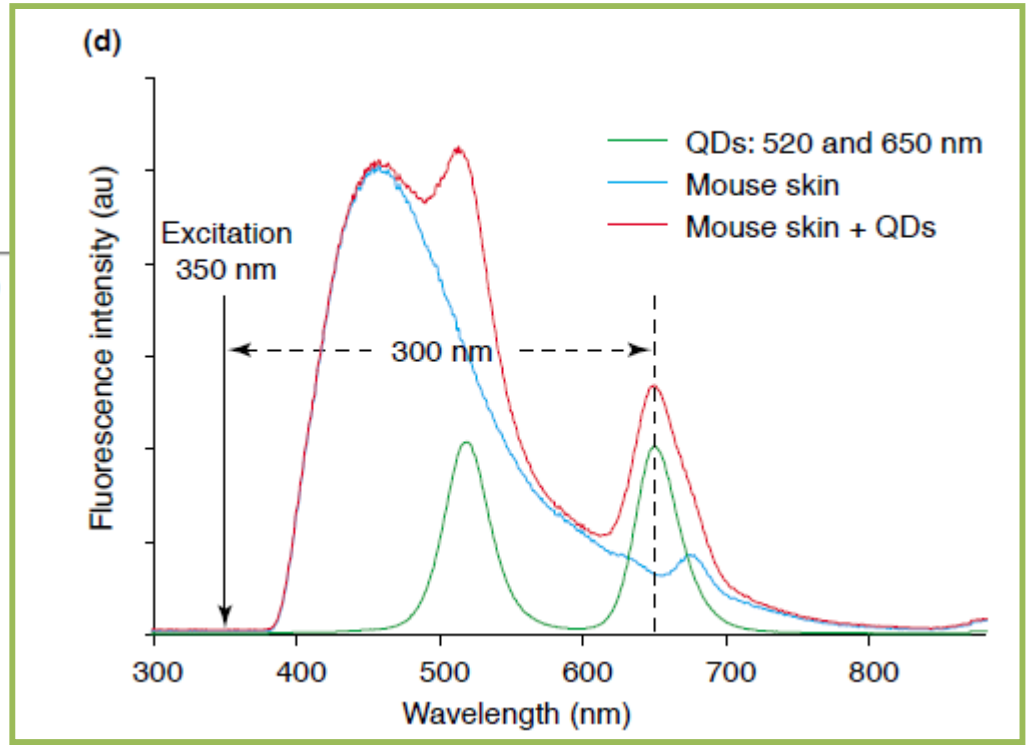

# Spherical quantum dots

Current Opinion in Chemical Biology 2006, 10:423–429 *Nanoscale controlled self-assembled monolayers and quantum dots*

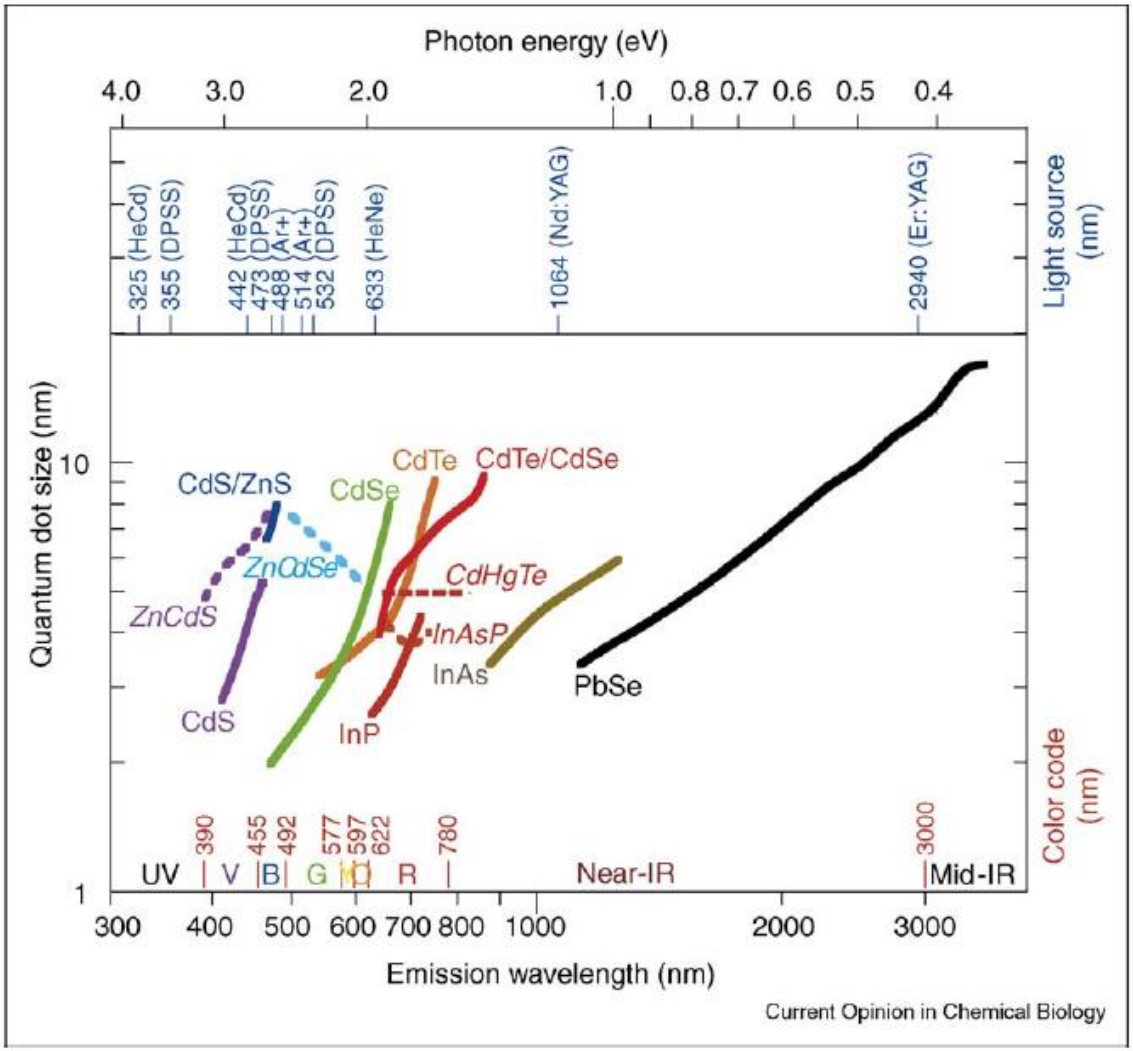

# Spherical quantum dots

Figure 4

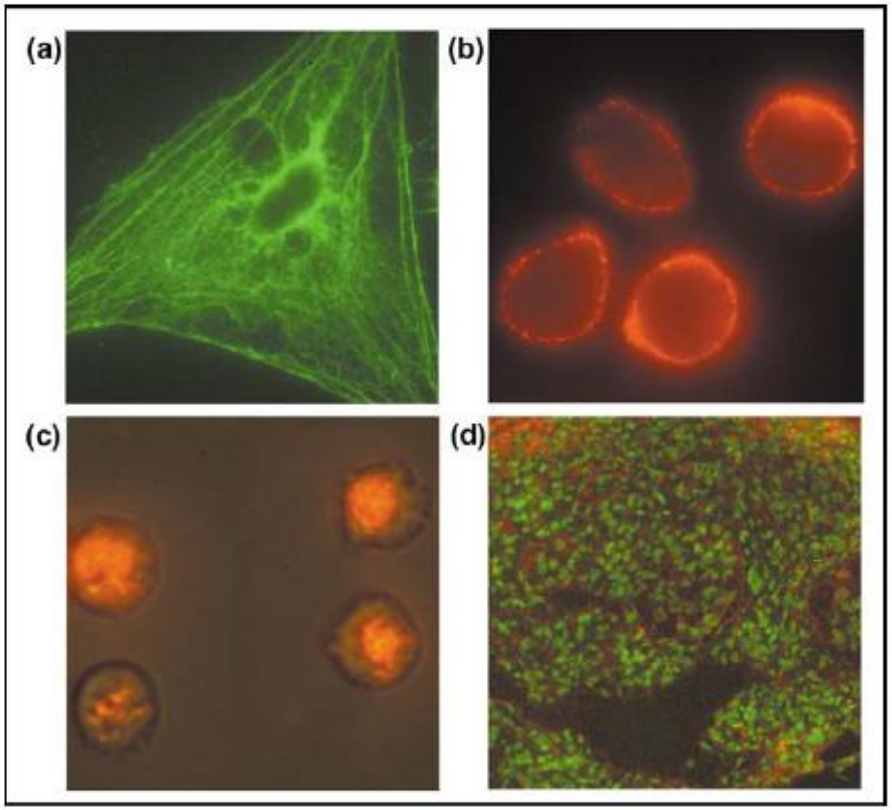


Fluorescence micrographs of QD-stained cells and tissues. **(a)** Actin staining (green QDs) on fixed 3T3 fibroblast cells. **(b)** Live MDA-MB-231 breast tumor cells labeled with a red QD–antibody conjugate targeting the urokinase plasminogen receptor. **(c)** Intracellular labeling of live mammalian cells using QD–Tat peptide conjugates [25••]. **(d)** Frozen tissue specimens stained with QDs (targeting the CXCR4 receptor, red) and a nuclear dye (green).

Figure 5

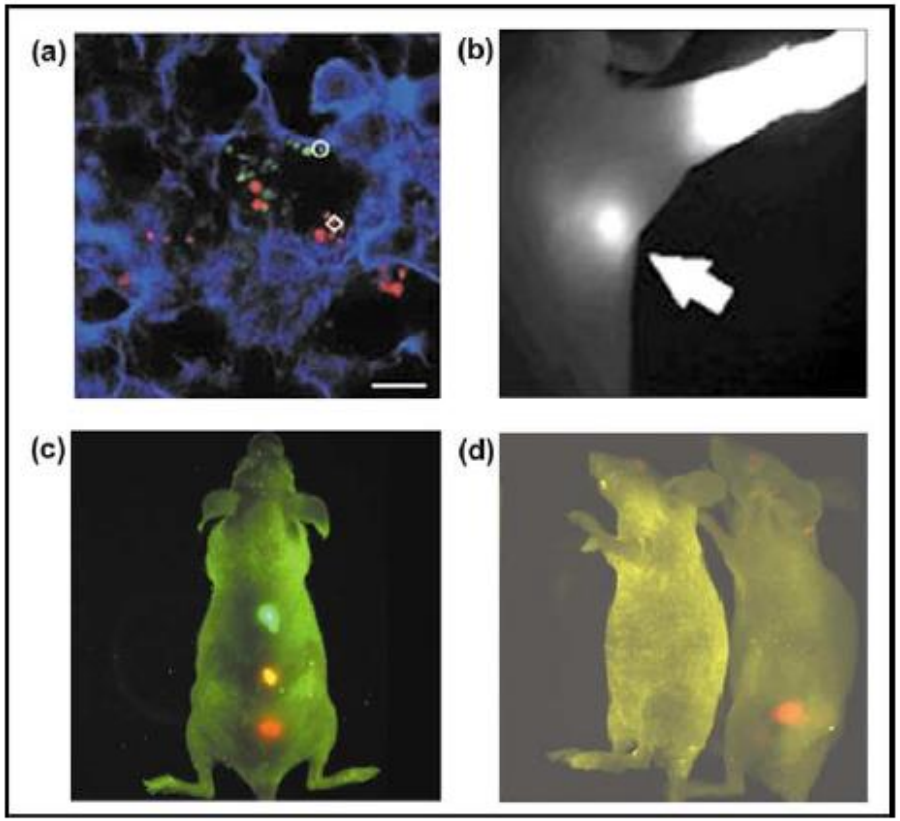


*In vivo* targeting and imaging with QDs. **(a)** *Ex vivo* tissue examination of QD-labeled cancer cells trapped in a mouse lung [44•]. **(b)** Near-infrared fluorescence of water-soluble type II QDs taken up by sentinel lymph nodes [49••]. **(c)** *In vivo* simultaneous imaging of multicolor QD-encoded microbeads injected into a live mouse [25••]. **(d)** Molecular targeting and *in vivo* imaging of a prostate tumor in mouse using a QD–antibody conjugate (red) [25••].

*In vivo molecular and cellular imaging with quantum dots*
Xiaohu Gao Current Opinion in Biotechnology 2005, 16:63–72

# Spherical quantum dots

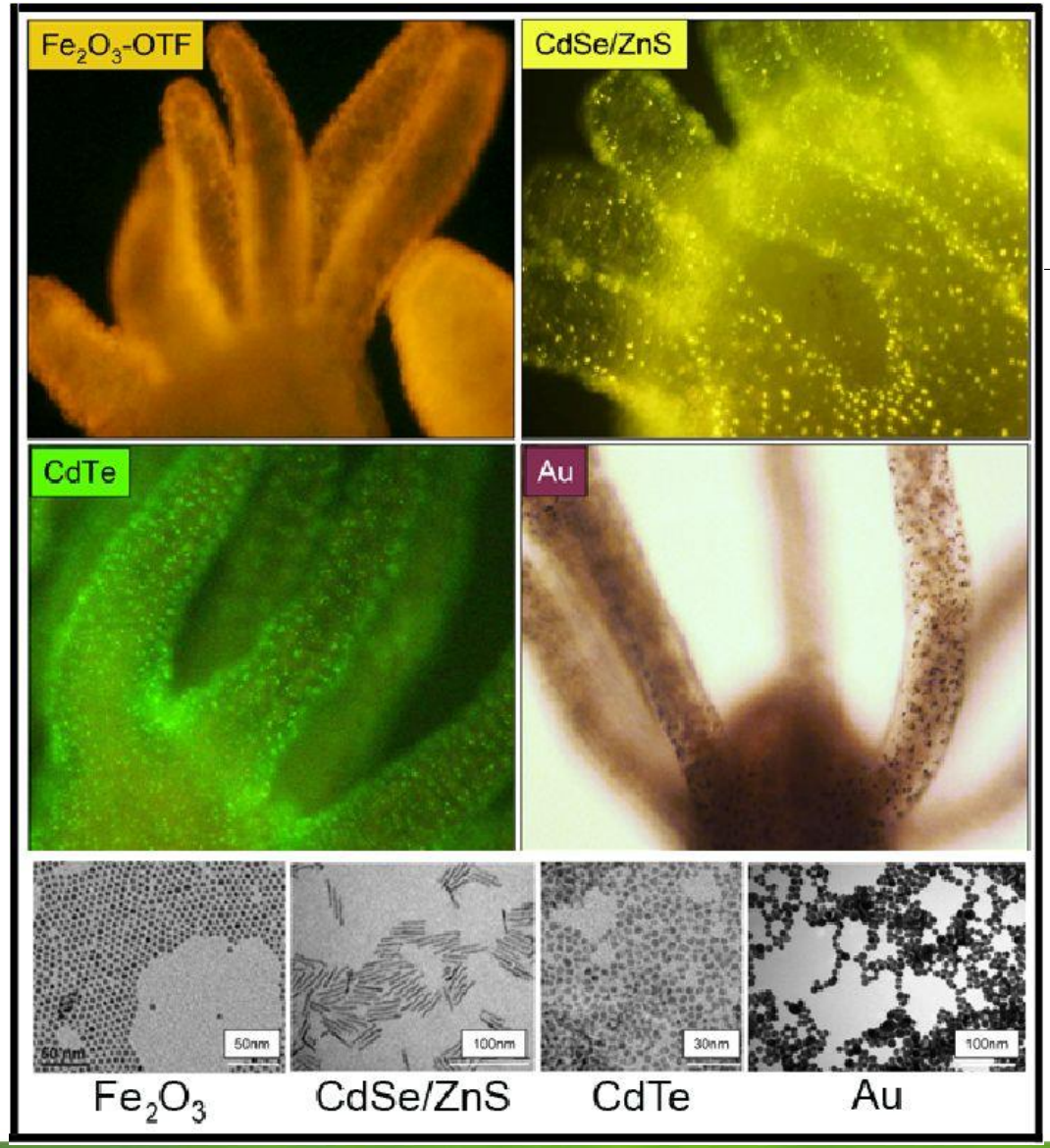


An Ancient Model Organism to Test In Vivo Novel Functional Nanocrystals

By Claudia Tortiglione

"Biomedical Engineering - From Theory to Applications", Edited by Reza Fazel-Rezai,

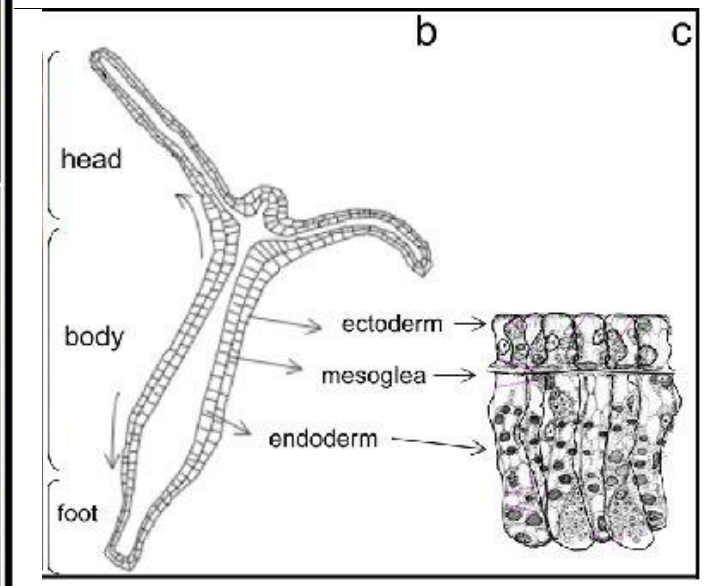


**Figure 1.**

Anatomical structure of *Hydra vulgaris*

**Figure 18.**

Labelling Hydra with nanocrystals

http://www.intechopen.com/books/biomedical-engineering-from-theory-to-applications/an-ancient-model-organism-to-test-in-vivo-novel-functional-nanocrystals

# Spherical quantum dots

**Magnetic Quantum Dot**

**What is MQD ?**

Justin Galloway

***Composite with A Novel Structure for Active Sensing in Living cells***

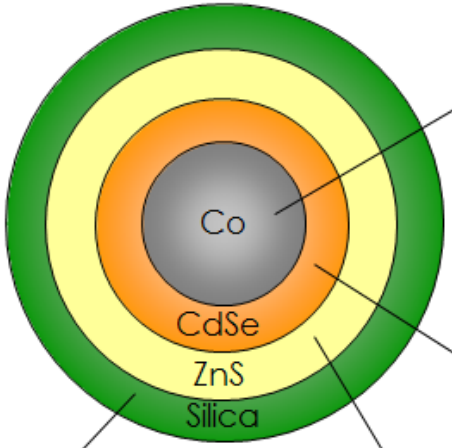


① **Cobalt core : active manipulation**

- diameter : ~10 nm
- superparamagnetic NPs

→ manipulated or positioned by an external field without aggregation in the absence of an external field

② **CdSe shell : imaging with fluorescence**

- thickness : 3-5 nm
- visible fluorescence (~450 – 700 nm)
- ability to tune the band gap

→ by controlling the thickness, able to tune the emission wavelength, i.e., emission color

③ **ZnS shell : electrical passivation**

- thickness : 1-2 nm
- having wider band gap (3.83 eV) than CdSe (1.91 eV)
- enhancement of QY

→ CdSe (5-10%) ⇒ CdSe/ZnS (~50%)

④ **Silica shell : bio-compatibility & functionalization with specific targeting group**

- thickness : ~10 nm
- bio-compatible, & non-toxic to live cell functions
- stable in aqueous environment
- ability to functionalize its surface with specific targeting group

# Spherical quantum dots

[1] Kawasaki et al. Nanotechnology, nanomedicine, and the development of new, effective therapies for cancer. *Nanomedicine: Nanotechnology, Biology, and Medicine.* 2005; 1:101, 109
[2] Alivisatos, et al. Quantum dots as cellular probes. *Annu. Rev. Biomed. Eng*. 2005; 7:55-76.
[3] Chan et al. Luminescent quantum dots for multiplexed biological detection and imaging. *Current opinion in biotechnology*. 2002; 13:40-46
[4] Michalet et al. Quantum dots for live cells, in vivo imaging, and diagnostics. *Science*. 2005; 307(5709): 538-544.
[5] Alivisatos A.P. Semiconductor clusters, nanocrystals, and quantum dots. *Science*. 1996; 271: 933-937.
[6] Gao et al. In vivo molecular and cellular imaging with quantum dots. *Current opinion in biotechnology*. 2005; 16:63-72.
[7] Shin et al. Nanoscale controlled self-assembled monolayers and quantum dots. *Current opinion in chemical biology.* 2006; 10(5): 423-429.
[8] Rogach et al. Infrared-emitting colloidal nanocrystals: synthesis, assembly, spectroscopy, and applications. *Small*. 2007; 3(4): 536-557.
[9] Weng, et al. Luminescent quantum dots: a very attractive and promising tool in biomedicine. *Current medicinal chemistry*. 2006; 13: 897-909.
[10] Fu, et al. Semiconductor nanoparticles for biological imaging. *Current opinion in neural biology*. 2005; 15:568-575.
[11] Hardman R. A toxicologic review of quantum dots: toxicity depends on physicochemical and environmental factors. *Environmental Health Perspectives*. 2006; 114(2): 165-172.

# Spectroscopy of nanostructures

131

# Selction rules in condensed matter

**Proof sketch**

Bloch function of a carrier in the crystal:

$$\Psi(\vec{r}) = \sum_{n,k} c_{n,k} u_{n,k}(\vec{r}) e^{i\vec{k}\vec{r}}$$

For the electron:

$$\Psi_{\mathrm{c}}(\vec{r}) \approx \sum_{k} c_{1,k} u_{\Gamma_6,0}(\vec{r}) e^{i\vec{k}\vec{r}} = u_{\Gamma_6,0}(\vec{r}) F_e(\vec{r})$$

For the hole:

$$\Psi_{\mathrm{v}}(\vec{r}) \approx \sum_{J_z = \pm 3/2, \pm 1/2, k} c_{J_z,k} u_{\Gamma_8,J_z}(\vec{r}) e^{i\vec{k}\vec{r}} = \sum_{J_z = \pm 3/2, \pm 1/2, k} u_{\Gamma_8,J_z}(\vec{r}) F_{J_z}(\vec{r})$$

Intersubband dipole optical transitions:

$$\langle \Psi_{\mathrm{c}}(\vec{r}) | \vec{p} | \Psi_{\mathrm{v},J_z}(\vec{r}) \rangle = \langle u_{\Gamma_6,0}(\vec{r}) | u_{\Gamma_8,J_z}(\vec{r}) \rangle \langle F_e(\vec{r}) | \vec{p} | F_{J_z}(\vec{r}) \rangle + \langle u_{\Gamma_6,0}(\vec{r}) | \vec{p} | u_{\Gamma_8,J_z}(\vec{r}) \rangle \langle F_e(\vec{r}) | F_{J_z}(\vec{r}) \rangle$$

# Time-dependent perturbation theory

General solution of Schrödinger equation

$$i\hbar \frac{\partial}{\partial t}\,\psi(\vec{r},t) = -\frac{\hbar^2}{2m}\,\nabla^2\psi(\vec{r},t) + V(\vec{r},t)\psi(\vec{r},t)$$

Time-independent potential

$$H_0 = -\frac{\hbar^2}{2m}\frac{\partial^2}{\partial x^2} + U(x) \qquad \psi(x,t) = A\varphi_m(x)e^{-iE_m t/\hbar}$$

Time-~~in~~dependent potential $\quad H = H_0 + V(t)$

The simplest case:

$$V(t) = \begin{cases} W(t) & \text{dla } 0 \le t \le \tau \\ 0 & \text{dla } t < 0 \text{ i } t > \tau \end{cases}$$

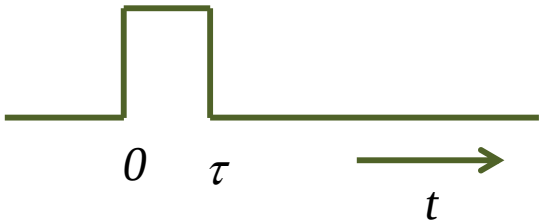

# Time-dependent perturbation theory

Time-dependent Schrödinger equation:

$$i\hbar\frac{\partial}{\partial t}\psi = H_0 + V(t)$$

$$\psi(x,t) = \sum_n A_n(t)\varphi_n(x)e^{-iE_n t/\hbar}$$

By analogy

Time-independent potential

$$H_0 = -\frac{\hbar^2}{2m}\frac{\partial^2}{\partial x^2} + U(x)$$

$$\psi(x,t) = A\varphi_m(x)e^{-iE_m t/\hbar}$$

Time-~~in~~dependent potential

$$H = H_0 + V(t)$$

The simplest case:

$$V(t) = \begin{cases} W(t) & \text{dla } 0 \le t \le \tau \\ 0 & \text{dla } t < 0 \text{ i } t > \tau \end{cases}$$

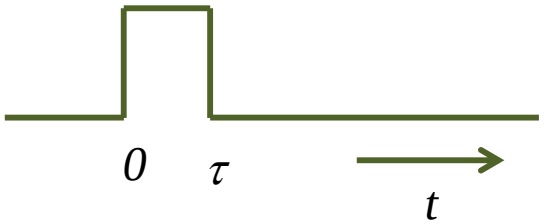

# Time-dependent perturbation theory

Time-dependent Schrödinger equation:

$$i\hbar\frac{\partial}{\partial t}\psi = H_0 + V(t)$$

$$\psi(x,t) = \sum_n A_n(t)\varphi_n(x)e^{-iE_n t/\hbar}$$

For $t < 0$ the system was in the initial state $m$

$$\psi(x, t < 0) = \varphi_m(x)e^{-iE_m t/\hbar}$$

For $t > \tau$ the system will be in a different state

$$\psi(x, t > \tau) = \sum_n A_{nm}(\tau)\varphi_n(x)e^{-iE_n t/\hbar}$$

wherein the probability that the system will be in a steady state of energy $E_n$ is given by the transition probability at time $\tau$ from an initial state $m$ to a state $n$.

$$w_{mn} = |A_{mn}(\tau)|^2$$

Functions $\varphi_n(x)$ are eigenstates of the Hamiltonian, i.e.: $H_0\varphi_n(x) = E_n^0\varphi_n(x)$

i.e. $H_0|n\rangle = E_n^0|n\rangle$

We have to compute: $i\hbar\frac{\partial}{\partial t}\psi(x,t)$

# Time-dependent perturbation theory

Time-dependent Schrödinger equation:

$$i\hbar\frac{\partial}{\partial t}\psi = H_0 + V(t)$$

$$\psi(x,t) = \sum_n A_n(t)\varphi_n(x)e^{-iE_n t/\hbar}$$

For $t < 0$ the system was in the initial state $m$

$$\psi(x, t < 0) = \varphi_m(x)e^{-iE_m t/\hbar}$$

For $t > \tau$ the system will be in a different state

$$\psi(x, t > \tau) = \sum_n A_{nm}(\tau)\varphi_n(x)e^{-iE_n t/\hbar}$$

wherein the probability that the system will be in a steady state of energy $E_n$ is given by the transition probability at time $\tau$ from an initial state $m$ to a state $n$.

$$w_{mn} = |A_{mn}(\tau)|^2$$

i.e. $H_0|n\rangle = E_n^0|n\rangle$

We calculate coefficients $A_{mn}$.

$$i\hbar\frac{d}{dt}A_{ml}(t) = \sum_n \langle l|W(t)|n\rangle A_{mn}e^{+i\omega_{ln}t}$$

$$\langle l|W(t)|n\rangle = \int \varphi_l{}^* W(t)\varphi_n dx$$

$$\hbar\omega_{ln} = E_l - E_n$$

# Time-dependent perturbation theory

Unfortunately, the exact solution of the equation is not possible

$$i\hbar \frac{d}{dt} A_{ml}(t) = \sum_n \langle l|W(t)|n\rangle A_{mn} e^{+i\omega_{ln}t}$$

$$\langle l|W(t)|n\rangle = \int \varphi_l{}^* W(t) \varphi_n dx$$

We calculate coefficents $A_{mn}$ iteratively

$$\hbar\omega_{ln} = E_l - E_n$$

$$A_{ml}^{(0)}(t) = \langle l|\varphi_m(x)\rangle = \langle l|m\rangle = \delta_{lm}$$

$$i\hbar \frac{d}{dt} A_{ml}^{(j)}(t) = \sum_n \langle l|W(t)|n\rangle A_{mn}^{(j-1)} e^{+i\omega_{ln}t}$$

New solution

Previous solution

Tutaj 2017.03.27

Odcałkowywujewujemy:

$$A_{ml}^{(1)}(t) = A_{ml}^{(0)}(0) + \frac{1}{i\hbar} \int_0^\tau \sum_n \langle l|W(t)|n\rangle A_{mn}^{(0)} e^{+i\omega_{ln}t}\, dt$$

$W(t)$ Is in the range of 0 to $\tau$

# Time-dependent perturbation theory

Unfortunately, the exact solution of the equation is not possible

$$i\hbar \frac{d}{dt} A_{ml}(t) = \sum_n \langle l|W(t)|n\rangle A_{mn} e^{+i\omega_{ln}t}$$

$$\langle l|W(t)|n\rangle = \int \varphi_l{}^* W(t) \varphi_n dx$$

We calculate coefficents $A_{mn}$ iteratively

$$\hbar\omega_{ln} = E_l - E_n$$

$$A_{ml}^{(0)}(t) = \langle l|\varphi_m(x)\rangle = \langle l|m\rangle = \delta_{lm}$$

Initially, the system was in state $m$

$$i\hbar \frac{d}{dt} A_{ml}^{(j)}(t) = \sum_n \langle l|W(t)|n\rangle A_{mn}^{(j-1)} e^{+i\omega_{ln}t}$$

New solution

Previous solution

Odcałkowywujewujemy:

$$A_{ml}^{(1)}(t) = A_{ml}^{(0)}(0) + \frac{1}{i\hbar}\int_0^\tau \sum_n \langle l|W(t)|n\rangle A_{mn}^{(0)} e^{+i\omega_{ln}t}\, dt =$$

$$= \delta_{lm} + \frac{1}{i\hbar}\int_0^\tau \sum_n \langle l|W(t)|n\rangle \delta_{mn} e^{+i\omega_{ln}t}\, dt = \delta_{lm} + \frac{1}{i\hbar}\int_0^\tau \langle l|W(t)|m\rangle e^{+i\omega_{lm}t}\, dt$$

# Time-dependent perturbation theory

Unfortunately, the exact solution of the equation is not possible

$$i\hbar \frac{d}{dt} A_{ml}(t) = \sum_n \langle l|W(t)|n\rangle A_{mn} e^{+i\omega_{ln}t}$$

$$\langle l|W(t)|n\rangle = \int \varphi_l{}^* W(t) \varphi_n dx$$

We calculate coefficents $A_{mn}$ iteratively

$$\hbar\omega_{ln} = E_l - E_n$$

$$A_{ml}^{(0)}(t) = \langle l|\varphi_m(x)\rangle = \langle l|m\rangle = \delta_{lm}$$

Initially, the system was in state $m$

$$i\hbar \frac{d}{dt} A_{ml}^{(j)}(t) = \sum_n \langle l|W(t)|n\rangle A_{mn}^{(j-1)} e^{+i\omega_{ln}t}$$

New solution

Odcałkowywujewujemy:

$$A_{ml}^{(1)}(t) = A_{ml}^{(0)}(0) + \frac{1}{i\hbar}\int_0^\tau \sum_n \langle l|W(t)|n\rangle A_{mn}^{(0)} e^{+i\omega_{ln}t}\, dt =$$

$$= \delta_{lm} + \frac{1}{i\hbar}\int_0^\tau \sum_n \langle l|W(t)|n\rangle \delta_{mn} e^{+i\omega_{ln}t}\, dt = \delta_{lm} + \frac{1}{i\hbar}\int_0^\tau \langle l|W(t)|m\rangle e^{+i\omega_{lm}t}\, dt$$

Only when the initial and final are the same. And we calculate the probability of transition to another state.

# Time-dependent perturbation theory

Substitute into the equation, we consider the initial condition (see *Quantum Mechanics* S.A Dawydov)

$$\mathcal{w}_{mn} = |A_{mn}(\tau)|^2 = \frac{1}{\hbar^2}\left|\int_0^\tau \langle m|W(t)|n\rangle e^{+i\omega_{mn}t}dt\right|^2$$

When $W(t) = const = W$ for $0 \le t \le \tau$ it is easy to obtain:

$$\int_0^\tau \langle n|W(t)|l\rangle e^{i\omega_{nl}t}dt = \frac{e^{i\omega_{nl}\tau} - 1}{i\omega_{nl}}\langle n|W|l\rangle$$

Then the corresponding probability of transition under perturbation is given by

$$\mathcal{w}_{mn} = |A_{mn}(\tau)|^2 = \frac{2}{\hbar^2}|\langle m|W|n\rangle|^2 \ \frac{1 - \cos\left[(E_n - E_m)\frac{\tau}{\hbar}\right]}{\left[(E_n - E_m)\frac{1}{\hbar}\right]^2}$$

# Time-dependent perturbation theory

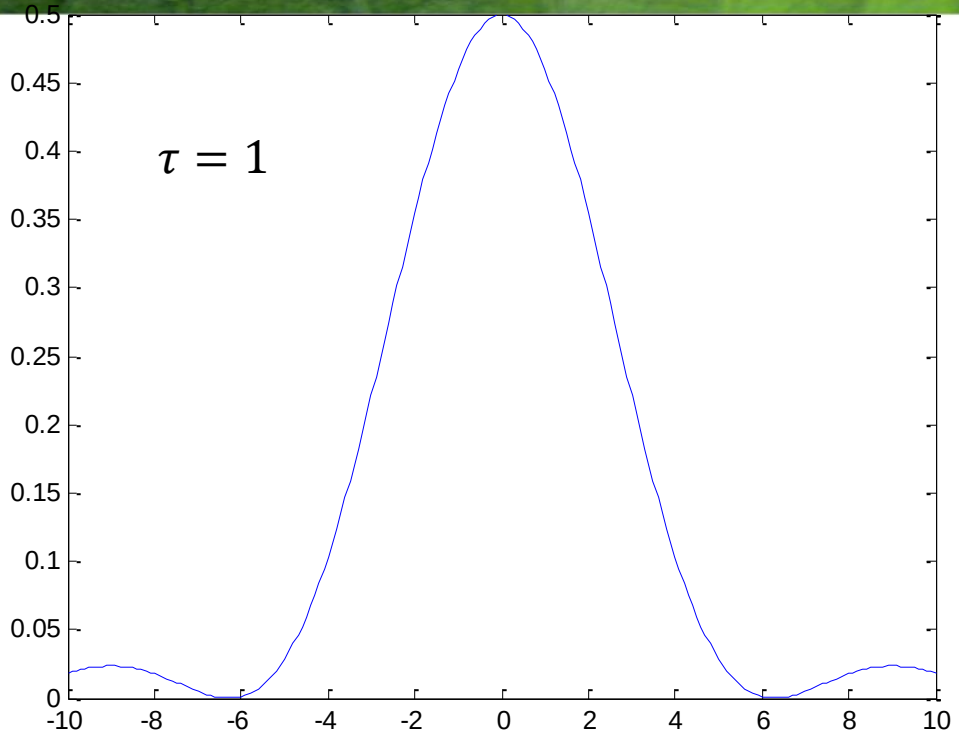


$$\frac{1-\cos\left[(E_n - E_m)\frac{\tau}{\hbar}\right]}{\left[(E_n - E_m)\frac{1}{\hbar}\right]^2}$$

# Time-dependent perturbation theory

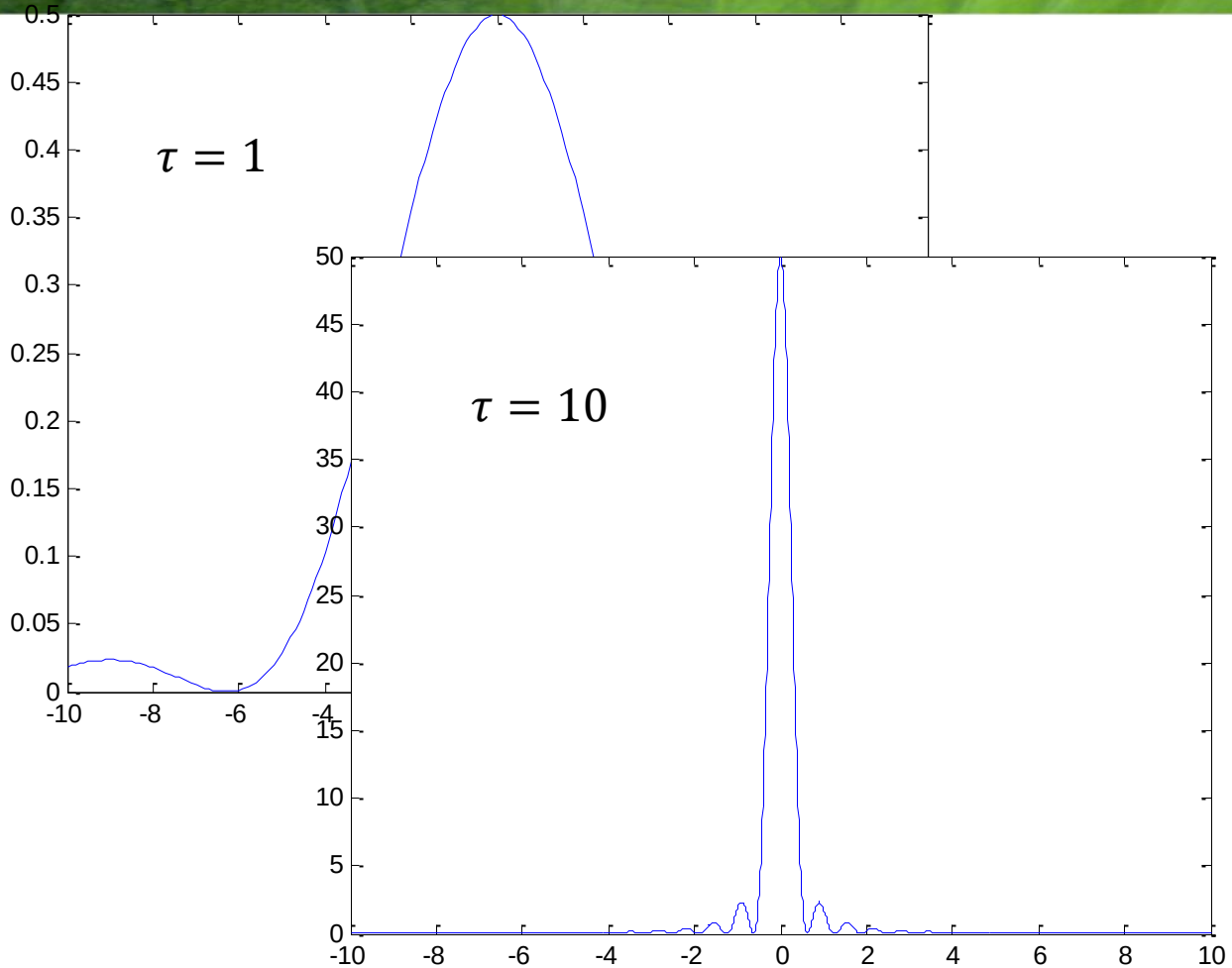


$$\frac{1-\cos\left[(E_n-E_m)\frac{\tau}{\hbar}\right]}{\left[(E_n-E_m)\frac{1}{\hbar}\right]^2}$$

# Time-dependent perturbation theory

$$\frac{1-\cos\left[(E_n-E_m)\frac{\tau}{\hbar}\right]}{\left[(E_n-E_m)\frac{1}{\hbar}\right]^2}$$

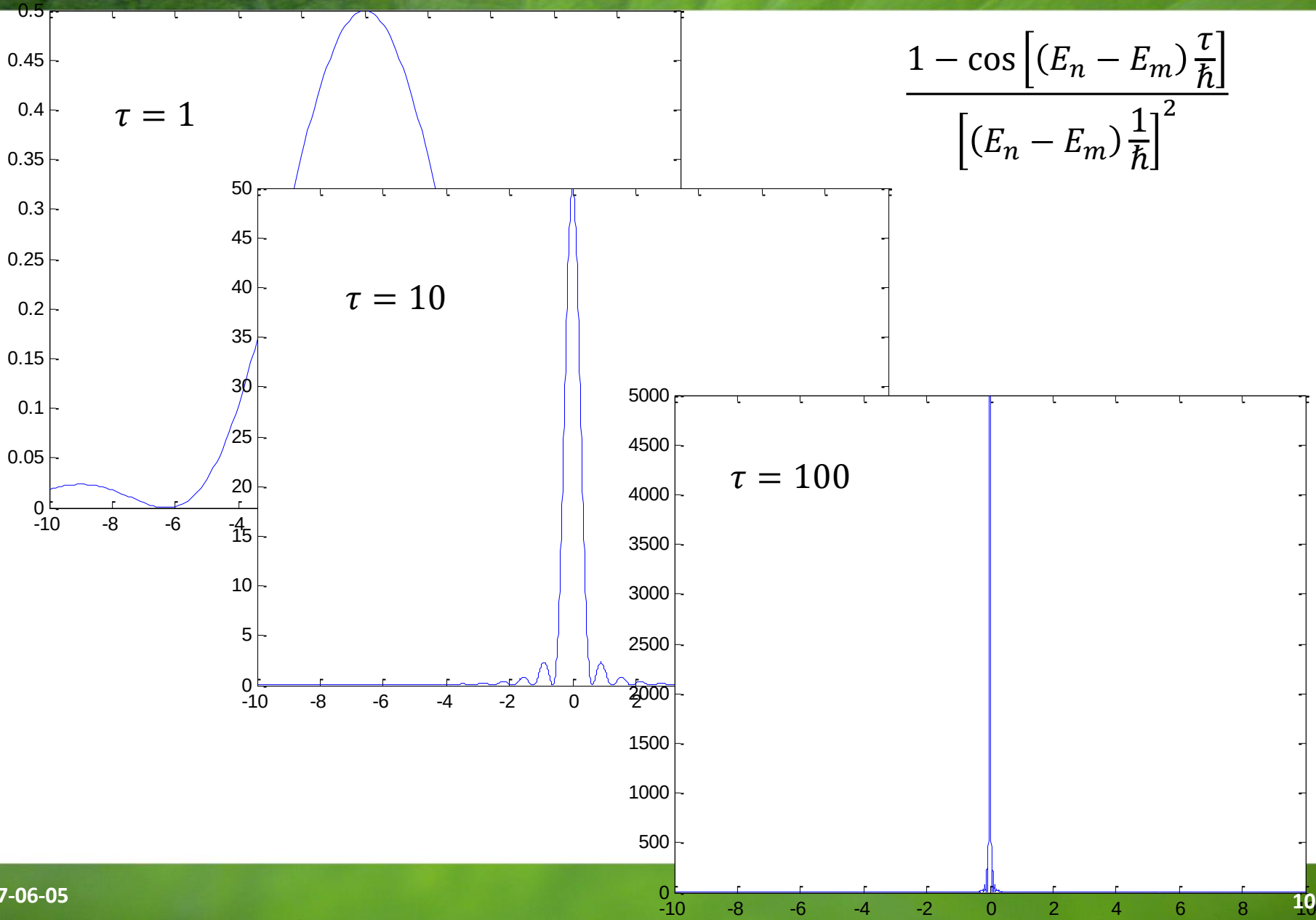

# Time-dependent perturbation theory

Substitute into the equation, we consider the initial condition (see *Quantum Mechanics* S.A Dawydov)

$$\mathcal{w}_{mn} = |A_{mn}(\tau)|^2 = \frac{1}{\hbar^2}\left|\int_0^\tau \langle m|W(t)|n\rangle e^{+i\omega_{mn}t}dt\right|^2$$

When $W(t) = const = W$ for $0 \le t \le \tau$ it is easy to obtain:

$$\int_0^\tau \langle n|W(t)|l\rangle e^{i\omega_{nl}t}dt = \frac{e^{i\omega_{nl}\tau} - 1}{i\omega_{nl}}\langle n|W|l\rangle$$

Then the corresponding probability of transition under perturbation is given by

$$\mathcal{w}_{mn} = |A_{mn}(\tau)|^2 = \frac{2}{\hbar^2}|\langle m|W|n\rangle|^2 \ \frac{1 - \cos\left[(E_n - E_m)\frac{\tau}{\hbar}\right]}{\left[(E_n - E_m)\frac{1}{\hbar}\right]^2}$$

For $\tau \gg \dfrac{\hbar}{E_n - E_m}$ $\quad \dfrac{1 - \cos\left[(E_n - E_m)\frac{\tau}{\hbar}\right]}{\left[(E_n - E_m)\frac{1}{\hbar}\right]^2} \approx \tau\pi\hbar\delta(E_n - E_m)$

# Time-dependent perturbation theory

Finally, the probability of transition

$$w_{mn} = \frac{2\pi}{\hbar} |\langle m|W|n\rangle|^2 \tau \delta(E_m - E_n)$$

The probability of transitions is proportional to the perturbation time, so the probability of transition per unit time is given by:

$$P_{mn} = \frac{w_{mn}}{\tau} = \frac{2\pi}{\hbar} |\langle m|W|n\rangle|^2 \delta(E_m - E_n)$$

# Time-dependent perturbation theory

If the perturbation is in the form of a **periodic wave** we back to the general formula:

$$w_{nm} = |A_{nm}(\tau)|^2 = \frac{1}{\hbar^2}\left|\int_0^\tau \langle n|W(t)|m\rangle e^{+i\omega_{nm}t}dt\right|^2$$

for the case where $W(t) = w^{\pm}e^{\pm i\omega t}$ for $0 \le t \le \tau$ it is easy to calculate:

$$\int_0^\tau \langle n|w^{\pm}|l\rangle e^{i(\omega_{nl}\pm\omega)t}dt = \frac{e^{i(\omega_{nl}\pm\omega)\tau} - 1}{i(\omega_{nl} \pm \omega)}\langle n|w^{\pm}|l\rangle$$

Transition probability:

$$w_{nm} = \frac{2\pi}{\hbar}\left|\langle n|w^{\pm}|m\rangle\right|^2 \tau\delta(E_n - E_m \pm \hbar\omega)$$

Transition probability per unit time:

$$P_{nm} = \frac{w_{nm}}{\tau} = \frac{2\pi}{\hbar}\left|\langle n|w^{\pm}|m\rangle\right|^2 \delta(E_n - E_m \pm \hbar\omega)$$

# Time-dependent perturbation theory

Conclusions:

$$W(t) = w^{\pm} e^{\pm i\omega t}$$
$$0 \leq t \leq \tau$$

$$\boxed{P_{nm} = \frac{\mathcal{w}_{nm}}{\tau} = \frac{2\pi}{\hbar} \left|\langle n | w^{\pm} | m \rangle\right|^2 \delta(E_n - E_m \pm \hbar\omega)}$$

The transitions are possible only for states $E_m = E_n \pm \hbar\omega$

The system can either gain energy (absorbs) or lose (emits).

# Electromagnetic wave

**The perturbation in a form of an electromagnetic wave.**

$$\boxed{P_{nm} = \frac{w_{nm}}{\tau} = \frac{2\pi}{\hbar}\left|\langle n|w^{\pm}|m\rangle\right|^2 \delta(E_n - E_m \pm \hbar\omega)}$$

General form of the hamiltonian in the electromagnetic field is given by tha vector potential $A$ and scalar $\varphi$:

$$H = \frac{1}{2m}\left(\vec{p} + e\vec{A}\right)^2 - e\varphi + V$$

Assuming suitable gauging (pol: „cechowanie”) $\varphi = 0$, $\mathrm{div}A = 0$ and neglecting terms with $A^2$ (low radiation, etc.)

$$H \approx \frac{e}{m}\vec{A}\vec{p}$$

Vector potential for an electromagnetic wave may be introduced in the form :

$$\vec{A} = \overrightarrow{A_0}\left\{e^{-i(\omega t - \vec{k}\vec{r})} + e^{i(\omega t - \vec{k}\vec{r})}\right\}$$

$$\vec{E} = -\nabla\varphi - \frac{\partial\vec{A}}{\partial t} \qquad \vec{E} = 2\omega\overrightarrow{A_0}\sin(\omega t - \vec{k}\vec{r})$$

$$\vec{B} = \nabla \times \vec{A} \qquad \vec{B} = 2(\vec{k} \times \overrightarrow{A_0})\sin(\omega t - \vec{k}\vec{r})$$

# Dictionary

$$\vec{D} = \varepsilon \vec{E}$$

$\varepsilon_0$ **vacuum permittivity, permittivity of free space** (przenikalność elektryczna próżni)
$\varepsilon_r$ relative permittivity (względna przenikalność elektryczna)
$\varepsilon = \varepsilon_0 \varepsilon_r$ permittivity (przenikalność elektryczna)

$$\vec{B} = \mu \vec{H}$$

$\mu_0$ **vacuum permeability, permeability of free space** (przenikalność magnetyczna)

$$\mu_0 = 4\pi \cdot 10^{-7} \text{H/m}$$

$\mu_r$ relative permeability (względna przenikalność magnetyczna)
$\mu = \mu_0 \mu_r$ permeability (przenikalność magnetyczna)

magnetic susceptibility $\chi_m = \mu_r - 1$

electric field $\vec{E}$ and the magnetic field $\vec{B}$
displacement field $\vec{D}$ and the magnetizing field $\vec{H}$

# Electromagnetic wave

**The perturbation in a form of an electromagnetic wave.**

$$P_{nm} = \frac{w_{nm}}{\tau} = \frac{2\pi}{\hbar}\left|\langle n|w^{\pm}|m\rangle\right|^2 \delta(E_n - E_m \pm \hbar\omega)$$

General form of the hamiltonian in the electromagnetic field is given by tha vector potential $A$ and scalar $\varphi$:

$$H = \frac{1}{2m}\left(\vec{p} + e\vec{A}\right)^2 - e\varphi + V$$

Assuming suitable gauging (pol: „cechowanie”) $\varphi = 0$, $\mathrm{div}A = 0$ and neglecting terms with $A^2$ (low radiation, etc.)

$$H \approx \frac{e}{m}\vec{A}\vec{p}$$

Vector potential for an electromagnetic wave may be introduced in the form :

$$\vec{A} = \overrightarrow{A_0}\left\{e^{-i(\omega t - \vec{k}\vec{r})} + e^{i(\omega t - \vec{k}\vec{r})}\right\}$$

$$\vec{E} = -\nabla\varphi - \frac{\partial\vec{A}}{\partial t} \qquad \vec{E} = 2\omega\overrightarrow{A_0}\sin(\omega t - \vec{k}\vec{r})$$

$$\vec{B} = \nabla \times \vec{A} \qquad \vec{B} = 2(\vec{k} \times \overrightarrow{A_0})\sin(\omega t - \vec{k}\vec{r})$$

# Electromagnetic wave

**The perturbation in a form of an electromagnetic wave.**

$$H \approx \frac{e}{m}\vec{A}\vec{p}$$

$$\boxed{P_{nm} = \frac{w_{nm}}{\tau} = \frac{2\pi}{\hbar}\left|\langle n|w^{\pm}|m\rangle\right|^2 \delta(E_n - E_m \pm \hbar\omega)}$$

$$\vec{A} = \overrightarrow{A_0}\left\{e^{-i(\omega t - \vec{k}\vec{r})} + e^{i(\omega t - \vec{k}\vec{r})}\right\}$$

expanding a series $\vec{p}\, e^{-i(\vec{k}\vec{r})} \approx \vec{p}\left[1 + \left(-i\vec{k}\vec{r}\right) + \frac{\left(-i\vec{k}\vec{r}\right)^2}{2!} + \cdots\right]$

We use the commutation rules $[\vec{r}, H_0] = \vec{r}H_0 - H_0\vec{r} = \frac{i\hbar}{m}\vec{p}$

we get $\langle n|\vec{p}|m\rangle = im\omega_{nm}\langle n|\vec{r}|m\rangle$

Subsequent terms in this expansion give: dipole magnetic transitions, quadrupole electric transitions etc.

# Electromagnetic wave

**The perturbation in a form of an electromagnetic wave.**

$$H \approx \frac{e}{m}\vec{A}\vec{p}$$

$$\vec{A} = \overrightarrow{A_0}\left\{e^{-i(\omega t-\vec{k}\vec{r})} + e^{i(\omega t-\vec{k}\vec{r})}\right\}$$

$$\boxed{P_{nm} = \frac{w_{nm}}{\tau} = \frac{2\pi}{\hbar}\left|\langle n|w^{\pm}|m\rangle\right|^2 \delta(E_n - E_m \pm \hbar\omega)}$$

expanding a series $\vec{p}\, e^{-i(\vec{k}\vec{r})} \approx \vec{p}\left[1 + \left(-i\vec{k}\vec{r}\right) + \frac{\left(-i\vec{k}\vec{r}\right)^2}{2!} + \cdots\right]$

after laborious calculations we get the probability of emission of electromagnetic radiation dipole (described by the operator $e\vec{r}$)

$$\boxed{A_{nm} = \frac{w_{nm}}{\tau} = \frac{{\omega_{nm}}^3 e^2}{3\pi\varepsilon_0\hbar c^3}|\langle n|\vec{r}|m\rangle|^2 = \frac{4\alpha}{3}\frac{{\omega_{nm}}^3}{c^2}|\langle n|\vec{r}|m\rangle|^2}$$

$$\alpha = \frac{e^2}{4\pi\varepsilon_0\hbar c} \approx \frac{1}{137}$$

It is one of the **Einstein coefficients** (lasers, etc. - next week!) for nondegenerated states.

# Electromagnetic wave

**The perturbation in a form of an electromagnetic wave.**

$$\boxed{A_{nm} = \frac{{\omega_{nm}}^3 e^2}{3\pi\varepsilon_0 \hbar c^3} |\langle m|\vec{r}|n\rangle|^2 = \frac{4\alpha}{3}\frac{{\omega_{nm}}^3}{c^2}|\langle m|\vec{r}|n\rangle|^2}$$

In the case o degenerated states we introduce „oscillator strength"

$$A_{nm} = \frac{4\alpha}{3}\frac{{\omega_{nm}}^3}{c^2}\frac{S_{mn}}{g_m} \qquad S_{nm} = \sum_i \sum_j \left|\langle n_i|\vec{r}|m_j\rangle\right|^2$$

the degeneracy of the initial state

In the case of the hydrogen atom states it is convenient to represent operator $\vec{r}$ in the circular form:

$$\left|\langle n_i|\vec{r}|m_j\rangle\right|^2 = \left|\langle n_i|z|m_j\rangle\right|^2 + \frac{1}{2}\left|\langle n_i|x+iy|m_j\rangle\right|^2 + \frac{1}{2}\left|\langle n_i|x-iy|m_j\rangle\right|^2$$

it is easy to then integrate spherical harmonics, because:

$$z = r\cos\vartheta$$

$$x \pm iy = re^{\pm i\varphi}\sin\vartheta$$

**Check it!**

# Electromagnetic wave

**Some final remarks**

$$A_{nm} = \frac{4\alpha}{3}\frac{{\omega_{nm}}^3}{c^2}\frac{S_{mn}}{g_m} \qquad S_{nm} = \sum_i \sum_j \left|\langle n_i|\vec{r}|m_j\rangle\right|^2$$

By calculating the Einstein coefficients of eg. the hydrogen atom, we can get the so called **optical transitions selection rules** , eg. for hydrogen:

$\Delta l = \pm 1$ momentum conservation rule – the photon has an integer spin

$\Delta m = \pm 1$ transition in circular polarization $\sigma$

$\Delta m = 0$ transition in linear polarization $\pi$

Optical transitions are possible only between atomic levels of **different symmetry**, since the operator $\vec{r}$ is antisymmetric

# Electromagnetic wave

**Some final remarks**

$$A_{nm} = \frac{4\alpha}{3}\frac{{\omega_{nm}}^3}{c^2}\frac{S_{mn}}{g_m} \qquad S_{nm} = \sum_i \sum_j \left|\langle n_i|\vec{r}|m_j\rangle\right|^2$$

We can introduce *radiative recombination rate* (recombination lifetime) $\tau_{mn}$

$$\tau_{nm} = \frac{1}{A_{nm}}$$

*czas życia*

In the case of dipole optical transition this lifetime is of the order of nanoseconds.

The power of the optical transition $P_{nm} = A_{nm}\hbar\,\omega_{nm}$

# Summary –Fermi golden rule

The probability of transition per unit time:

$$W(t) = W$$
$$0 \le t \le \tau$$

$$\boxed{P_{mn} = \frac{w_{mn}}{\tau} = \frac{2\pi}{\hbar}|\langle m|W|n\rangle|^2 \delta(E_m - E_n)}$$

Transitions are possible only for states, for which $E_m = E_n$

$$W(t) = w^{\pm} e^{\pm i\omega t}$$
$$0 \le t \le \tau$$

$$\boxed{P_{nm} = \frac{w_{nm}}{\tau} = \frac{2\pi}{\hbar}\left|\langle n|w^{\pm}|m\rangle\right|^2 \delta(E_n - E_m \pm \hbar\omega)}$$

Transitions are possible only for states, for which $E_m = E_n \pm \hbar\omega$

**The perturbation in a form of an electromagnetic wave:**

$$\boxed{A_{nm} = \frac{{\omega_{nm}}^3 e^2}{3\pi\varepsilon_0 \hbar c^3}|\langle m|\vec{r}|n\rangle|^2 = \frac{4\alpha}{3}\frac{{\omega_{nm}}^3}{c^2}|\langle m|\vec{r}|n\rangle|^2}$$

$$\boxed{P_{nm} = A_{nm}\delta(E_n - E_m \pm \hbar\omega)}$$

# Summary –Fermi golden rule

The transition rate – the probability of transition per unit time – from the initial state $|i\rangle$ to final $|f\rangle$ is given by:

Szybkość zmian – czyli prawdopodobieństwo przejścia na jednostkę czasu – ze stanu początkowego $|i\rangle$ do końcowego $|f\rangle$ dane jest wzorem:

$$\boxed{P_{mn} = \frac{2\pi}{\hbar}|\langle f|W|i\rangle|^2 \rho(E_f)}$$

$W$ - interaction with the field

$\rho(E_f)$ - the density of final states

**Perturbation $W$ does not have to be in the form of an electromagnetic wave.**

# Selction rules in condensed matter

**Proof sketch**

Bloch function of a carrier in the crystal:

$$\Psi(\vec{r}) = \sum_{n,k} c_{n,k} u_{n,k}(\vec{r}) e^{i\vec{k}\vec{r}}$$

For the electron:

$$\Psi_{\mathrm{c}}(\vec{r}) \approx \sum_{k} c_{1,k} u_{\Gamma_6,0}(\vec{r}) e^{i\vec{k}\vec{r}} = u_{\Gamma_6,0}(\vec{r}) F_e(\vec{r})$$

For the hole:

$$\Psi_{\mathrm{v}}(\vec{r}) \approx \sum_{J_z = \pm 3/2, \pm 1/2, k} c_{J_z,k} u_{\Gamma_8,J_z}(\vec{r}) e^{i\vec{k}\vec{r}} = \sum_{J_z = \pm 3/2, \pm 1/2, k} u_{\Gamma_8,J_z}(\vec{r}) F_{J_z}(\vec{r})$$

Intersubband dipole optical transitions:

$$\langle \Psi_{\mathrm{c}}(\vec{r}) | \vec{p} | \Psi_{\mathrm{v},J_z}(\vec{r}) \rangle = \underbrace{\langle u_{\Gamma_6,0}(\vec{r}) | u_{\Gamma_8,J_z}(\vec{r}) \rangle}_{=0} \langle F_e(\vec{r}) | \vec{p} | F_{J_z}(\vec{r}) \rangle + \langle u_{\Gamma_6,0}(\vec{r}) | \vec{p} | u_{\Gamma_8,J_z}(\vec{r}) \rangle \langle F_e(\vec{r}) | F_{J_z}(\vec{r}) \rangle$$

# Optical transitions

$E_f$ final energy
$E_i$ initial energy

$E_f = E_i + \hbar c Q$ energy conservation rule
$K_f = K_i + Q$ momentum conservation rule

Photon momentum $\hbar\omega = \hbar c Q$. For $\hbar\omega = 1$ eV we got $Q \approx 10^7 m^{-1}$. The size of the Brillouin zone is about $\frac{\pi}{a} \approx \frac{\pi}{0.5\,nm} = 10^{10} m^{-1}$. Therefore $K_f = K_i + Q \approx K_i$

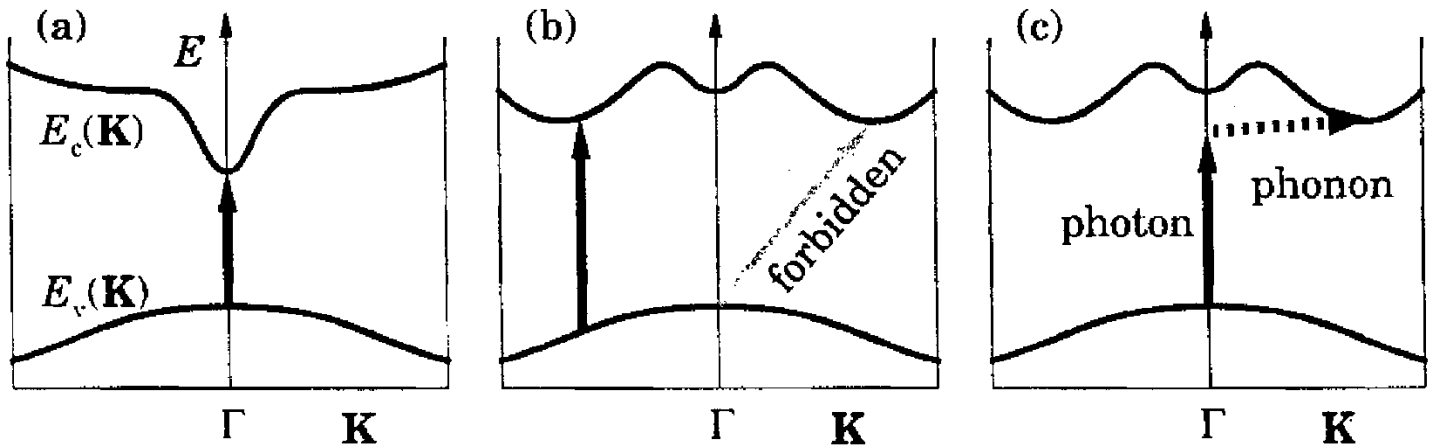


**FIGURE 2.20.** Optical absorption across the band gap in different types of semiconductor. (a) Absorption across a direct band gap at Γ. (b) Absorption across an indirect band gap is forbidden but vertical transitions occur for all **K**. (c) Transition across an indirect band gap with absorption of both a phonon and a photon.

# Optical transitions

$$\varepsilon_{e,n_e} = E_c^{GaAs} + \frac{\hbar^2\pi^2 n_e^2}{2m_0 m_e a^2}$$

$$\varepsilon_{h,n_h} = E_v^{GaAs} - \frac{\hbar^2\pi^2 n_h^2}{2m_0 m_h a^2}$$

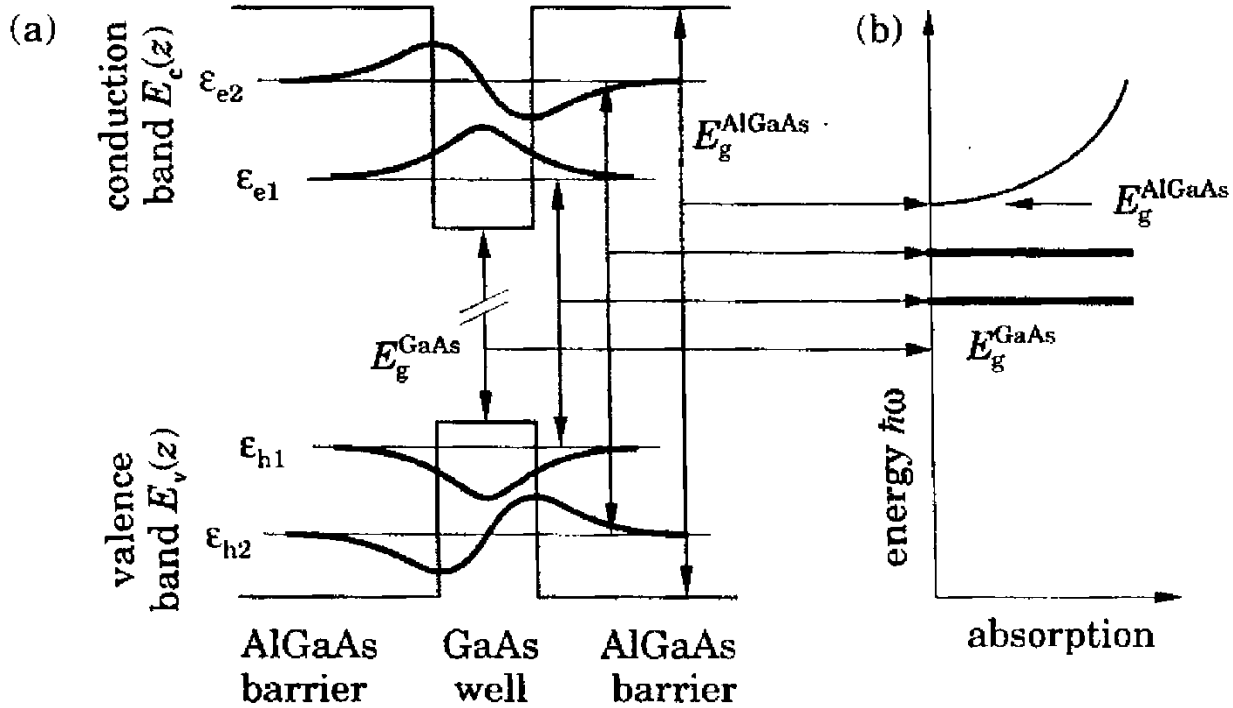


$$\hbar\omega_n = \varepsilon_{e,n_e} - \varepsilon_{h,n_h} = E_g^{GaAs} + \frac{\hbar^2\pi^2 n^2}{2m_0 a^2}\left(\frac{1}{m_e} + \frac{1}{m_h}\right) = E_g^{GaAs} + \frac{\hbar^2\pi^2 n^2}{2m_0 m_{eh} a^2}$$

Optical effective mass $\frac{1}{m_{eh}} = \frac{1}{m_e} + \frac{1}{m_h}$

# Optical transitions

$$\varepsilon_{e,n_e} = E_c^{GaAs} + \frac{\hbar^2\pi^2 n_e^2}{2m_0 m_e a^2}$$

$$\varepsilon_{h,n_h} = E_v^{GaAs} - \frac{\hbar^2\pi^2 n_h^2}{2m_0 m_h a^2}$$

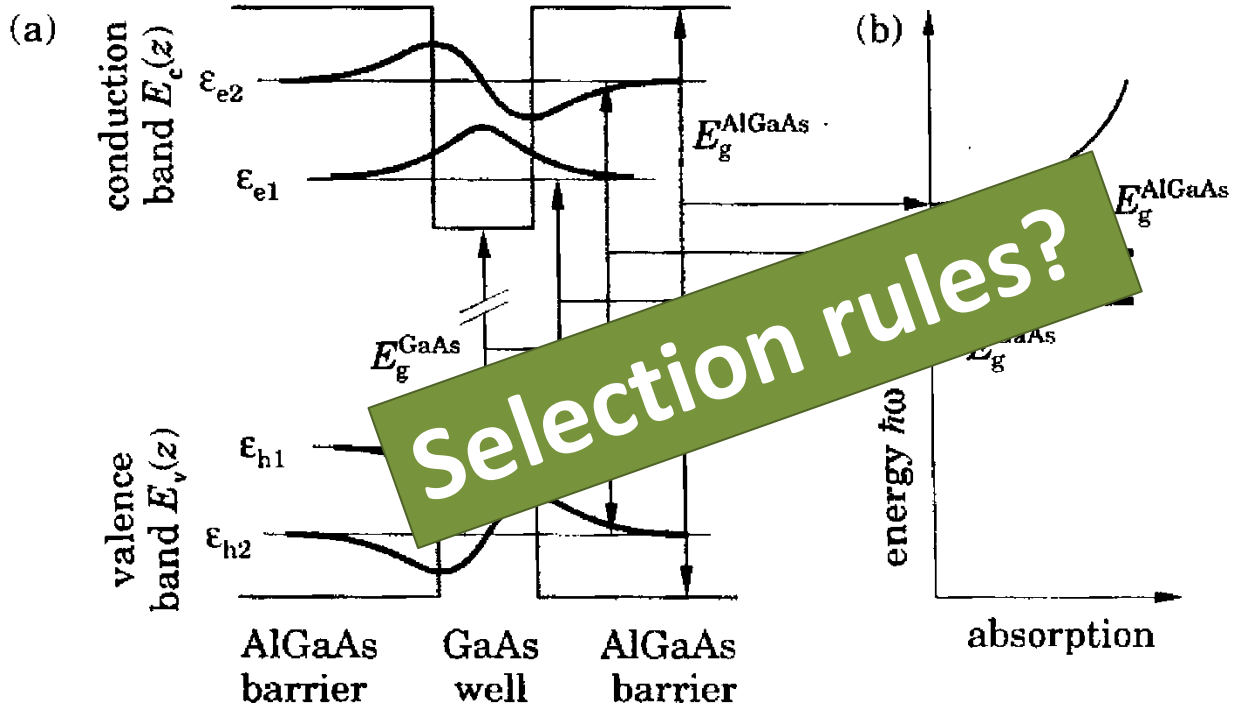


$$\hbar\omega_n = \varepsilon_{e,n_e} - \varepsilon_{h,n_h} = E_g^{GaAs} + \frac{\hbar^2\pi^2 n^2}{2m_0 a^2}\left(\frac{1}{m_e} + \frac{1}{m_h}\right) = E_g^{GaAs} + \frac{\hbar^2\pi^2 n^2}{2m_0 m_{eh} a^2}$$

Optical effective mass $\frac{1}{m_{eh}} = \frac{1}{m_e} + \frac{1}{m_h}$

# Optical transitions

$$\varepsilon_{e,n_e} = E_c^{GaAs} + \frac{\hbar^2\pi^2 n_e^2}{2m_0 m_e a^2}$$

$$\varepsilon_{h,n_h} = E_v^{GaAs} - \frac{\hbar^2\pi^2 n_h^2}{2m_0 m_h a^2}$$

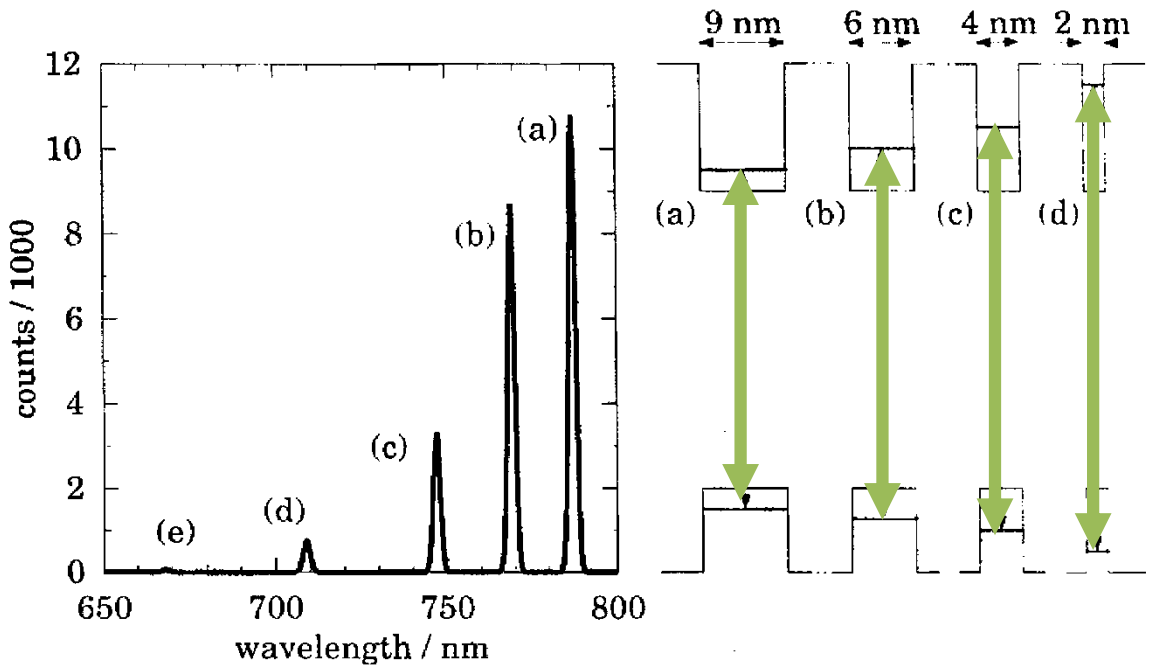


**FIGURE 1.4.** Photoluminescence as a function of wavelength for a sample with four quantum wells of different widths, whose conduction and valence bands are shown on the right. The barriers between the wells are much thicker than drawn. [Data kindly supplied by Prof. E. L. Hu, University of California at Santa Barbara.]

$$\hbar\omega_n = \varepsilon_{e,n_e} - \varepsilon_{h,n_h} = E_g^{GaAs} + \frac{\hbar^2\pi^2 n^2}{2m_0 a^2}\left(\frac{1}{m_e} + \frac{1}{m_h}\right) = E_g^{GaAs} + \frac{\hbar^2\pi^2 n^2}{2m_0 m_{eh} a^2}$$

Optical effective mass $\frac{1}{m_{eh}} = \frac{1}{m_e} + \frac{1}{m_h}$

# Optical transitions

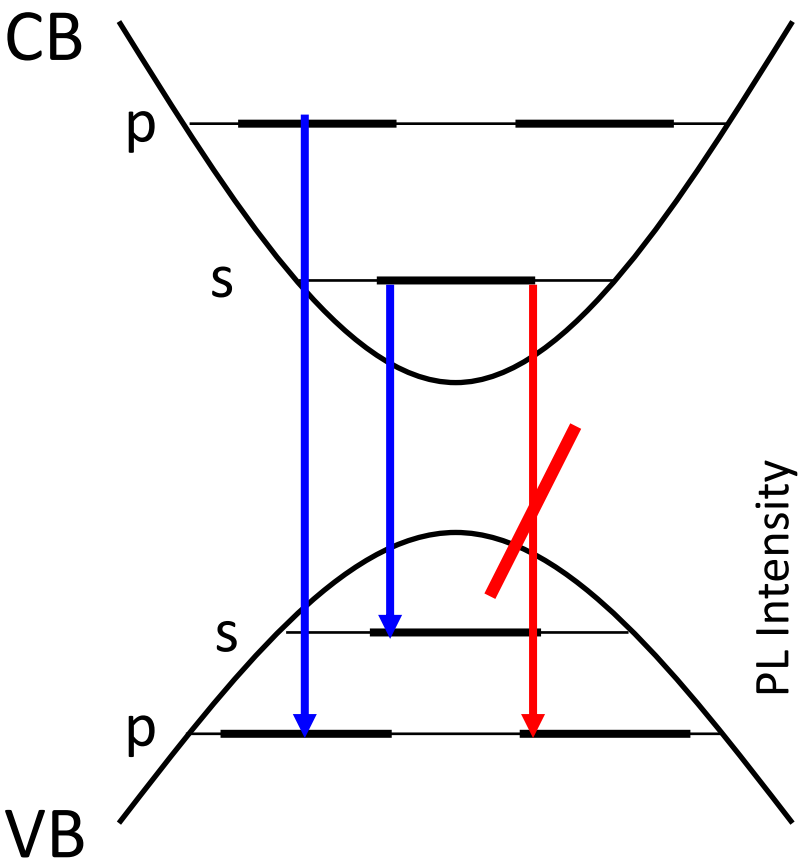


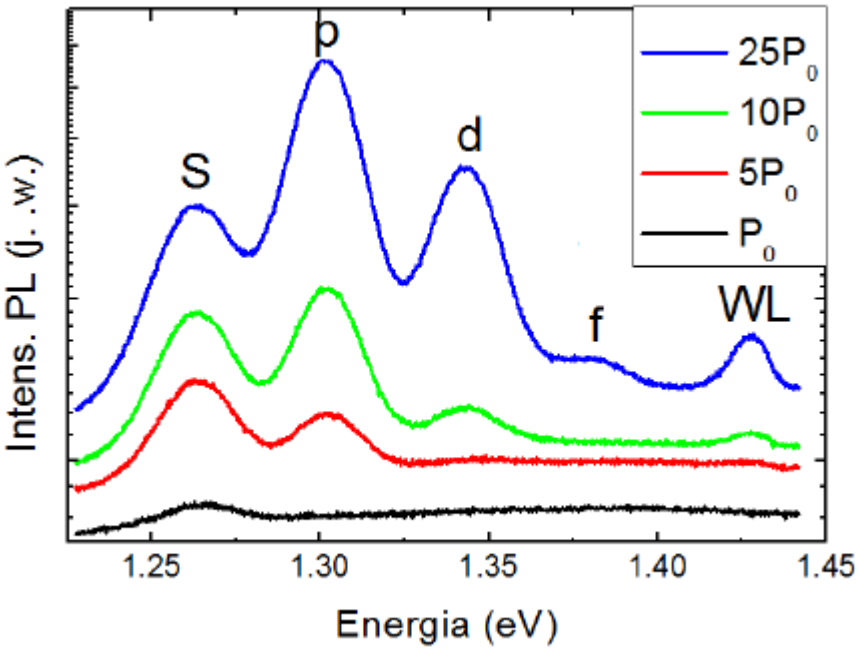


The power dependence of photoluminescence spectra at temperatures close to liquid helium temperatures (approx. 5 K) for a large number set (several million) of quantum dots InAs/GaAs

# Optical transitions

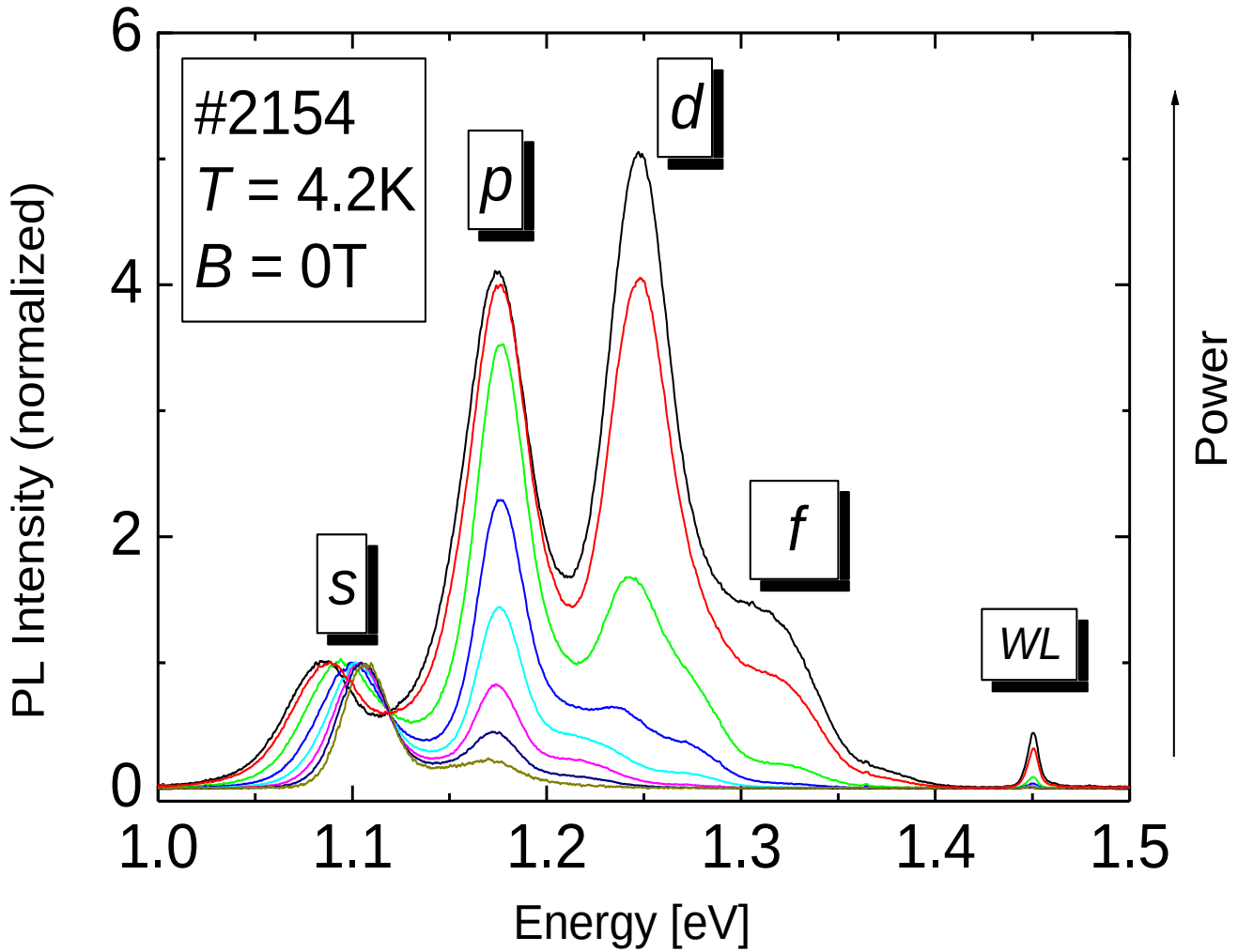


Adam Babiński

# Optical transitions

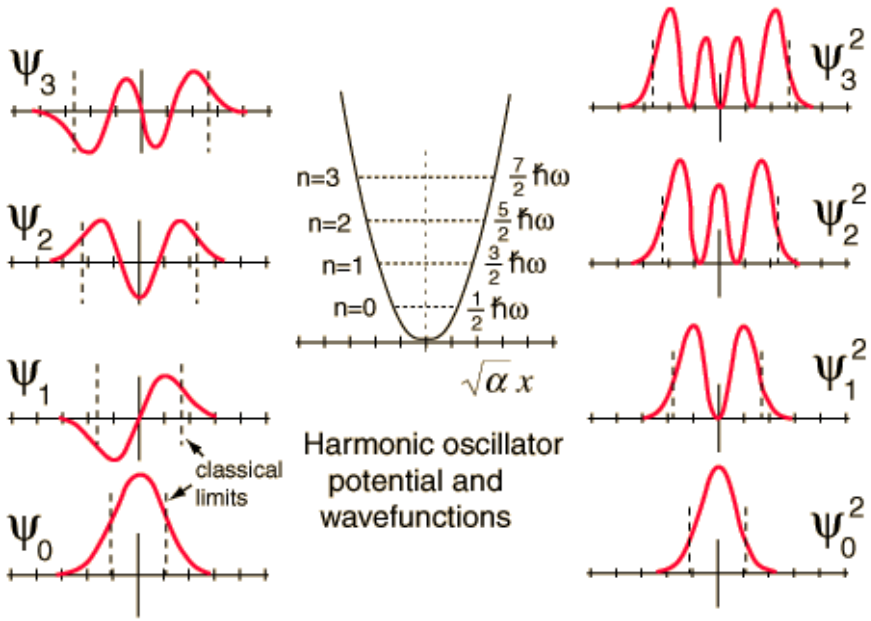


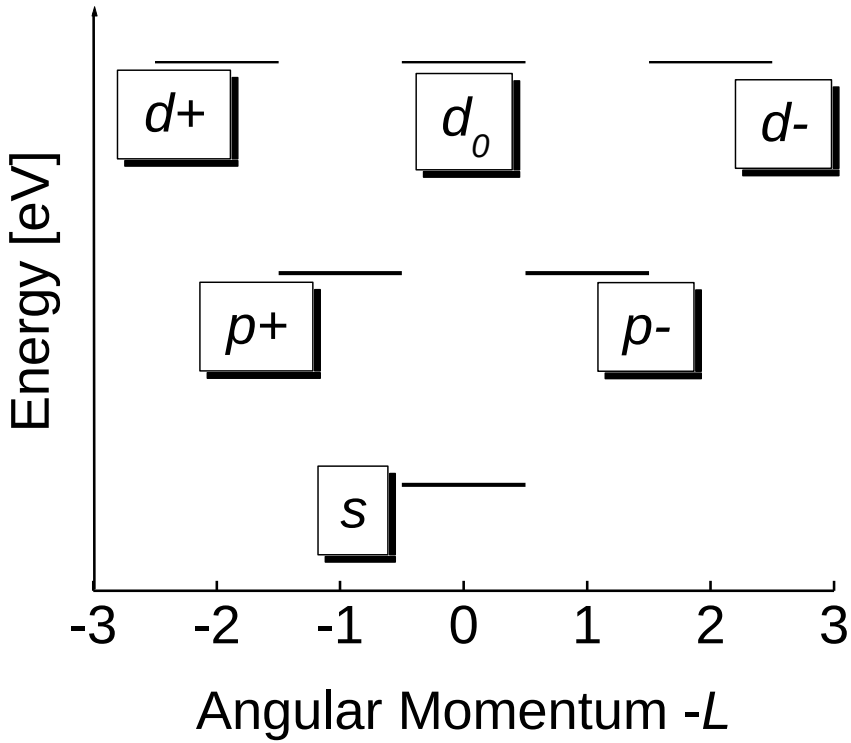


$n, m = 0,1,2...$

$L = n - m$ (elektron)

Adam Babiński